Project Acronym	CORMORAN (ANR 11-INFR-010)
Document Title	D3.4 - PHY/MAC Cross-Layer Design for Enhanced WBAN Communications through Cooperation – Final Document
Contractual Date of Delivery to ANR	M34 (10/2014) / M40 (04/2015) **[Approved extension]**
Actual date of Delivery	M40
Editor	Arturo Mauricio JIMENEZ GUIZAR (INSA)
Authors	Arturo Mauricio JIMENEZ GUIZAR (INSA), Claire GOURSAUD (INSA), Anis Ouni (TPT), Claude CHAUDET (TPT)
Participants	INSA, TPT, UR1
Related Task(s)	T3
Related Sub-Task(s)	T3.1
Security	Public
Nature	Technical Report
Version Number	1.0
Total Number of Pages	82

Key Words: *Scheduling, Resource slot allocation, Wireless Sensor Network, Cooperative Communications, Body Area Networks, Positioning, Mobility Model, Channel Model, IR-UWB*

Table of Content

CONTACTS & CORRESPONDENCE

Arturo Mauricio JIMENEZ GUIZAR (INSA)

- Address: Département de Télécommunications, Services & Usages, CITI INRIA Laboratory – SOCRATE TEAM, INSA Lyon, 6 Avenue des Arts, Bât. Claude Chappe, 69621 Villeurbanne Cedex
- Email: arturo.guizar@insa-lyon.fr
- Tel: (+33) (0)4 72 43 76 15

Claire GOURSAUD (INSA)

- Address: Département de Télécommunications, Services & Usages, CITI INRIA Laboratory – SOCRATE TEAM, INSA Lyon, 6 Avenue des Arts, Bât. Claude Chappe, 69621 Villeurbanne Cedex
- Email: claire.goursaud@insa-lyon.fr
- Tel: (+33) (0)4 72 43 63 27

Anis OUNI (TPT)

- Address: Télécom ParisTech ; Dept. INFRES ; 23 avenue d'Italie ; CS 51237 - 75214 Paris Cedex 13
- Email: anis.ouni@telecom-paristech.fr

Claude CHAUDET (TPT)

- Address: Télécom ParisTech ; Dept. INFRES ; 23 avenue d'Italie ; CS 51237 - 75214 Paris Cedex 13
- Email: claude.chaudet@enst.fr
- Tel: (+33) (0)1 45 81 71 51

Table of Acronyms

A&B	Aggregate and Broadcast
AWGN	Additive White Gaussian Noise
CAP	Contention Access Period
CDF	Cumulative Density Function
CIR	Channel Impulse Response
CFP	Contention Free Period
CGN	Coordinated Group Navigation
CM3	IEEE 802.15.6 - Channel Model 3
CRLB	Cramer Rao Lower bound
GCS	Global Coordinates System
(G)TS	(Guaranteed) Time Slots
IR-UWB	Impulse Radio – Ultra Wideband
ISM	Industrial Scientific & Medical radio bands
LMDS	Local Multi-Dimensional Scaling
LCS	Local Coordinates System
LoS	Line of Sight
LQE	Link Quality Estimator
LSIMC	Large-Scale Individual Motion Capture
MDS	Multi-Dimensional Scaling
MF	Matched Filtering
ML	Maximum Likelihood
MAC	Medium Access Control
MoCap	Motion Capture
NB	Narrow Band

NLoS	Non-Line of Sight
PDF	Probability Density Function
PER	Packet Error Rate
PHY	Physical layer
PL	Path Loss
P_{Succ}	Positioning success rate
P2P	Peer-to-Peer transmission
P2P-B	Peer-to-Peer transmission mixed with Broadcast
RMSE	Root Mean Squared Error
RSSI	Received Signal Strength Indicator
(RT-)ToF	(Round Trip -) Time Of Flight
R_{Succ}	Ranging success rate
Rx	Receiver device
SNR	Signal to Noise Ratio
ToA	Time of Arrival
TDoA	Time Difference Of Arrival
TDMA	Time Division Multiple Access
ToA	Time of Arrival
2-WR	Two Way Ranging
3-WR	Three Way Ranging
Tx	Transmitter device
WBAN	Wireless Body Area Network
WSN	Wireless Sensor Networks

ABSTRACT

This deliverable summarises our investigations on WBAN cooperative communications and cross-layer mechanisms to perform *individual motion capture (LSIMC)* and more marginally here, *coordinated group navigation (CGN)* (D1.1). For this purpose, we exploit the advantages of the *Wireless Body Area Networks (WBAN)* communicating through *Impulse Radio - Ultra Wideband (IR-UWB).* Accordingly, we recall the main parameters (e.g. nodes synchronisation, WBAN channel variations and mobility of the human body) to consider when using IR-UWB radio for WBAN localization at the different protocol layers (D2.3, D2.4, D3.1).

First, we investigate the problem of mobility and we characterize its impact on the quality of range estimation. Then, we extend the problem by quantifying the errors related to the WBAN channel variations. From this study, we have found that the latter errors are significantly higher than that caused by the lack of space-time coherence between acquired radio metrics and actual inter-node distances (under practical protocol and latency constraints).

Based on the previous results, we propose new cooperative mechanisms to reduce the mobility impact on ranging. For this sake, we evaluate the resulting positioning error with different packet scheduling strategies and node slots allocation at the MAC layer under realistic mobility scenarios obtained by measurement (D4.1).

Finally, we consider packet loss in the network and its impact on the positioning success rate of on-body nodes. Accordingly, we have proposed a cross-layer cooperative approach to increase this success rate, which consists in choosing the most adequate cooperative virtual on-body anchors for ranging, based on link quality estimation.

We invite the reader to look at the Deliverables D1.1 D2.3 D2.4 D2.5 D3.1 D3.2 D4.1 of the CORMORAN project for more details about the inputs considered in this work.

1. INTRODUCTION

Recent works on radiolocation with Wireless Body Sensor Networks (WBSN) or Wireless Body Area Networks (WBAN) [1] [2] [3] [4] [5] [6] show this technology as a key for several applications and public/private services, e.g. civil security, health care monitoring, sport tracking activity. In this document, we aim at proposing cross-layer PHY/MAC/NWK cooperative mechanisms adapted to on-body nodes localization so as to enable the application scenarios presented in Deliverable D1.1 of the CORMORAN project, namely ***large-scale individual motion capture*** (LSIMC) and more marginally here, ***Coordinated group navigation*** (CGN). Indeed, the performance of communication protocols for WBAN can dramatically be degraded due to several channel variations in time domain. In fact, the body's absorption of RF energy and the movement create temporal variations of the channel, which produce a significant loss of transmitted packets. One way to avoid this problem consists in implementing cooperation mechanisms between the different on-body nodes of a WBAN [7] [8] [9]. In proposals such as [10] [11] [12] [13] [14] [15], it is possible to appreciate the advantages of cooperation as a solution for robust communications in harsh environments sensing (e.g. temperature, heartbeat, blood pressure). In this project, we generally consider to explore the potential of jointly cooperative and heterogeneous WBAN contexts with e.g., the use of IEEE 802.15.6 standard [16] with an Impulse Radio Ultra Wideband (IR-UWB) PHY layer at the body scale and a Narrowband (NB) PHY Layer (e.g. RSSI measurement at 2.4GHz) for body-to-body and off-body links. Hereafter, we will however focus mostly on cooperative on-body communications for LSIMC.

1.1. SELECTED APPLICATION SCENARIOS AND RELATED NEEDS

1.1.1 LARGE-SCALE INDIVIDUAL MOTION CAPTURE

One first scenario of interest is related to LSIMC applications. The aim is to propose alternative stand-alone solutions to achieve Motion Capture (MoCap) at larger scale than conventional technologies (e.g., optical systems). Thus, we consider three sub-scenarios:

- ***Relative On-Body Nodes Ranging*** where a group of wireless nodes embedded on the body and with unknown positions communicate between them to estimate their relative Euclidean distances.

- ***Relative On-Body Nodes Positioning*** considers two categories of on-body devices, the **mobile nodes** with unknown positions and the **anchor nodes** composing a ***Local Coordinates System (LCS)***. Here, the anchors are placed onto the body and they know their relative positions at any time, independently of the body attitude and/or direction (e.g. on the chest or on the back).

- ***Absolute On-Body Nodes Positioning:*** describes an extended scenario from the previous one, where a set of wireless anchors are deployed in the environment. Thus, the on-body anchors communicate with the off-body anchors to calculate their absolute positions. Moreover, they are time-variant in the ***Global Coordinates System (GCS)***

under pedestrian mobility. And they also depend on the body attitude, the motion direction et/or speed.

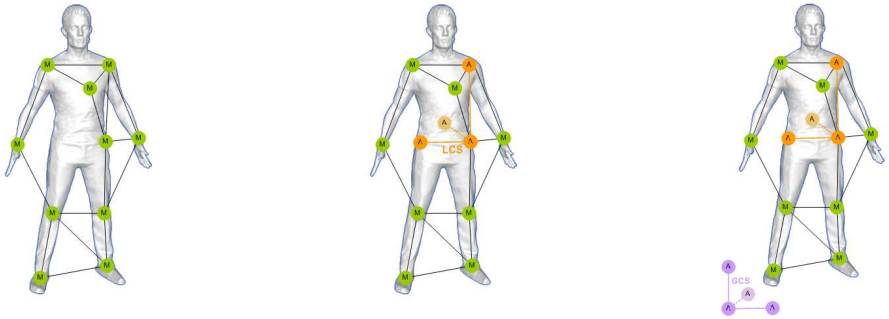

Figure 1-1: Examples of relative on-body nodes ranging (a), relative on-body nodes positioning (b) and absolute on-body nodes positioning (c) configurations for large-scale single-user motion capture applications.

1.1.2 COORDINATED GROUP NAVIGATION APPLICATION

The second application scenario concerns CGN, where we consider a group of wearable BAN deployed in different agents (including benefits through inter-body or off-body interactions). Here, we propose cooperative strategies to improve the availability and accuracy of group navigation applications. For that, we identified two sub-scenarios:

- ***Relative Body-to-Body Ranging in a Group*** where a group of mobile users wearing a WBAN perform inter-body localization to estimate the distances between each mate of the group. Accordingly, no external anchor nodes would be required in this embodiment.

- ***Absolute Body Positioning in a Group*** where a group of fixed and known devices placed in the infrastructure communicate with the group of WBAN to provide the absolute positions within a GCS composed by the off-body anchor nodes.

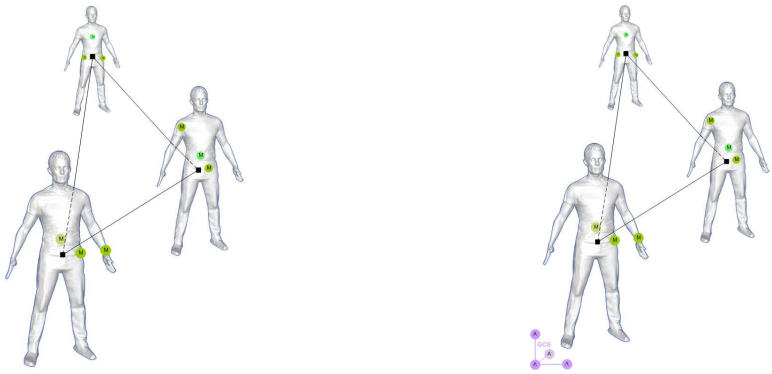

Figure 1-2: Examples of relative body-to-body ranging (a) and absolute body positioning (b) configurations for coordinated group navigation applications.

1.1.3 TECHNICAL REQUIREMENTS

Table 1-1 summarizes the main requirements for both LSIMC and CGN, as defined in D1.1 at the beginning of the CORMORAN project. Note that we will focus hereafter mostly on the LSIMC scenario, in compliance with the description of subtask 3.1. The results related to CGN scenario, which is mostly addressed by subtask 3.3, will be reported in D3.6.

	Large-Scale Individual Motion Capture		**Coordinated Group Navigation**
	Low Precision	High Precision	
On-Body Nodes Location Precision (Relative)	$\varepsilon_{90} < 25$ cm (worst case CDF @ 90%) $\varepsilon_{50} \approx 5$ cm (median CDF @ 50%)	$\varepsilon_{90} < 5$ cm (worst case CDF @ 90%) $\varepsilon_{50} \approx 1$ cm (median CDF @ 50%)	N/A
Average Body Location Precision (Absolute)	$\varepsilon_{90} < 1$ m (worst case CDF @ 90%) $\varepsilon_{50} \approx 0.3$ m (median CDF @ 50%)		
Nodes Location Refreshment Rate	100 ms	10 ms	1s
Maximum Speed	{5, 15} km h^{-1}		
Anchors Density	< 0.05 anchors / m^2		< 0.01 anchors / m^2
Nb Persons per Group	N/A		{5, 10}
Maximum Inter-Body Distances	N/A		{1, 5, 10, 50}
Nb of On-Body Nodes	{5, 10, 20}		{2, 5}
Rank of Preferred On-Body Nodes Location	**An-He-Wr-To-Hi-Lg-Ba-Sh-Kn-Bd**		**Sh-To-Ba-Hi-Wr**
Environment	{Outdoor, Indoor}		Indoor
Place for Final Location Info	{Server, User}		User
Pre Calibration (Deployment Convention to be Respected)	{None, Precise Deployment Pattern}		{None, Rough Deployment Pattern}

Table 1-1 : Summary of application needs in both large-scale individual motion capture (Within low precision and very high precision modes) and group navigation applications[1].

1.2. RADIOLOCATION-BASED MOTION CAPTURE WITH WIRELESS BODY AREA NETWORKS

In the initial document (Deliverable D3.1), we accounted for preliminary investigations on cooperative communications for localization purposes. We also presented an overview of the technical requirements and needs through a qualitative analysis to evaluate existing cooperative protocols considering different aspects, i.e. fairness, adaptability, reliability,

[1] An : Ankles ; He : Head ; Wr : Wrist ; To: Torso; Hi: Hips; Lg: Legs; Ba: Back; Sh: Shoulders; Kn: Knees; Bd: Bends

mobility and power saving. From this analysis, we highlighted that the cooperation strategy for localization purposes should be based on cross-layer design. PHY layer provides to the MAC layer the channel measurements to help on the cooperative decision. NWK layer will help to find cooperative path in order to mitigate interferences between inter/intra BAN flows and the application layer will seek to aggregate and compress on the fly the information detected by the sensors to reduce traffic. But before using cooperative cross-layer mechanisms, we need to understand the ranging and positioning challenges to consider when using radiolocation. Thus, we note that one big challenge for cross-layer mechanisms to enable LSIMC or CGN is to reduce the error on positioning estimation related to channel variations, clock synchronisation, interferences and nodes mobility.

As explained in the Derivable D1.1, positioning systems can be divided into three main categories [17] [18] [19]: 1) *Signal Strength (SS)* approach where nodes measure the energy of the received signal from the other node in order to calculate their distance; 2) *Direction of Arrival (AoA)* where the target node use an antenna arrays to measure the angle of the straight line with the reference nodes; and 3) *Time of Arrival (ToA)* based systems where the distance is estimated from the measure of the time taken by the radio signal to fly from one node to another. In BAN, the *AoA* solution is difficult to implement because of the cost and complexity of the antenna arrays. Moreover, in an indoor environment the receiver will have problems to estimate an accurate angle because of the high probability of multipath interference. In the case of *SS* techniques, the distance estimation becomes challenging due to the absence of Lin of Sight (NLOS) to transmit around the body, the antenna orientation and the possibility of multipath in indoor leading to high variations on the received signal strength (RSSI). In [17] [20] authors show that the best achievable limit (i.e. Cramér-Rao lower bound (CRLB)) depends on the channel parameters and the distance between the two nodes, i.e. the variance of the range estimation is proportional to the distance and shadowing effect. This is a major problem considering that it is already difficult to extract the shadowing and fast fading components of the received signal [21] to analyse only the path loss component. When we look at the properties of the channel models for BAN in literature [22], we observe that the path loss model presents a normal distributed variable (for frequencies of 2.4-2.5 GHz and 3.1-10.6 GHz). Therefore, it makes impossible the association between a path loss model based on RSSI with the real distance for localization purposes. Finally, the *time based* approach also aims to calculate the distance from the estimation of the travel times of signals between two nodes. In this case, the accuracy of the distance estimated is inversely proportional to the occupied bandwidth [17] [23] [24], i.e. the accuracy can be improved by increasing the SNR or the effective signal bandwidth. For this reason, IR-UWB signal is considered as a potential candidate due to the high time resolution and the large bandwidth to reduce the multipath fading effects. Thus, IR-UWB allows a centimeter accuracy (in theory a bandwidth on the order of 500MHz would achieve a ranging precision of 10 cm at -5dB), along with low-power and low-cost implementation for localisation with WBAN. However, there are theoretical limits for ToA-based location estimation [17], e.g. when a mobile node is very close to some reference nodes which can measure only signal strength. In such case, the use of hybrid TOA/SS scheme can be useful for obtaining an accurate location estimation.

1.2.1 IR-UWB LOCALIZATION BASICS

As explained before, Impulse Radio Ultra Wideband (IR-UWB) systems [25] are a good solution thanks to the high time resolution using the Time of Arrival which can be accurately estimated for precise range measurements between two nodes. Accordingly, motion capture can be possible with the Three Way Ranging protocol (3-WR) which estimates the distance between two nodes with the transmission of three packets by evaluating the time of flight (ToF) of packets.

For sake, we consider a mesh of IR-UWB WBAN under full connectivity containing N_T nodes of two kinds as in [25] , on-body mobile nodes that do not know their own position ($i = 1 \ldots N_m$) and on-body anchor nodes that know their own position ($j = 1 \ldots N_A$), $N_T = N_A + N_M$. A set of anchor nodes define a Local Coordinate System (LCS) to localize nodes under mobility. We define the instantaneous distance of the node i with the anchor j as (d_{ij}) and the estimated distance as ($\hat{d}_{ij}$) which is calculated through ToA estimation.

The distance ($\hat{d}_{ij}(t)$) between two nodes is deduced with the 3-WR protocol by combining the typical timers obtained from 3 transmissions [26], as shown in **Figure 1-3**. First, the mobile node i sends a request packet Q_{ij} to an anchor j. Then the anchor answers with a response packet $R1_{ji}$, to complete a round trip to estimate the distance with the ToF (Two-Way Ranging 2-WR). Finally, the anchor sends a second response packet $R2_{ji}$ to complete the 3-WR and compensate the clock drift between the nodes clocks. During these transactions, the on-body nodes collect the different timers of the 3-WR packets transmission and reception. Thus, the distance ($\hat{d}$) is evaluated as follows:

$$\hat{d}_{ij}(t) = \frac{1}{2} c \left[\left((T_4 - T_1) - (T_3 - T_2) \right) - \left((T_6 - T_4) - (T_5 - T_3) \right) \right] \qquad \textbf{(1-1)}$$

Time of Flight — Clock Drift

where c is the light speed. We define $\Delta t1 = T_3 - T_2$ (resp. $\Delta t2 = T_5 - T_3$) as the delay between the reception of a request packet and the transmission of a response 1 packet (resp. the delay between the transmission of the response packets).

$$\hat{d}_{ij}(t) = \frac{1}{2} c \left[\left((T_4 - T_1) - \Delta t1 \right) - \left((T_6 - T_4) - \Delta t2 \right) \right] \qquad \textbf{(1-2)}$$

From this transaction, the goal is that each on-body mobile node *i* calculates its position after estimating its distance with the anchors. Accordingly, the instantaneous position for a node is defined as (P_i) and the estimated position is defined as a function of estimated distances $(\hat{P}_i) = f((\hat{d}_{i1}), (\hat{d}_{i2}), \ldots, (\hat{d}_{iN_A}))$. This function differs depending on the position algorithm, e.g. conventional algorithms (Linear Least Square Error (LLSE), Time Difference of Arrival (TDOA) [24]) and cooperative techniques (Maximum Likelihood (ML), Cooperative Constrained (CDWMDS) [27]).

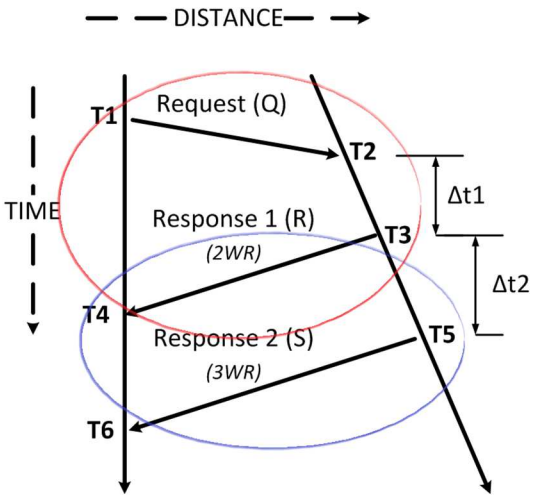

Figure 1-3: IR-UWB 2WR and 3-WR protocol

1.2.2 SPECIFIC TECHNICAL ASPECTS TO CONSIDER WITH IR-UWB FOR MOTION CAPTURE

From this modeling, we can notice that there are several parameters that may affect the 2-WR and 3-WR based ranging estimators [28]. Such parameters can be the clock synchronization between the nodes, the channel variations, the mobility of nodes, the variation of Δt1 and Δt2, the number of nodes/anchors and the scheduling of the 3-WR (2-WR) packets.

The clock synchronization between the nodes is critical to achieve a high accuracy of the ToA estimation [29] and maintaining clock usually increases the complexity of the node hardware. In literature, we can find several works leading with clock synchronization, e.g. [29] [30] [31]. In [29], authors proposed to study the performance of the loop filter to reduce the effect of the clock jitter. In [30] [31], the time-hopping code is used for the synchronization by comparing the estimated distances between the received pulses and those predicted with the knowledge of the TH sequence. Moreover, in the case of de-/miss-synchronization between two nodes, a round-trip time can be estimated to estimate the clock drift [26] (e.g. 3-WR). But this can be a problem for positioning if there is no synchronization between the mobile node and the anchor nodes. In this case, it is suitable to synchronize the reference nodes to employ the time-difference-of-arrival (TDOA) technique [17] [24].

Another problem is the channel variations impact on the pulses detection (Deliverables D2.2, D2.3, D2.4, D2.5) leading into ranging errors and packet loss. In literature, we can find two ToA ranging detection methods (Peak detection, leading edge detection) within three types of receivers for IR-UWB [32] [33] (coherent, differential and non-coherent). The ranging detection method choice depends on the channel conditions [19], in the peak detection approach the ToA aims to estimate the strongest multipath component; alternatively, the leading edge detection is based on the first multipath component arriving at the receiver. In BAN, most of the ToA measurements are affected by NLoS due to the shadowing of the body and the high

mobility of nodes. Therefore, the direct path is attenuated in most of the cases and in this case the strongest multipath will not arrive first. For this reason, leading edge returns a better ranging estimation. For the receiver choice, we discussed in Deliverable D2.5 about the possibilities of the non-coherent receiver [33] due to the low cost and low complexity of implementation in the BAN context. As the BAN channel presents high packet loss, the low complexity of the non-coherent approach let us create a joint solution with the performance of cooperative strategies at PHY and MAC level [21]. For example, we can imagine comparing the performance of a specific MAC for PHY cooperative algorithms e.g. Amplify and Forward (AF) [34] [35] , Decode and Forward (DF) [10] or Compress and Forward (CF) [13] [36].

However, most of this solutions are based on the WSN scenarios where the nodes are assumed to be quasi-static. The mobility of nodes depends on the kind of human activity and it may have an impact on the capacity of the BAN system to estimate accurate positions for motion capture. Moreover, the physical channel between anchors and mobile nodes depends on the speed of nodes and we can have high packet loss rate under high speeds. Furthermore, the position of a mobile node evolves during the 3-WR packets transmission, so the delay of $\Delta t1$ and $\Delta t2$ needs to be as smaller as possible to achieve accurate positioning estimation. This is a major problem because the introduction of errors in the ranging estimations will cause an error on the position estimation. Indeed, as stated in Section 1.2.1, the position estimation depends on the accuracy of the distances calculated with the anchor nodes. This is possible in the case of WBAN, during the transmission of 3-WR packets the mobile nodes are always moving and the estimated distances with the anchors are not performed at the same time for the position of the node, which can lead into an error estimation on the positioning **Figure 1-3.**

Moreover, if we consider a bigger topology of mobile nodes performing 3-WR transactions, the positioning error may increase because of the high traffic of packets in the network. Therefore, it is necessary to find new cooperative strategies at MAC/NWK layer to mitigate the positioning error within an acceptable latency, e.g. Aggregated & Broadcast [26], scheduling of 3-WR packets and enhanced slot allocation for nodes under mobility.

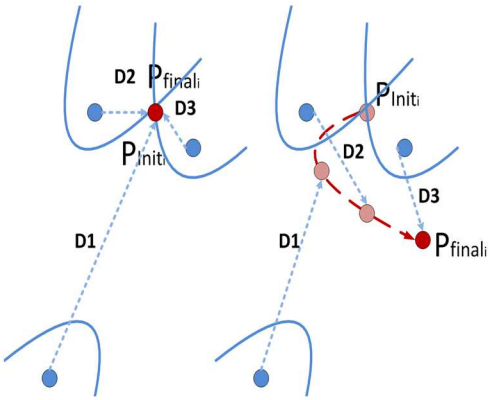

Figure 1-4: Error on ranging estimation with TDOA (static node vs mobile node)

1.2.3 GENERAL DISCUSSION ON CROSS-LAYER DESIGN FOR LOCALIZATION

The design of the PHY/MAC/NWK layer has to be seen as an independent black box offering the service of enhanced communications for the localization applications. The adoption of new cooperative algorithms has to match with the use of the IR-UWB PHY layer defined on the standard IEEE802.15.6. A cross-layer design will lead to strategies for system optimization considering the throughput, the delay, the degree of fairness, the energy consumption and the positioning accuracy. The recent works in localization with WBAN focused on the radio issues and localization algorithms performances without rigorous scope on MAC or NWK strategies.

Previous works focusing on MAC design for localization with UWB systems proposed protocol strategies based on beacon-enabled Time Division Multiple Access and evaluated the performance in terms of accuracy and latency. In [26], they proposed cooperative ranging with Aggregated and Broadcast schemes to reduce the delay of 3-WR transactions. In [37], they focus on better resource management with priority levels for communication. In [38], they focus on the relation between MAC delay and UWB accuracy related to the number of anchors and the communication range of nodes under mobility. However, all these works focus on localization applications for WSN which do not present the same problems of WBAN and they do not consider the impact of the scheduling of localization packets on the positioning estimation nor more accurate routes for enhanced communication between the nodes. In [39], they proposed scheduling schemes for cooperative distributed localization with two different policies (node neighborhood and links quality) to reduce positioning convergence, latency and overhead. However, they consider a 2D Positioning for WSN which again is not realistic for WBAN location-aware applications.

As discussed in Deliverable D3.1, the main functions on MAC design that we have to consider for localization purposes [40] are the medium sharing, topology organization, admission control, packet scheduling, power control and quality of service. Thus, while the MAC layer attempt to decide whether or not cooperation is necessary and select the optimal relaying entities among the network, the NWK layer defines the routing protocols to deliver the 3-WR packets between the mobile node and the anchors with cooperative strategies. In this case, the NWK has several challenges to be addressed, i.e. specific link definition, cost of route establishment and maintenance, multi-flow throughput and multi path interference, optimization of path delays. Thus, the application layer will seek to aggregate and compress on the fly the information detected by the sensors to reduce traffic and perform enhanced/distributed positioning algorithms. The NWK and positioning issues will be more detailed in Deliverables D3.5 and D3.6.

In this Deliverable, we aim to propose cross-layer PHY/MAC strategies by quantifying their behavior and compare their performance on positioning estimation under realistic WBAN scenarios. In this task, a single WBAN is considered for most of the studies in this Deliverable. Thus, this work is divided and organized in three Chapters as follows.

Chapter 2 consists on the study of the ranging estimation with a complete protocol stack by crossing physical up to the application layer dedicated to WBAN radio-location applications.

For this purpose, we use a discrete-event simulator, WSNet, which takes into account the real time constraints for maintaining the peer-to-peer ranging transactions along the network and addresses all the layers. With this framework, we investigate and characterize the impact of nodes mobility and the WBAN channel variations (Deliverable 2.2, 2.3, 2.4) on the distance estimation. We consider both LSIMC and CGN in navigation application with respect to on-, off- or inter-body links. Then, we quantify and compare both impacts in order to propose an adapted cooperative cross-layer mechanism for localization.

Chapter 3 is share with D3.5 (for positioning investigation) and aims at providing design specifications concerning Application, NWK, MAC and PHY layers in a cross-layer perspective. From the results on Chapter 2, we address the problems of positioning error due to the latency and WBAN mobility MAC scheduling strategies of 3-WR packets and adapted resource allocation. For this, we provide a comparison of different scheduling strategies dealing with the mobility and the latency of ranging packets between the nodes and the anchors that triggers positioning error. Moreover, we consider a mobility model based from two realistic LSIMC scenarios.

In Chapter 4, we quantify the impact of the WBAN channel on the positioning success rate of on-body mobile nodes. Then, we propose a cooperative mechanism at MAC layer to overcome the packet loss by choosing virtual on-body anchors. We thus adopted a bottom-up approach for our protocol evaluation with two different channel models i) an on-body empirical model as defined by the CM3 IR-UWB channel (D2.3-D2.4) and ii) a channel model calculated with a ray-tracing simulation (D2.5). In this study, the very challenging issue is to propose an algorithm allowing several nodes to find the best virtual anchor without degrading the positioning accuracy under an acceptable latency.

Finally, Chapter 5 concludes the deliverable and comments on the current CORMORAN outcomes to consider for further investigation on LSIMC and CGN applications.

2. IMPACT OF CONVENTIONAL MAC CONSTRAINTS ON WBAN-BASED IR-UWB RANGING UNDER REALISTIC MOBILITY

2.1. INTRODUCTION

In this chapter we focus on the study of the mobility and channel characterization for the ranging estimation. In the literature, the considered challenges on Individual Motion Capture using IR-UWB are mainly the clock synchronization, the NLOS case (Non Line of Sight), the interference and multipath [28]. When considering mobility, some nodes located in the body moves always and the positions of the nodes changes at each frame transmission, thus introducing error in the estimation [25] [41]. In [42], the authors have considered the mobility issue, for the localization of a pedestrian in a room. They present the issues of ranging error, position update latency and calculation algorithms under mobility. But, no rigorous analysis was provided. Besides, the considered speed is much lower than the one in a BAN. They show the impact of MAC allocation resources on the capacity of the tracking system for Wireless Sensor Networks (WSN) scenarios. Therefore, it is necessary to understand the drawbacks between the mobility and channel constraints before the design of any protocol at the upper layer.

In terms of protocols, the PHY layer considered for the LSMIC scenario is the UWB proposed in the IEEE 802.15.6 group. We will consider the cases when we are in the ideal case for the localization (i.e. study of the mobility impact on localization with Line of Sight) and the case with realistic channel models with enhanced localization algorithms. For the MAC layer, we will study the protocol defined by the standard but depending on the final application, we will propose to adapt some MAC features, especially to comply with constraints for cooperative transmissions and localization applications. Then, considering the co-simulator between WSNET and Pylayers presented in the Deliverable D2.5, we will be able to implement the protocols and algorithms in order to study the behavior and performances under realistic scenarios, as the one performed during the measurement campaign at ENS Cachan Bretagne, Deliverable D4.1.

2.2. IMPACT OF MOBILITY ON RANGING ERROR

As explained on the introduction, the objective of the Task 3.1 of the CORMORAN project is to propose new cooperative algorithms in order to collect information to achieve enhanced communications and location, to enable Individual Motion Capture applications. In the last case, the posture of On-Body nodes is expected to be estimated with an Impulse Radio-Ultra Wide-band (IR-UWB) system [24]. The high temporal resolution of the pulses makes possible to calculate the distance between two nodes by estimating the Time of Flight (ToF) of three packets as defined by the Three Way Ranging Protocol (3-WR) [26]. However, this technique was proposed in the case of WSN, where the node has a regular motion and the coordination between anchors and mobiles nodes is easy to achieve and maintain. In the case of WBAN, nodes are affected by different variations in the speed of the human body. Therefore, the distances estimated vary during the 3-WR transactions, inducing positioning errors.

Moreover, the delays of packets can also be affected by the number of nodes/anchors; the order of the slot allocation for the nodes; but also by the strategies used to schedule the 3-WR packets. This means that the system needs a MAC protocol as flexible as possible to consider all these parameters and adapt the system to different human activities. Thus, the study of these parameters is important for a cross layer protocol design and it will be more discussed on the Chapter 3.

For this purpose, we focus on the study of the impact of mobility on ranging estimation considering the LSIMC scenario along with the consideration for the MAC design. First, we defined a system model considering the LSIMC scenario for the study on the impact of mobility for positioning estimation. Then we propose to extend the study with a theoretical model of this issue by considering the speed of nodes and the delays of packets.

2.2.1 LOCALIZATION ERROR RELATED TO THE DELAYS OF RANGING PACKETS

When considering mobility for localization applications in WBAN, we explained in Chapter 1.2.2 that the distance between a pair of node and anchor changes at each transmission of the 3-WR packets, thus introducing error in the ranging estimation [25]. There are few works considering this issue, in [42] the authors have considered the mobility issue, for the localization of a pedestrian in a room. But, no rigorous analysis was provided. Besides, the considered speed is much lower than the one in a BAN. For this reason, we propose a preliminary study for Individual Motion Capture to quantify the impact of mobility on the ranging estimation [43]. First, we analyze the distance estimation between 2 nodes, a mobile sensor and an anchor attached to a human body. The anchor has a known position with respect to a global 3D coordinate system while the sensor does not have any knowledge of its own position. We assume that the sensor follows a back-and-forth linear motion.

2.2.2 SIMULATION AND PERFORMANCE EVALUATION

We defined a physical (PHY) Layer based on the IEEE802.15.6 PHY UWB [44] in default mode (OOK modulation, data rate 0.4875 Mbps) and we consider a Line of Sight (LOS) channel without packet loss. Therefore, we assume that our radio is capable to detect the first path of IR-UWB to detect the precise TOA at the receiver. At the Medium Access Control (MAC) Layer, we define a protocol based on the TDMA protocol and we assume that it is beacon enabled. Then, we reserve three transmission periods corresponding to the 3-WR (2-WR) protocol (Section 1.2.1) and we considered two types of parameters: (i) the speed of nodes; (ii) the values of $\Delta t1$ and $\Delta t2$. Then, we quantify the impact of mobility by using the Root Mean Square Error (RMSE).

$$RMSE = \sqrt{\frac{\sum_1^N |d_{ref} - d_{est}|^2}{N}} \quad \textbf{(2-1)}$$

The RMSE compare the estimated distance d_{est} with three reference distances d_{ref} as follows: d_{ref1} is the distance at the beginning of the first request, d_{ref2} is the distance at the reception of the last response, and d_{avg} is the average of d_{ref1} and d_{ref2}.

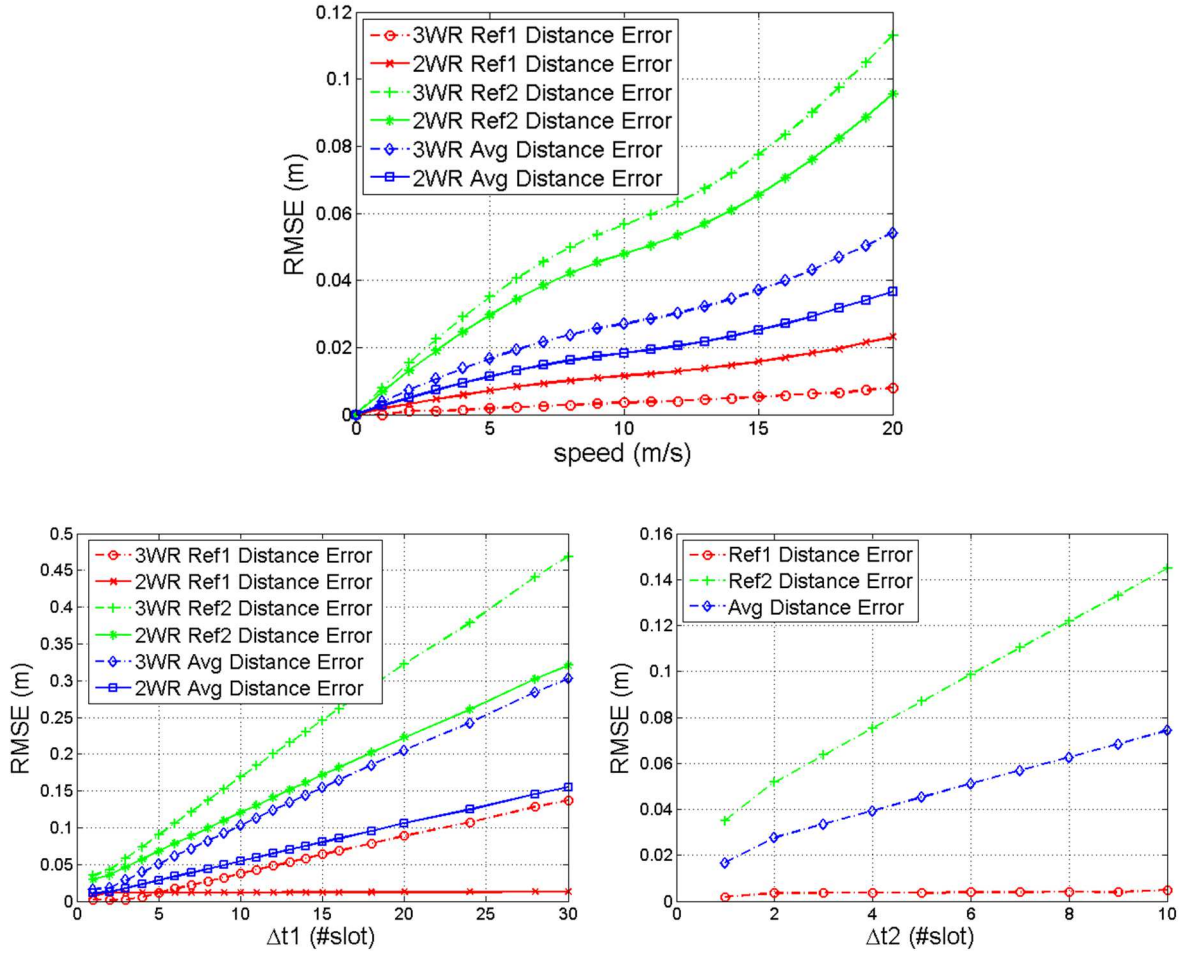

Figure 2-1: (a) RMSE of estimated distance between 2-WR/3-WR as function of speed. (b) RMSE of estimated distance between 2-WR/3-WR as function of $\Delta t1$. (c) RMSE of estimated distance with 3-WR as function of $\Delta t2$.

Figure 1-1 shows that RMSE increases with the speed and the response time Δt1 and Δt2. This means that increasing one of these parameters leads to a higher distance between the nodes due to the node mobility, and hence an error in the ranging estimation is introduced. The results show that depending on the speed and the chosen reference point, the 2WR can be better than 3-WR if only mobility is taken into account. This would mean that the channel would be less used since sends a packet less. Moreover, the results show that $\Delta t1$ has more

impact on the ranging estimation than the speed since the RMSE can reach an important ranging error (>50cm) while with 20m/s (i.e. human fist speed) of speed RMSE do not exceed 12cm of error. This leads us to investigate more in the optimization of the scheduling problem (3-WR) in order to reduce the response time $\Delta t1$.

2.3. THEORETICAL MODEL OF THE MOBILITY IMPACT

In section 2.2, we conclude that the ranging accuracy depends on the speed of nodes and the duration of $\Delta t1$ and $\Delta t2$. In particular, the delay $\Delta t1$ to send the first response $R1_{ji}$ has more impact than the time taken $\Delta t2$ for the second response $R2_{ji}$. Therefore, the nodes present a bigger displacement when these delays increase. In this study, we aim to analyze the impact of speed on the ranging estimation. For this, we propose a theoretical model that takes into account this impact [45]. Then, we show the relation of speed of nodes with the estimated distances by evaluating our theoretical model with the simulated ranging estimation. Moreover, we give some important key points to consider when designing MAC protocols to perform localization applications. Our results show a high correlation between the type of performed movement (and therefore, the speed of nodes) and the error in the ranging estimation.

2.3.1 MODELLING THE MOBILITY IMPACT

In this work, we consider a WBAN embedded on a person in full-mesh where all nodes N_T can directly communicate in pairs with the same topology described in Section 1.2.1. Accordingly, we model the 3-WR communication between the mobile node i and the anchor node j as follows (**Figure 2-2**):

- At time t_0, the mobile node i sends a request packet Q_{ij} to the anchor.
- At time t_1, the anchor answers with a response packet $R1_{ji}$. Thus, the node is able to estimate the ToF of the pulses and therefore, a first ranging estimation (2-WR).
- Finally, at t_2, the anchor sends a second response packet $R2_{ji}$ to complete the 3-WR.

From these transactions, we define the times T_1, T_3 and T_5 as the moments where the nodes sends the Q_{ij}, $R1_{ji}$ and $R1_{ji}$ packets respectively. Similarly, we note T_2, T_4 and T_6 as the ToA of these same packets respectively. Thus, the distance ($\hat{d}$) is evaluated with Eq. **(1-1)** as presented in Section 1.2.1. In order to quantify the impact of node speed on the ranging estimation, we consider a three-Dimensional Euclidean space (O_g, x_g, y_g, y_g). We define $\vec{P}(t) = \overrightarrow{O_gP}$ as the position vector between the origin point and the node's position at time t. Moreover, we note $\vec{d}_{ij} = \vec{P_j}(t) - \vec{P_i}(t)$ as the distance vector between node i and anchor j during a 3-WR packet transmission.

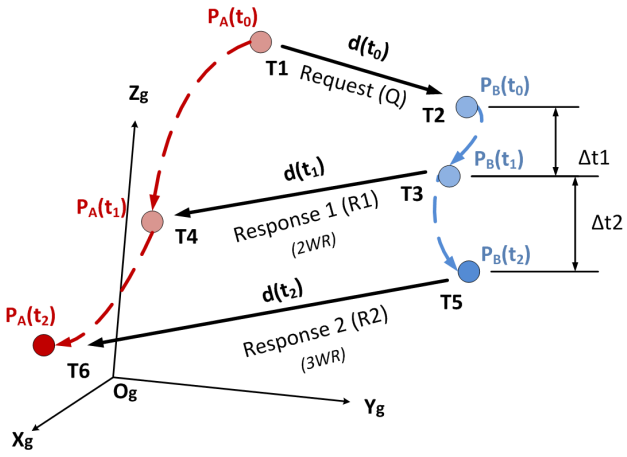

Figure 2-2: 3-Way ranging protocol applied with mobile nodes

As the 3-WR packets are send at different moments (Figure 2-2), while the nodes are moving, the initial distance is affected by different displacements ($t_0 \rightarrow t_1$ and $t_1 \rightarrow t_2$), leading to 3 distances for the same ranging estimation. As result, Eq. **(1-1)** can be written as:

$$\hat{d}_{ij}(t) = \frac{1}{2}\left[\, \|\vec{d}_{ij}(t_0)\| + 2\,\|\vec{d}_{ij}(t_1)\| - \|\vec{d}_{ij}(t_2)\| \,\right] \qquad \textbf{(2-2)}$$

where $\|\vec{d}_{ij}(t)\|$ represents the distance vector norm terms of c (speed propagation pulse). In our model, we aim to express $\hat{d}_{ij}(t)$ as a function of the nodes speed $\vec{V}_i(t)$ and the initial distance $\vec{d}_{ij}(t_0)$. Accordingly, we obtain the following system of equations with 3 variables:

$$\begin{cases} \vec{d}_{ij}(t_0) = \vec{P}_j(t_0) - \vec{P}_i(t_0) \\ \vec{d}_{ij}(t_1) = \vec{d}_{ij}(t_0) - \vec{V}_i(t_1)(T_4 - T_1) + \vec{V}_j(t_1)\,\Delta t1 \\ \vec{d}_{ij}(t_2) = \vec{d}_{ij}(t_1) - \vec{V}_i(t_2)(T_6 - T_4) + \vec{V}_j(t_2)\,\Delta t2 \end{cases} \qquad \textbf{(2-3)}$$

In practice, we can find a first approximation if we neglect the speed of a node (<10m/s) compared to the pulse speed propagation (c) during a packet transmission. Thus the system of equations yields to:

$$\begin{cases} \vec{d}_{ij}(t_0) = \vec{P}_j(t_0) - \vec{P}_i(t_0) \\ \vec{d}_{ij}(t_1) = \vec{d}_{ij}(t_0) - (\,\vec{V}_i(t_1) - \vec{V}_j(t_1)\,)\,\Delta t1 \\ \vec{d}_{ij}(t_2) = \vec{d}_{ij}(t_1) - (\,\vec{V}_i(t_2) - \vec{V}_j(t_2)\,)\,\Delta t2 \end{cases} \qquad \textbf{(2-4)}$$

2.3.2 CONVENTIONAL MAC WITH SCHEDULING STRATEGIES

For positioning estimation within a three-dimensional space, the node estimates its distance through 3-WR with (at least) 4 anchors, and then calculates its position with a positioning algorithm (e.g. TDOA). However, in function of the number of nodes to locate, the scheduling of 3-WR packets becomes a problem due to the possible delays for ranging estimation. This issue will be more investigated on Chapter 3. For instance, we implement two scheduling MAC strategies [46] order to validate our theoretical analysis where the frame holds enough slots for an individual location of all nodes. Moreover, $\Delta t1$ and $\Delta t2$ are fixed by the scheduling strategies at the MAC layer:

- **Single node localization (P2P-B)** where each node i intend to send the requests Q_i to the anchors in broadcast. Then, each anchor answers with $R1_{ji}$ and $R2_{ji}$ successively in single-links to the nodes.
- **Aggregated and Broadcast (A&B)** [26] where nodes send the requests Q_i in broadcast. Thereafter, each anchor j gathers the ToA of each request and sends an aggregated response ($R1_j$) to all nodes, followed by the second response ($R2_j$). Thus, A&B increases the $\Delta t1$ delay even though it reduces the frame size.

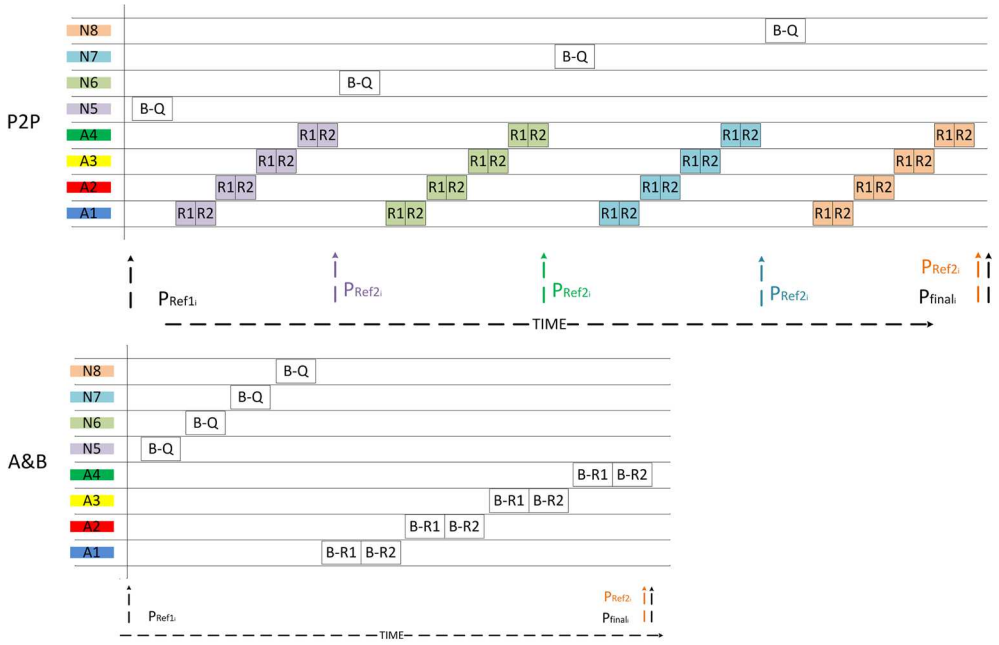

Figure 2-3: P2P-B and A&B scheduling mechanisms

2.3.3 MOBILITY MODEL

We consider a realistic Yoga Model, obtained by measurement during the CORMORAN project at the M2S laboratory, ENS Cachan, France in June 2014 [47]. This model was generated using an optical motion capture system (Vicon [48]) based on infrared at a rate of 100 Hz. For this, we deployed 16 cameras in a confined space of 10x6 m² and we considered a scenario timing of 100s to perform a Yoga activity. The interest in this scenario is the study of the presence or absence of movement which separates the impact of the speed and the other error factors on the accuracy. The series of the static positions (realizing yoga postures (e.g. put both feet together and hands above the head)) is performed in the same place, so only the articulations of the body perform a movement. Here, we consider a network composed of 4 anchors and 4 mobile nodes, as shown in **Figure 2-4**. The anchors are positioned on the most static parts of the body: the right chest (A_1), the left chest (A_2), the left hip (A_3) and the back (A_4). The mobile nodes are located on the right arm (N_5) the left arm (N_6), the right foot (N_7) and the head (N_8). Thus, we were able to calculate the position and the instantaneous velocity of each node.

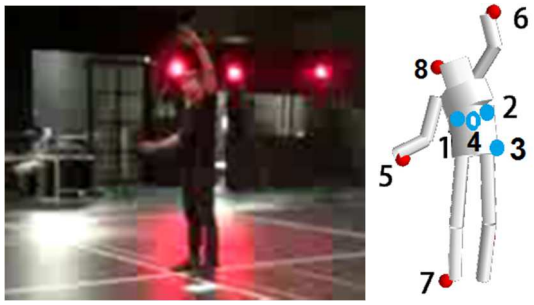

Figure 2-4: a) Camera snapshot during the measurement of the Yoga activity. b) Multi-cylinder Body reconstruction - the red (resp. blue) points refer to the mobile nodes (resp. anchors).

2.3.4 SIMULATION AND PERFORMANCE EVALUATION

In this work, we adopt a discrete event simulation with WSNet [49], suitable for the test of our theoretical model on the experiment movement traces. In particular, we implemented an UWB PHY layer as defined by the standard IEEE802.15.6 in default mode (OOK modulation and 0.4875 Mb/s), as detailed in the Deliverable D2.5. At the MAC layer, we implemented the protocols based on TDMA, the P2P-B and A&B algorithms, as detailed in Section 2.3.2. Finally, we created a mobility model, which exploits the traces of the Yoga scenario (Section Mobility Model2.3.3) during the 100 ms of acquisition. Within this framework, we evaluate the ranging error over time between the real distance and the distance estimated in function of the packet delays and the speed of nodes.

A. Relation between nodes speed and ranging estimation

For a preliminary analysis, we evaluate by simulation the error on the estimated distances and quantify the impact on the design of the MAC layer. For this purpose, we simulated the P2P-B and A&B strategies to perform the 3-WR ranging estimation for the Yoga scenario. For our network composed of 4 anchors and 4 nodes, the TDMA frame duration depends on the strategy, for P2P-B $T_{P2P} \approx 54\ ms$ and for A&B $T_{A\&B} \approx 18\ ms$.

For instance, if we analyze the calculated speed of nodes (**Figure 2-5**), we observe that the anchors are quasi-static (not presented) compared to the mobile nodes (<3 m/s) which move according to the performed Yoga positions (**Figure 2-7**). Accordingly, the range estimation will be affected mostly by the movement of mobile nodes.

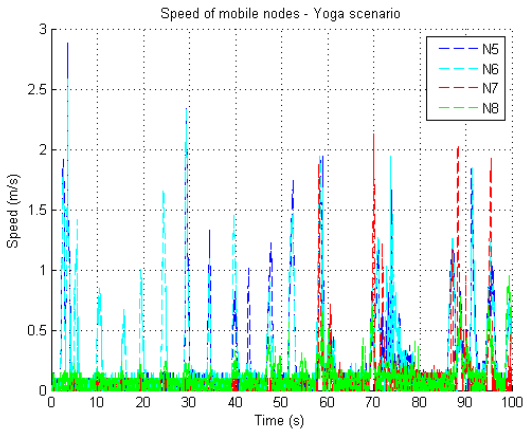

Figure 2-5: Speed of mobile nodes

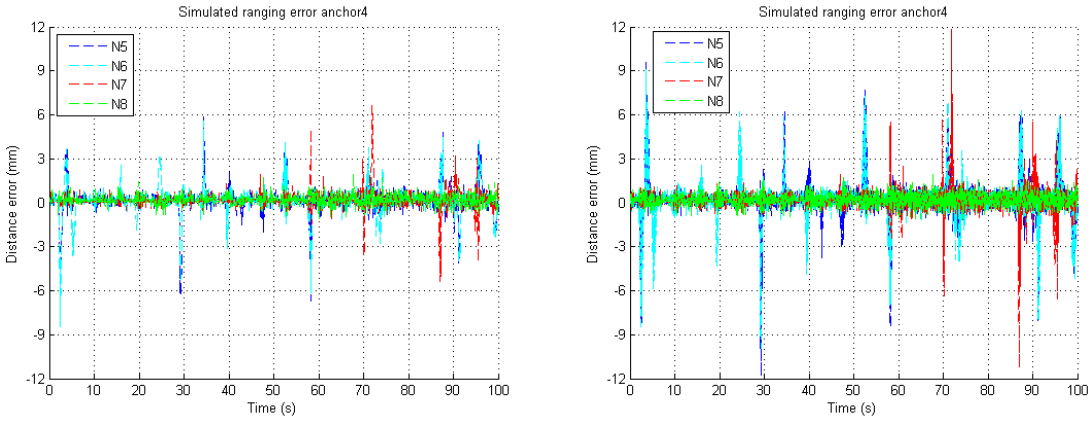

Figure 2-6: Comparison of the simulated ranging error with a) P2P-B and b) A&B between the mobile nodes and A_4

We give in **Figure 2-6 (a)** and **(b)** the ranging error obtained by simulation with P2P-B and A&B respectively, when the mobiles nodes try to estimate their distance with the A_4. The general trend of the curves shows that the ranging error (for both strategies) follows the evolution of the node speed (Figure 2-5). Thus, we can observe three main periods of activity (**Figure 2-7**): Sb1 (0-50 s), Sb2 (50-70 s) and Sb3 (70-100 s).

- In Sb1, the subject realized the half moon and mountain poses by raising and dropping both hands several times above his head. Therefore, nodes on the hands (N_5 and N_6) show the most of variation errors, whereas the nodes on the foot (N_7) and the head (N_8) are quasi-static.
- In Sb2, the subject realized the warrior and tree poses by stretching his legs. This explains the error on the ranging estimation with the leg (N_7). In particular, we observe a quick change from negative to positive error at the end.
- In Sb3, the subject leans forward to touch his feet with his hands (bend forward pose) where the mobile nodes come close to the anchors, yielding errors on all the nodes.

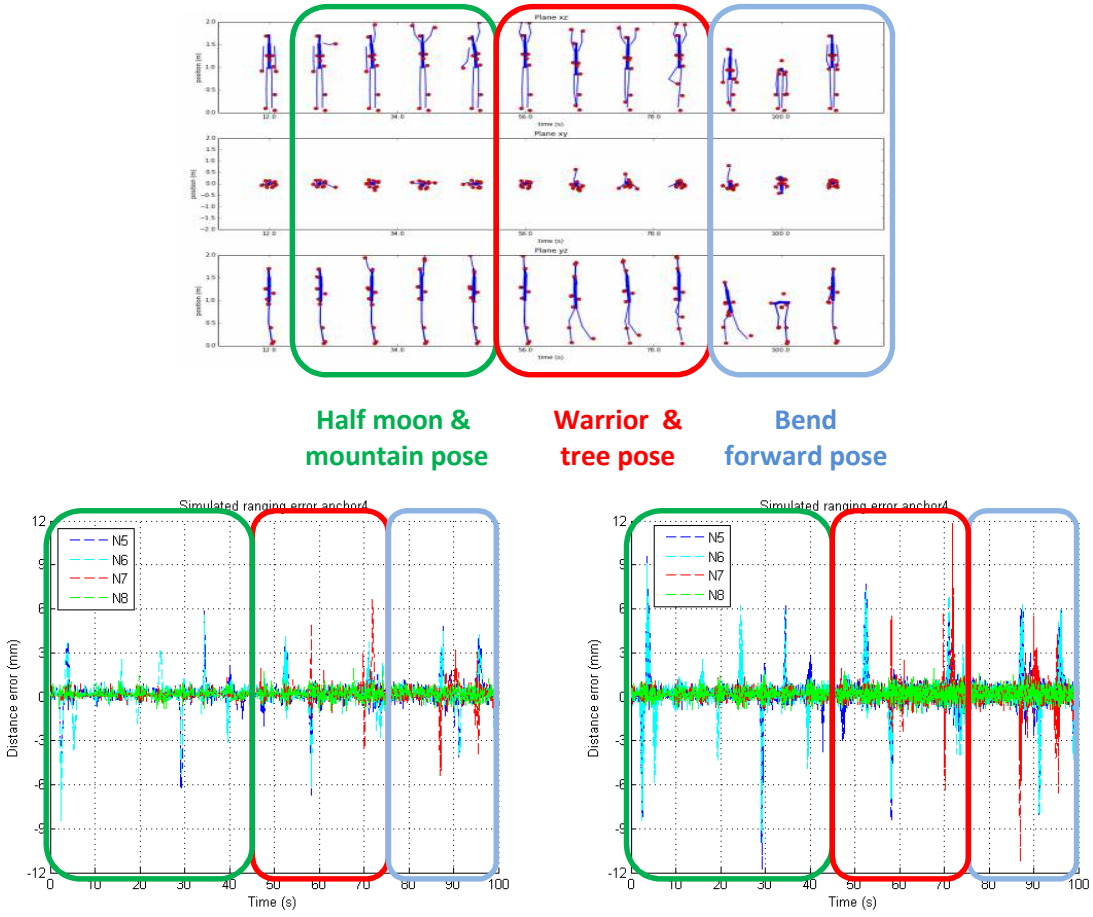

Figure 2-7: Three main periods of activity: Sb1 (0-50) s, Sb1 (50-70) s and Sb1 (70-100) s

B. Validation of our theoretical model

In the following study, we quantify the error between the initial distance $\|\vec{d}_{ij}(t_0)\|$ and the dijt with our theoretical model (**d**ijt= 12 dijt0+ 2 dijt1− dijt2 **(2-2)**. Then, we compare this theoretical error with the error obtained by simulation (**Figure 2-6** and **Figure 2-9**), by fixing Δt1 and Δt2 with the delays related with P2P-B and A&B. First, we observe that the theoretical error (**Figure 2-9**) is correlated with the evolution of the speed (**Figure 2-5**). Moreover, we can observe an association between the variation of the distances estimated with A_4 (**Figure 2-8**) and the theoretical error. In fact, when nodes and anchors move away (resp. get closer), there is an increase (resp. decrease) of the distance estimated by simulation, but also a theoretical negative (resp. positive) error. This kind of information may help to reduce the ranging error. If we compare the ranging error (**Figure 2-9**) between A&B and P2P-B, we observe that A&B has visibly an increased level of error compared to P2P-B. In fact, P2P-B subsample the motion and A&B detects the movements with more detail. These observations are more visible with the simulated errors for both strategies.

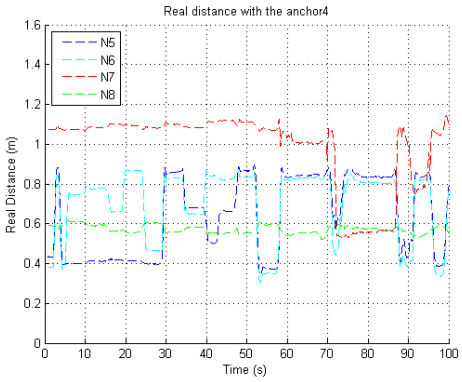

Figure 2-8: Real distance evolution between the nodes and A_4

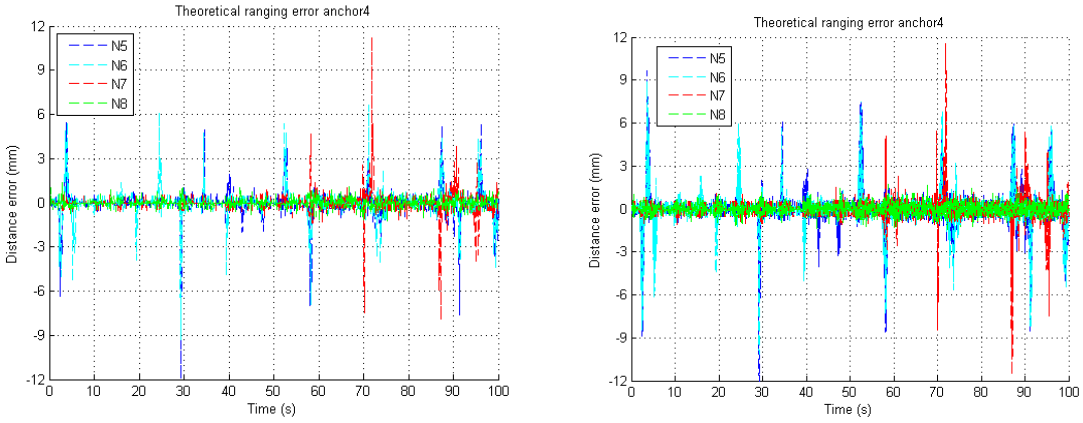

Figure 2-9: Comparison of the theoretical ranging error with a) P2P-B and b) A&B between the mobile nodes and A_4

C. Consequences of the comparison theoretical model – simulations.

At this point of the investigation, the difference between the simulated errors and theoretical errors (for both strategies) is due to the limit of simulation related to the mobility model. **Figure 2-10** shows the theoretical error with the P2P-B delays for anchors (A_1), (A_2) and (A_3). We observe that the variance of the theoretical error evolves progressively for each anchor in function of the delays and the speed of nodes. However, this is not the case by simulation which depends on frame duration and mobility sampling. In fact, when designing MAC protocols through simulation, it is necessary to consider the correct sampling for the mobility model (in our case T_{vicon} = 10 ms). If the duration of one 3-WR transaction is lower than 10 ms, the level of error will not be affected by the speed, since the simulation changes the positions of nodes according to the mobility sampling. Considering this issue with more anchors, we can expect to have the same level of ranging error with the anchors performing their transactions during the same interval.

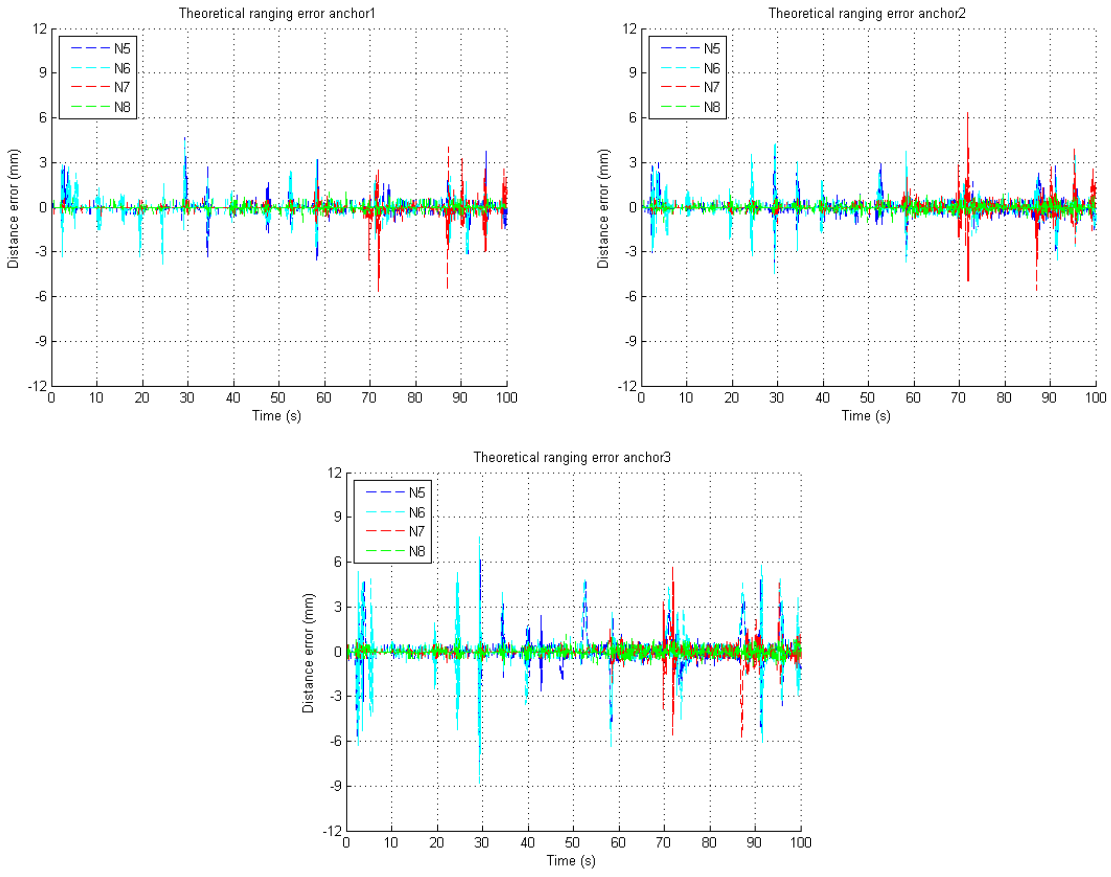

Figure 2-10: Comparison of the theoretical ranging error with P2P-B between the mobile nodes and (a) A_1 , (b) A_2, (c) A_3

D. Impact of the speed of nodes on the positioning estimation.

In order to complete this study, we estimated by simulation (**Figure 2-11**) the error on the positions estimated with A&B and TDOA [24] and we compare this error with the normalized ranging error between the nodes and A_4. We observe that there is a correlation between the positioning error and the theoretical error on the distance estimation. However, the positioning error is higher due to the cumulated errors with the other anchors during the positions calculation with TDOA. Moreover, the results show that the error on the distance estimation ($< 2\ cm$) and positioning ($< 5\ cm$) is small relative to the distance traveled (**Figure 2-8**) (40 – 120 cm), and exhibits a variation correlated with the speed of nodes (**Figure 2-5**).

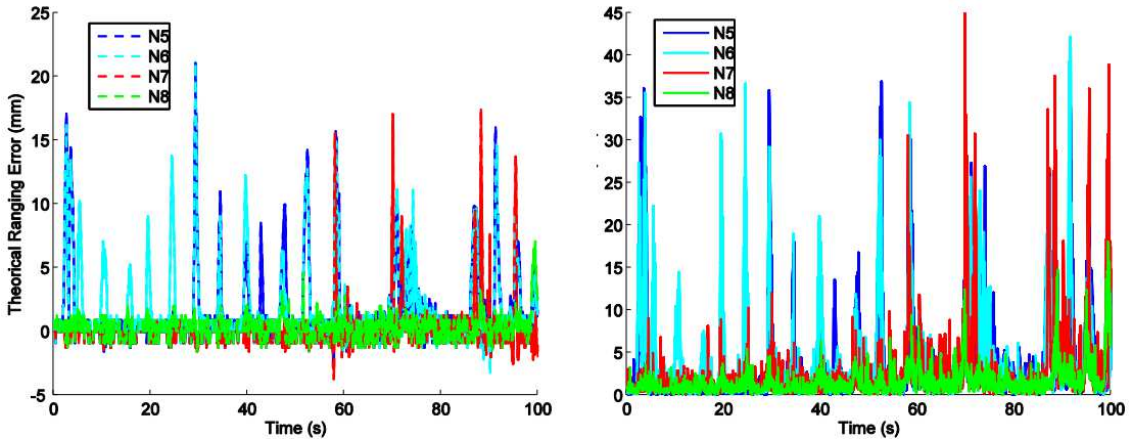

Figure 2-11: Comparison of (a) the normalized ranging error calculated theoretically between nodes and A_4 and (b) the error on positions estimated with A&B by simulation

2.3.5 CONCLUSION

This section presents the impact of speed on the ranging estimation of mobile nodes in a WBAN. We modeled this impact with a theoretical model of the 3-WR protocol in function of the speed and the packets delays. We quantified this effect by using a realistic Yoga scenario and we evaluated the ranging error by simulation with two MAC strategies: P2P-B and A&B. One of the main features of this work is the observation of a correlation between the distance and the theoretical error. In fact, knowing when the error is positive or negative give us the key to predict when the nodes are getting closer or not. This kind of information is important to collect in order to make a control of the distance estimations. We can imaging a joint inertial - radio location system with accelerometers to estimate the speed of nodes, then as the MAC frame is synchronized and beacon enabled, we can obtain the duration of delays Δt1 and Δt2, therefore, we can evaluate the ranging error related with the mobility of nodes to increase the distance estimation. Finally, we show with the theoretical results that the nodes speed (and its associated mobility model) has an impact on the design of MAC strategies and the positioning estimation. In the next Section, we will extend this analysis to other scenarios and with a

physical channel in order to compare the ranging error produced by the mobility and the channel variations.

2.4. CHARACTERIZATION OF RANGING ERRORS OVER VARIOUS LINK KINDS UNDER REALISTIC MOBILITY

In this section, we aim to quantify and compare the ranging error produced by the mobility of nodes and the WBAN channel for localization purposes [50]. From one side, as explained in Sections 2.2 and 2.3, the mobility of nodes affects the ranging estimation during the packets exchange between a node trying to estimate its position and a reference anchor. In WBAN, the protocols proposed in literature do not consider that the estimation of one position is calculated with distances evaluated at different times with nodes moving all the time (**Figure 1-4**). On the other hand, the shadowing of the body and the multipath may compromise the ToA estimation of pulses. However, due to the high difficulty of radio-location experiments (i.e. lack of IEEE 802.15.6 integrated devices), most works of literature [25] [42] [51] [52] are focused on theoretical studies using often unrealistic assumptions and inaccurate abstraction of wireless communications, or focusing on a given layer, ignoring the other network layers. For this reason, we considered a realistic navigation group scenario composed of three WBANs communicating through on-body, body-to-body and off-body links.

2.4.1 NETWORK CONFIGURATION

As shown in **Figure 2-12**, we consider a WBAN in full-mesh connectivity with two types of nodes: the mobile nodes which are placed on the body and they have no knowledge of their own position and the anchors nodes having knowledge of their positions in all the time. We have three kinds of links between these nodes: the on-body links to communicate nodes placed in a single WBAN, the inter-body nodes to connect nodes between different WBANs and the off-body links to exchange packets with fixed nodes in the infrastructure. A set of anchors define a Local Coordinated System (LCS) to locate the mobile nodes within a Global Coordinated System (GCS) related to the infrastructure. In this coordinated system, all the on-body nodes communicate peer-to-peer with the anchors or even between them using IR-UWB, to estimate the ToA with 3-WR (Section 1.2.1.). In order to avoid the interference between communications, a TDMA-based MAC layer is used by all the nodes and we assume that is synchronized and beacon enabled. We refer to non-cooperative localization (resp. cooperative localization) when a node performs the 3-WR with the anchors only (resp. with the anchors and the other on-body nodes).

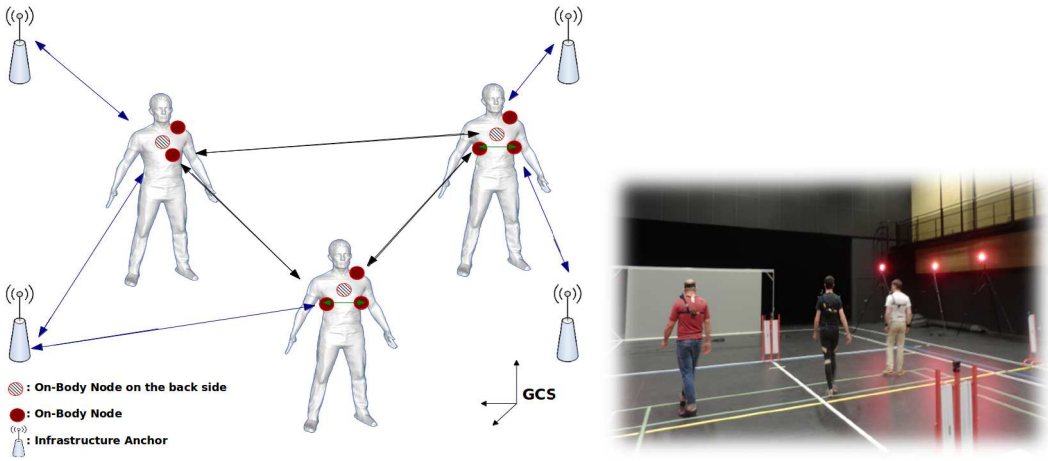

Figure 2-12: Deployment of the group navigation scenario. There are three kinds of links: on-body links (green colour), inter-body links (black colour) and off-body links (blue colour). The on-body nodes (red colour) must be positioned relatively to the fixed anchors.

2.4.2 POSITIONING AND RANGING ASSESSMENT

As explained in Section 2.4.1, the distances are estimated through RT-TOF with 3-WR. Once all the distances are estimated between the on-body nodes with the anchors and/or with the other on-body nodes, the on-body nodes positions can be calculated using a localization algorithm. However, the traffic sent over the wireless medium quickly increases with the number of devices and the MAC protocol employed. Moreover, the distance between the nodes can change between the beginning and the end of the 3-WR, reducing the accuracy of the ranging estimations. Thus, we can expect that the main source of ranging error is related to the involved WBAN channel and the mobility of nodes along with the algorithm to collect the ToF from the 3-WR packets. Quantifying the ranging error due to these three parameters is beneficial for the phase of the resolution of the localization problem.

In this study, we implanted three scheduling strategies with different delays in order to quantify their related ranging error. The first strategy consists in a classical peer-to-peer transaction (P2P) realizing the 3-WR transactions for each couple of devices. Then, we implemented the procedure proposed in [26] called Aggregate-and-Broadcast (A&B), to reduce the volume of control traffic. With this strategy, each node initiates the ranging transactions by broadcasting a request packet to all the other nodes, instead of querying each node separately. The concerned nodes then aggregate its response and broadcast the response packets by order. The last solution is an intermediate peer-to-peer strategy (P2P-Broadcast) where nodes broadcast the requests and then, the responses are transmitted one by one (Section 2.3.2).

2.4.3 MOBILITY MODEL

The mobility model was calculated by ray-tracing simulation with PyLayers [53] using the mobility traces obtained from the CORMORAN measurement campaign (Section 2.3.3). In this campaign, we deployed 16 cameras based on the Vicon [48] optical technology in a restricted area of 10x6 m². In this study, we consider a real scenario with three persons in random navigation with the presence of four fixed anchors (**Figure 2-12**). Two subjects are embedded with four devices each, while the third subject is equipped with three devices (due to the limited number of devices). The devices are placed at the chest left, the chest right, the shoulder and the back. We equipped each wireless device with a Vicon marker in order to record its exact position alongside in addition to the movements of each subject.

2.4.4 SIMULATION AND PERFORMANCE EVALUATION

We use a discrete-event simulator, WSNet [49], which takes into account the real time constraints for maintaining the peer-to-peer ranging transactions along the network and addresses all the layers. We implemented a complete protocol stack by crossing the physical up to the application layer dedicated to WBANs localization applications, particularly, based on IR-UWB physical layer with OOK modulation as defined by IEEE 802.15.6 and TDMA-based access control layer that mimics the scheduled access of a group of WBANs. We implemented a mobility model resulting from real experiments (Section 2.4.3). To perform a ranging estimation, we added the 3-WR protocol with the possibility of using A&B, P2P or P2P-B. We quantify the ranging error with the Root Mean Square Error (RMSE), computed as the absolute difference of measured and real distances. All simulation results are obtained over 20 independent trial runs. Over each run of 100s, the number of ranging updates between each pair of nodes is about 1300 times.

A. Preliminary study: determining elements of mobility

For a preliminary analysis, we evaluate by simulation the impact of the on-body nodes speed with perfect channel. Here, we use a scenario of Individual Motion Capture similar to the one presented in Section 2.4.3. We embedded 11 nodes in a single body as follows: one at the head, two at the torso, one at the back, one by hand, one by foot, one at the knee and one by elbow. **Figure 2-13** illustrates the evolution of the cumulative distribution function (CDF) of the range RMSE. If we compare the RMSE of three different on-body links (**Figure 2-13** (a)), the ranging error is more affected when the nodes mobility is considered faster, confirming the conclusions from Section 2.3. In **Figure 2-13** (b), we observe that the ranging accuracy also depends on the involved transaction protocol. In fact, P2P and P2P-B shows a similar behavior compared to A&B which perform better. These results confirm that by reducing the delays of the 3-WR transactions, we can improve the ranging estimation, e.g. as showed in Section 2.2 and 2.3.

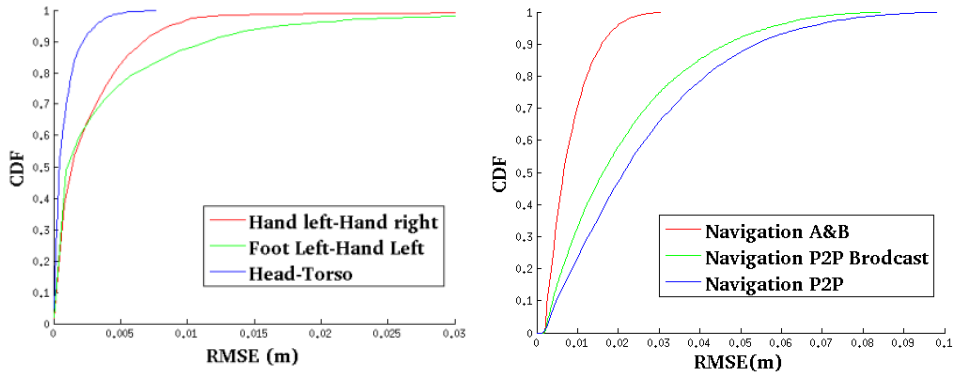

Figure 2-13: CDFs of Root Mean Square Error (RMSE) of ranging errors using the Yoga scenario. (a) The RMSE for different on-body links. (b) The RMSE for different transaction protocols

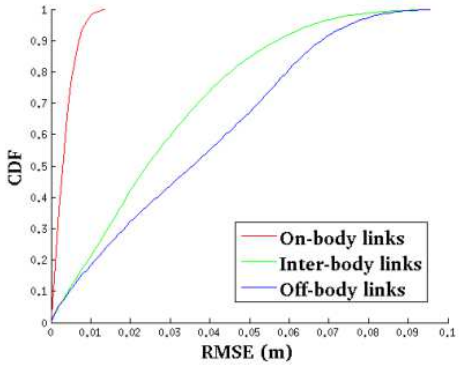

Figure 2-14: CDFs of Root Mean Square Error (RMSE) of ranging errors on the on-, off- and inter-body link using the Group Navigation Scenarios and A&B.

When we analyze the results for the group navigation scenario (**Figure 2-14**) with A&B, we observe that the ranging accuracy varies depending on the type of link. In particular, the on-body ranging error is relatively negligible with respect to the error of inter-body and off-body links. This observation refers to the fact that the nodes mobility is bounded at the body scale, but unbounded at the large scale where the body-to-body and the off-body links are involved. This observation is very important for cooperative context, since it leads to promote and enhance the use of on-body cooperation.

2.4.5 CONCLUSION

This preliminary study let us observe the effect of mobility on ranging estimation considering the different constraints for the MAC design. Accordingly, we focused on the localization application with WBAN communicating in full-mesh using IR-UWB. For this, we considered a realistic scenario with on-body, body-to-body and off-body links where nodes estimate their

distances through 3-WR with a set of anchors composing a reference system. By quantifying the ranging error for the on-body, inter-body and off-body links under a realistic scenario, we observed that the ranging error varies depending on the scheduling MAC protocol, but also the kind of link (on-/body-to-/off- body). This founding is important to consider by the positioning system, especially at the MAC layer and the optimization of the resource utilization (e.g. slot allocation or scheduling of packets). This study [50] will be extended with the Deliverable D3.5 to compare the ranging error produced by the mobility and the channel variations to improve the localization accuracy, e.g. by using cooperative extended Kalman filter.

2.5. DISCUSSION AND PERSPECTIVES

In this Chapter, we characterized the ranging error due to the mobility and the WBAN channel which is necessary for the estimation of nodes position in a WBAN. In Section 2.2, we showed that the classic n-WR protocols (e.g. 2-WR and 3-WR) used for ranging estimation can be affected by the mobility of WBAN nodes. This is because, under mobility, the position of an on-body node may not be the same between the moment it sends a request packet and at the moment it receives the response packets from the anchors. A tradeoff was found between the ranging accuracy and the latency of 3-WR packets that has to be suited to the localization applications with WBAN.

In Section 2.3, we quantified through a theoretical model the ranging error due to the mobility and we showed that depending on the speed of nodes, the error increases. From this study, we infer that the MAC design has to use maximum knowledge on biomechanics intra-BAN model in order to guarantee a minimum and acceptable positioning results. Therefore, we propose to extend the study in Chapter 3 to evaluate the impact on positioning estimation with different scheduling strategies to minimize the ranging and positioning error for the LSIMC scenario.

Finally, in Section 2.4, we investigated and compared the ranging error generated by the mobility of nodes and the channel variations in the on-, off-, inter-body links (with the off-body as the worst case). For the following, we aim to investigate the robustness of the cooperative EKF in delivering high positioning accuracy for group navigation purposes while exploiting cross layer information, i.e., channel and nodes mobility. This study will be extended in Deliverable D3.5.

3. ADVANCED SCHEDULING AND RESOURCES ALLOCATION FOR IMPROVED WBAN-BASED COOPERATIVE RANGING AND POSITIONING

3.1. INTRODUCTION

As presented on the last chapters, the positioning of the on-body nodes consists in collecting the range measurements either in a centralized manner (at a central node), or in a distributed scheme (each node collects its range measurements with respect to its neighborhood devices for its own localization). In Chapter 2, we explained that the range is estimated through several transactions based on 3-WR; therefore, the collect of the distances from devices may conduct to high latency, which depends on the network size as well as the addressed scheduling [54]. In turn, this latency triggers ranging error, as the body can change its position and its gesture during this elapsed time. Besides, another main source of ranging error is related to the involved WBAN channel, in which the signal may suffer from NLOS propagation effects and dense multipath situation. These errors source, if not properly mitigated, generally yield severe degradation of positioning accuracy.

3.1.1 RANGING AND POSITIONING ERRORS

In the context of ranging estimation, [42] presents the issues of ranging error, position update latency and calculation algorithms under mobility. The authors are limited to the impact of MAC allocation resources on the capacity of the tracking system for Wireless Sensor Networks scenarios. In [25], the authors modeled the ranging error in terms of TOA estimation with real IR-UWB channel measurements in order to perform better localization algorithms but without any focus on the statistics of ranging error. [51] realizes a realistic measurement setup to achieve accurate positioning of WBAN nodes and compare the results with a different localization system. The study, however, requires special attention on the ranging accuracy, i.e., characteristics of the on-body ranging error.

3.1.2 RESOURCE ALLOCATION AT MAC LAYER

Previous works focusing on MAC design for localization with UWB systems proposed protocol strategies based on beacon-enabled Time Division Multiple Access and evaluated the performance in terms of accuracy and latency. In [26], they proposed cooperative ranging with Aggregated and Broadcast schemes to reduce the delay of 3-WR transactions. In [37], they focus on better resource management with priority levels for communication. In [38], they focus on the relation between MAC delay and UWB accuracy related to the number of anchors and the communication range of nodes under mobility. However, all these works focus on localization applications for WSN [55] which do not present the same problems of WBAN [56] and they do not consider the impact of the scheduling of localization packets on the positioning estimation. In [39], they proposed scheduling schemes for cooperative distributed localization with two different policies (node neighborhood and links quality) to reduce positioning convergence, latency and overhead. However, they consider a 2D Positioning for WSN which again is not realistic for WBAN location-aware applications.

3.1.3 IMPACT ON POSITIONING ALGORITHMS

In the context of localization estimation, various positioning algorithms have been developed in the past few years. [52] used the Non Linear Least Squares (NLLS) algorithm, which consists in minimizing a global quadratic cost function using the Gradient descent method incorporating the peer-to-peer range measurements. [57] and [58] adapt a centralized classical Multidimensional Scaling (MDS) for on-body motion capture applications and pose estimation. In [58], the authors introduce additional constraints relying on the prior knowledge of minimal and maximal feasible distances related to the body dimensions (and thus some kinds of geographical limitations). In [59] the centralized Maximum Likelihood estimator has been considered, introducing other constraints relying on the actual positions of on-body mobile nodes. More recently, the problem of cooperative localization based on the extended Kalman filtering (EKF) has been developed which incorporates the cooperative peer-to-peer range measurements with the on-body nodes as well as the anchors [60]. The existing contributions do not exploit the potential information of the lower layers.

In this chapter, we propose to reduce the ranging error due to the mobility and WBAN channel. In Section 3.2, we deal with the problem of mobility in a perfect channel by proposing different scheduling strategies of the 3-WR packets at the MAC layer in order to find the best strategy reducing the delays, thus, the ranging and positioning errors. In Section 3.3, we analyze the slot allocation performances in function of nodes mobility without noisy channel, in order to increase the positioning estimation according with different reference positions at the MAC frame duration. Finally, we conclude the chapter by giving some key points to consider in case of scenarios with noisy channel affecting the ranging estimation.

3.2. STUDY OF 3-WR PACKETS SCHEDULING FOR POSITION ESTIMATION

In Section 2.2 and 2.3, we investigated the impact of mobility on the ranging accuracy where the distances are estimated with a IR-UWB system [24]. For this, we measured the ToA of three different packets, as defined by the 3-WR protocol [26]. However, we observed that when considering a mobile target in a WBAN, the actual positions may be different for each packet. This may increase the error distance estimation, in particular, when the time between packets transmission increases. Therefore, the scheduling of 3-WR packets is of primary importance to perform an effective location. Thus, the MAC layer must consider the rapid mobility of WBAN nodes by reducing the delays to complete the ranging estimations.

In this section, we study different scheduling strategies at MAC layer in order to reduce the impact of mobility on the position estimation accuracy and location-aware applications. For this, we consider a perfect channel with a realistic mobility scenario (Section 2.3.3).

3.2.1 SYSTEM CONFIGURATION

In this study, we consider a mesh of IR-UWB WBAN under full connectivity containing N_T nodes of two kinds as in [25] , on-body mobile nodes that do not know their own position ($i = 1 \ldots N_M$) and on-body anchor nodes that know their own position ($j = 1 \ldots N_A$), $N_T = N_A + N_M$. A set of anchor nodes define a Local Coordinate System (LCS) to localize nodes under mobility. We define the instantaneous distance of the node i with the anchor j as (d_{ij}) and the estimated distance as ($\hat{d}_{ij}$) which is calculated through ToA estimation. As presented in Section 1.2.1, we use the 3-WR to estimate the positions and distances between the nodes in real time by combining the typical timers obtained from 3 transmissions. During these transactions, the on-body nodes collect the different timers of the 3-WR packets transmission and reception. Thus, the distance ($\hat{\mathrm{d}}$) is evaluated as follows:

$$\hat{\mathrm{d}}_{\mathrm{ij}}(\mathrm{t}) = \frac{1}{2}\,\mathrm{c}\left[\left((\mathrm{T}_4 - \mathrm{T}_1) - \Delta\mathrm{t}1\right) - \left((\mathrm{T}_6 - \mathrm{T}_4) - \Delta\mathrm{t}2\right)\right]$$

where c is the light speed and $\Delta t1 = \mathrm{T}_3 - \mathrm{T}_2$ (resp. $\Delta t2 = \mathrm{T}_5 - \mathrm{T}_3$) is the delay between the reception of a request packet and the transmission of a response 1 packet (resp. the delay between the transmission of the response packets). The positions of nodes are estimated with the Time Difference of Arrival (TDOA) technique [24] where the position is determined as the intersection of hyperboloids in a tridimensional space. For this purpose, each node communicates with at least four anchors for a distributed localization, which is the minimum needed for a tridimensional positioning ($\hat{\mathrm{d}}_{\mathrm{i,j}} = \sqrt{(\mathrm{x} - \mathrm{x_j})^2 + (\mathrm{y} - \mathrm{y_j})^2 + (\mathrm{z} - \mathrm{z_j})^2}$), as described by the following equations:

$$\begin{aligned}
{d_2}^2 - {d_1}^2 &= (x_2 - x)^2 + (y_2 - y)^2 + (z_2 - z)^2 - (x_1 - x)^2 + (y_1 - y)^2 + (z_1 - z)^2 \\
{d_3}^2 - {d_2}^2 &= (x_3 - x)^2 + (y_3 - y)^2 + (z_3 - z)^2 - (x_2 - x)^2 + (y_2 - y)^2 + (z_2 - z)^2 \\
{d_4}^2 - {d_3}^2 &= (x_4 - x)^2 + (y_4 - y)^2 + (z_4 - z)^2 - (x_3 - x)^2 + (y_3 - y)^2 + (z_3 - z)^2
\end{aligned}$$

Then, we use a Linear Least Square (LLS) approach to estimate the position of the node ($\widehat{\mathrm{P}}_{\mathrm{i}}(\mathrm{t}) = \{\mathrm{x}, \mathrm{y}, \mathrm{z}\}$) by reorganizing the equations into a linear equation and an intermediate variable is added (linearization function) to estimate the source position (Deliverable D3.1). For the TDOA technique, we assume that the anchor nodes have a common time reference, but not with the mobile nodes. Therefore, the clock drift between the anchors and mobile nodes is mitigated with the 3-WR packets.

3.2.2 CONSIDERED PROTOCOLS

TDOA is good solution in the case of WSN localization, where the node has a regular motion and the coordination between anchors and mobiles nodes is easy to achieve and maintain. In the case of WBAN, during the transmission of 3-WR packets the mobile nodes are always moving and the estimated distances with the anchors are not performed at the same time for the position of the node, which can lead into an error estimation on the positioning (**Figure 1-4**). As explained in Section 2.2, the 3-WR accuracy depends on the delays taken to receive the response. If we consider a topology with many mobile nodes performing 3-WR transactions

for localization with the anchors, the positioning error can also be a problem for the motion capture. Therefore, it is necessary to find new scheduling schemes at MAC layer to mitigate the positioning error within an acceptable latency. To this aim, we define a Medium Access Control (MAC) layer based on the TDMA protocol and we assume that it is beacon enabled. Then, we reserve three transmission periods for the 3-WR packets. For the sake of our study, the scheduling of the 3-WR periods is flexible to allow the comparison of different scheduling strategies to reduce the ranging error. Our first contribution consists to evaluate the scheduling strategies to increase the positioning accuracy of 1 mobile node in a WBAN. Whereas the second contribution propose different scheduling strategies to achieve a Motion Capture application where several mobile nodes try to estimate a human posture.

3.2.3 SCHEDULING STRATEGIES FOR ACCURATE POSITIONING

In this study, we consider four peer-to-peer (P2P) scheduling strategies for position estimation (Figure 3-1) of one node with four anchors based on 3-WR and TDOA. For each scheme, we considered to reduce as much as possible the time to send the first response (delay Δt1) as follows:

- **All request first (S1):** The request packets Q_{ij} are sent in priority to all the anchors. Then each anchor answers at its turn with responses $R1_{ji}$and $R2_{ji}$ consecutively.
- **Ordered transaction (S2):** The node starts a 3-WR transaction with each anchor in order.
- **Three period order (S3):** The MAC Frame is divided into three periods dedicated to send the different 3-WR packets in order: the Q_{ij}, the $R1_{ji}$ and $R2_{ji}$at the end.
- **Priority for Response 1 (S4):** The node sends the Request and the anchor send a Response 1 packet immediately. Then, the anchors send $R2_{ji}$ the at the end of the frame.

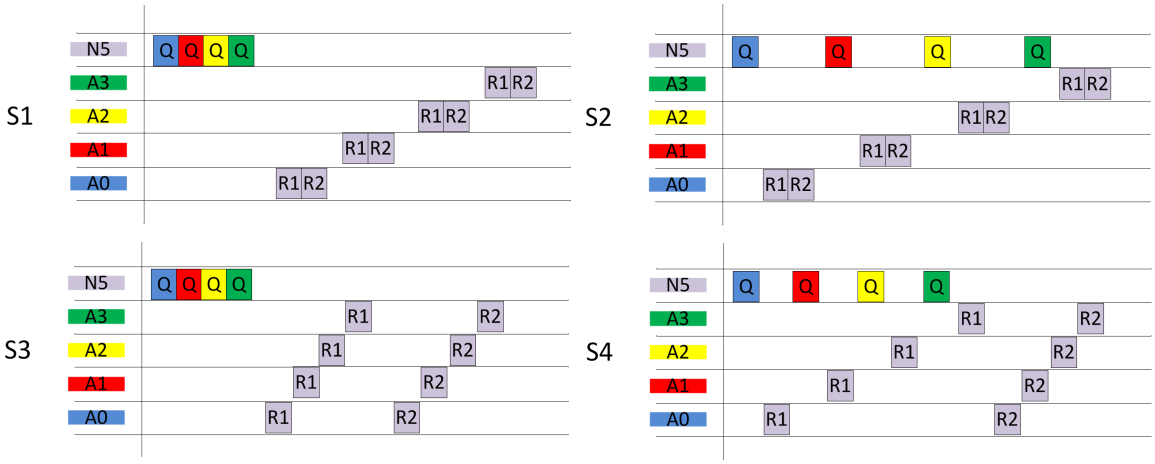

Figure 3-1: Scheduling strategies with 1 node and 4 anchors. (a) All request first - S1, (b) Ordered transaction - S2, (c) Three period order - S3 and (d) Priority for Response 1 - S4

A. Mobility model

We consider two mobility models. The first consist in a controlled scenario composed by 5 sensors: four anchors located at the chest, back, hip right and hip left and one node on the right wrist performing a periodic linear movement (e.g. walking) at different speeds (1-20 m/s). The anchors stay fixed and the node moves in a linear space of 30 cm. Besides, we consider a realistic scenario obtained by measurement as presented in Section 2.3.3. The mobile node is on the right wrist (N_5) and the four anchors are on the right chest (A_1), the left chest (A_2), the left hip (A_3) and the back (A_4) as shown in **Figure 3-2**. We use a speed factor (1 to 10) in order to accelerate the movement traces.

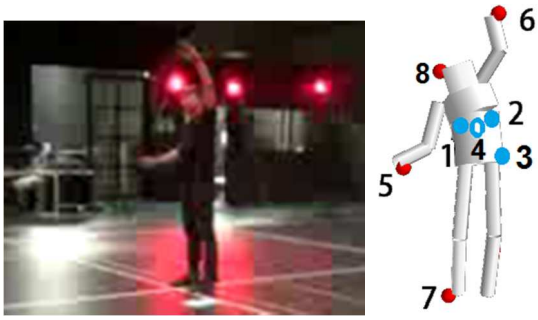

Figure 3-2: Multi-cylinder Body reconstruction - the red (resp. blue) points refer to the mobile nodes (resp. anchors).

B. System configuration

We adopt a discrete-event simulation approach using the WSNet simulator [49]. At the physical (PHY) layer, we defined a protocol based on the IEEE802.15.6 PHY UWB [44] in default mode (OOK modulation, data rate 0.4875 Mbps). For the sake of simplicity, we assume a line of sight (LOS) channel without packet loss in order to focus on the ranging error related to the mobility. Therefore, we assume that our radio is capable to detect the first path of IR-UWB to detect the precise ToA at the receiver. We implemented a MAC scheduling based on TDMA synchronized and beacon enabled. Within this framework, we evaluate the impact on positioning estimation with the RMSE as follows:

$$\mathrm{RMSE}(i, \mathrm{ref}_r) = \sqrt{\frac{\sum_1^{N_f} \left| P_{\mathrm{ref}_{r,i}}(t) - \hat{P}_i(t) \right|^2}{N_f}} \qquad (3\text{-}1)$$

where N_f is the number of frames during the simulation and $P_{\mathrm{ref}_{r,i}}(t)$ represents a reference position to compare with the estimated positions. Finally, we implemented the mobility models from section B where the results are obtained over a simulation of 100s.

C. Performance evaluation

In this study, we compare the estimated position ($\hat{P}_i(t)$) with the real position at the end of each frame $P_{final_i}(t)$. **Figure 3-3** shows the RMSE for both mobility scenarios in function of the speed. We observe that the RMSE of all the strategies increases with the speed. This is because the node covers a bigger distance as the speed increases for the same among of time for the 3-WR transactions. Moreover, we note for both scenarios that S1 and S2 perform a better positioning than S3 and S4. This is an interesting observation between prioritizing the ranging estimation or positioning, i.e. we showed in Section 2.2 that Δt1 needs to be reduced for an accurate ranging estimate. If we consider a global comparison of the delays, S3 and S4 have the smaller Δt1 compared to S1 and S2. Therefore, S3 and S4 perform better ranging accuracy. However, this turns with the position estimation, in our scenario we compare the estimated position with the real position at the end of the frame. Thus, the distances estimated by S1 and S2 are closer to the real distances corresponding to the position at the end of the frame. To complete this study, we consider the case of broadcast transmissions for the request parquets for the best strategy (B-S1). Theoretically, this yields a gain of 3 slots. We can observe in **Figure 3-3** that the broadcast on strategy S1 permits to reduce both error on positioning estimation and delay.

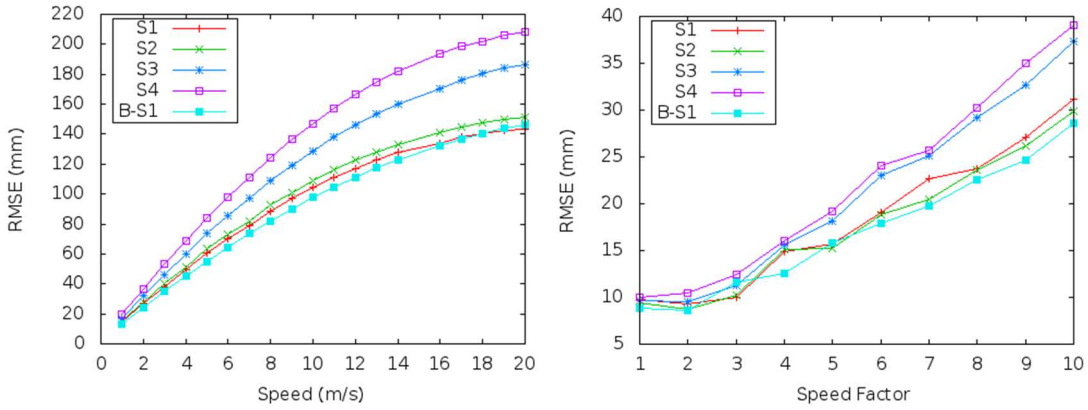

Figure 3-3: RMSE in function of the speed to evaluate the impact of the scheduling schemes (a) under linear mobility and (b) with a realistic human scenario

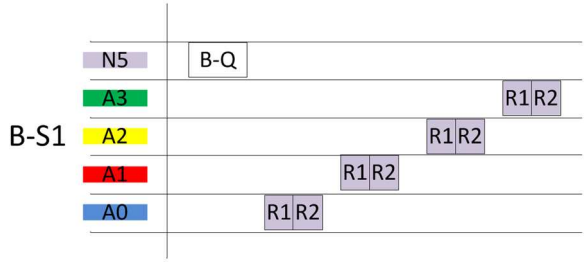

Figure 3-4: Scheduling strategy S1 with request in broadcast

3.2.4 SCHEDULING STRATEGIES FOR LSIMC

Based on the previous results, we extend the study with a complete WBAN network to enable a motion capture application. In this study, we consider a WBAN with several mobile nodes trying to locate with the anchor nodes with 3-WR and TDOA. Thus, we propose three P2P scheduling strategies based on S1 and S2 for position estimation (**Figure 3-5**) as follows:

- **All request first, anchor priority (S5)** where the nodes send the Q_{ij} packets at the beginning, then each anchor answer in order to all nodes with $R1_{ji}$and $R2_{ji}$.
- **All request first, node priority (S6):** As the previous, the nodes send Q_{ij} first then all anchors answer node by node with $R1_{ji}$and $R2_{ji}$.
- **Ordered node positioning (S7):** Each node repeat the scheme S1 one by one.

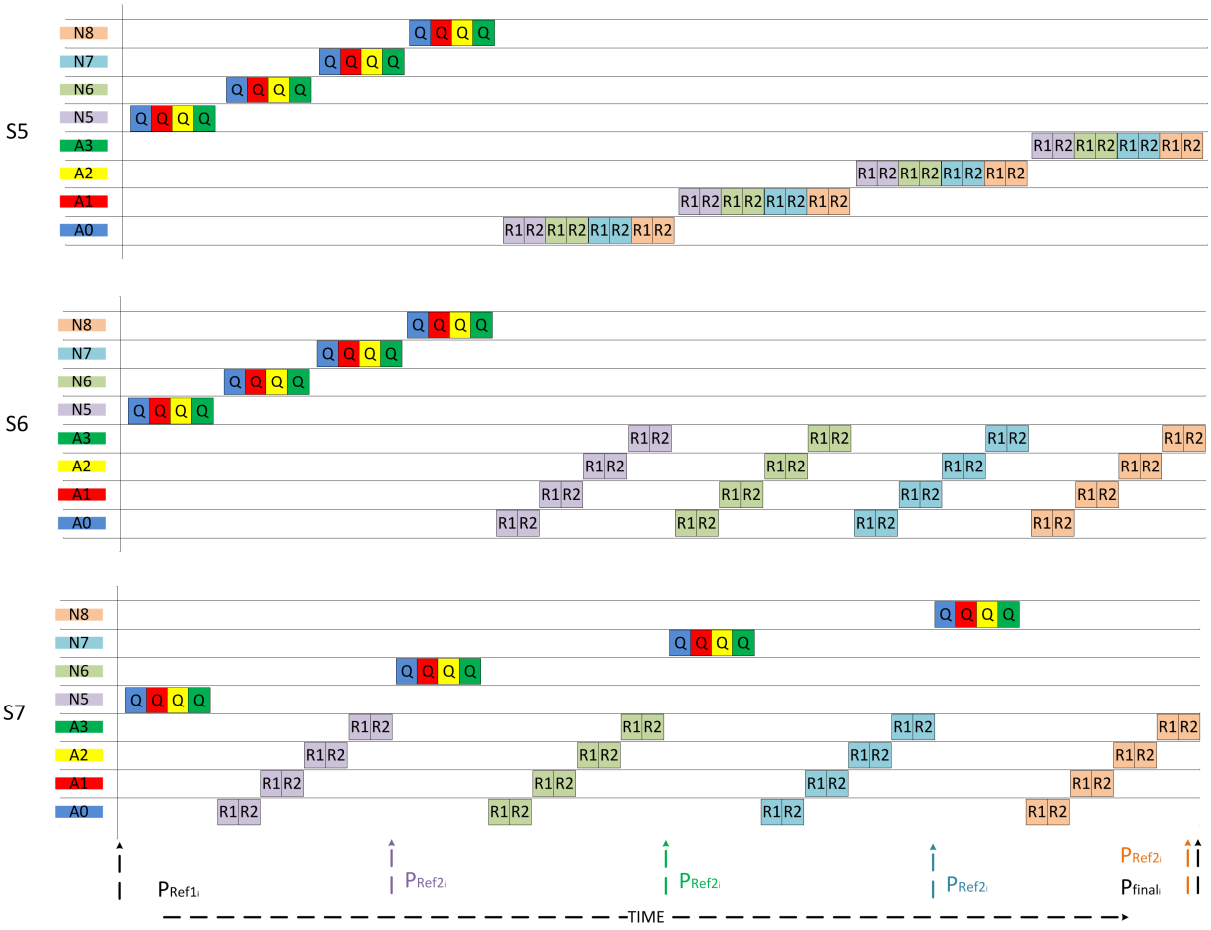

Figure 3-5: Scheduling strategies with 4 nodes and 4 anchors. (a) All request first, anchor priority - S5 (b) All request first, node priority - S6 (c) Ordered node positioning - S7

A. Mobility model

We consider the realistic scenario obtained by measurement as presented in Section 2.3.3. The mobile nodes are located on the right wrist (N_5), the left wrist (N_6), the right ankle (N_7) and the head (N_8). Besides, the anchors are on the right chest (A_1), the left chest (A_2), the left hip (A_3) and the back (A_4) as shown in Figure 3-2.

B. System configuration

In this study, we use the same framework presented before (Section 3.2.3). We evaluate the performance of the different scheduling schemes with the RMSE between the positions estimated with a three reference positions, as shown in **Figure 3-5**: $P_{ref1_i}(t)$ is the position of nodes at the beginning of a MAC frame, $P_{ref2_i}(t)$ represents the instantaneous position when a mobile node performs 3-WR with all the anchors and $P_{\text{final}_i}(t)$ is the position of nodes at the end of the frame. As for the last study, we evaluate the performance of the best strategies with the request packet in broadcast (**Figure 3-6**).

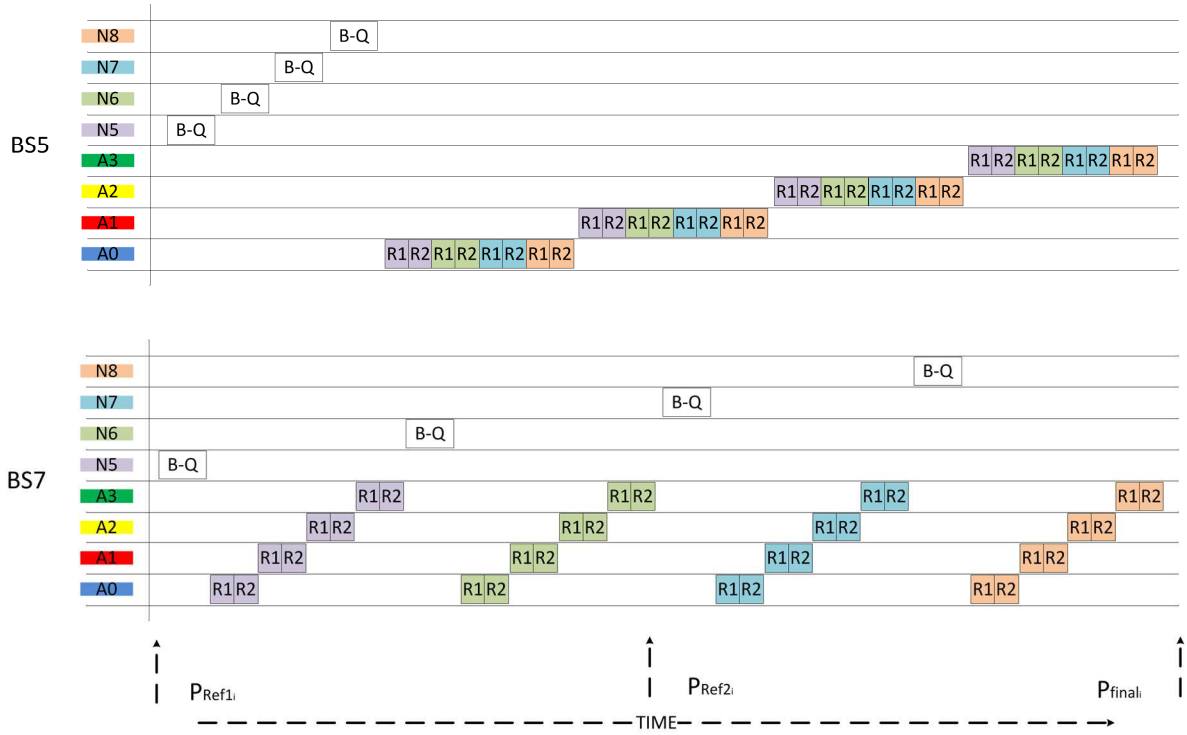

Figure 3-6: Best scheduling strategies with request in broadcast (a) B-S5 (b) B-S7

C. Performance evaluation

Figure 3-7, **Figure 3-8** and **Figure 3-9** present the RMSE on the position estimation in function of the speed for the all the nodes. **Figure 3-7** shows that nodes at start of frame (N_5 and N_6) have better estimation of P_{ref1_i} with S7. Inversely, nodes at end of frame (N_8) have better estimation of P_{ref1_i} with S5. Moreover, we note that the RMSE is small (< 5cm) when applying a broadcast transmission on the request for the best strategies depending with the position of the node (B-S7 and B-S5). If we analyze the performance to estimate P_{ref2_i}, we observe in **Figure 3-8** that S7 permits to estimate more accurate instantaneous positions (RMSE < 5cm over all speeds) with high refreshment rate. Finally, **Figure 3-9** shows that nodes at start of frame have better estimation of P_{final_i} with S5, without a remarkable precision (RMSE > 5cm) for high speed. On the contrary nodes at end of frame have better estimation of P_{final_i} with S7, with good precision (RMSE < 3cm) under high speed.

Based on these results, we find that in the case of an application looking for individual motion capture of the nodes (estimation of P_{ref2_i}) with high refreshment rate, the best scheduling is a Broadcast transmission with S7. If we enlarge the scope to applications looking for posture recognition (estimation of positions at the end (resp. start) of frame P_{final_i} (resp. P_{ref1_i})), it is possible with a Broadcast transmission with S5.

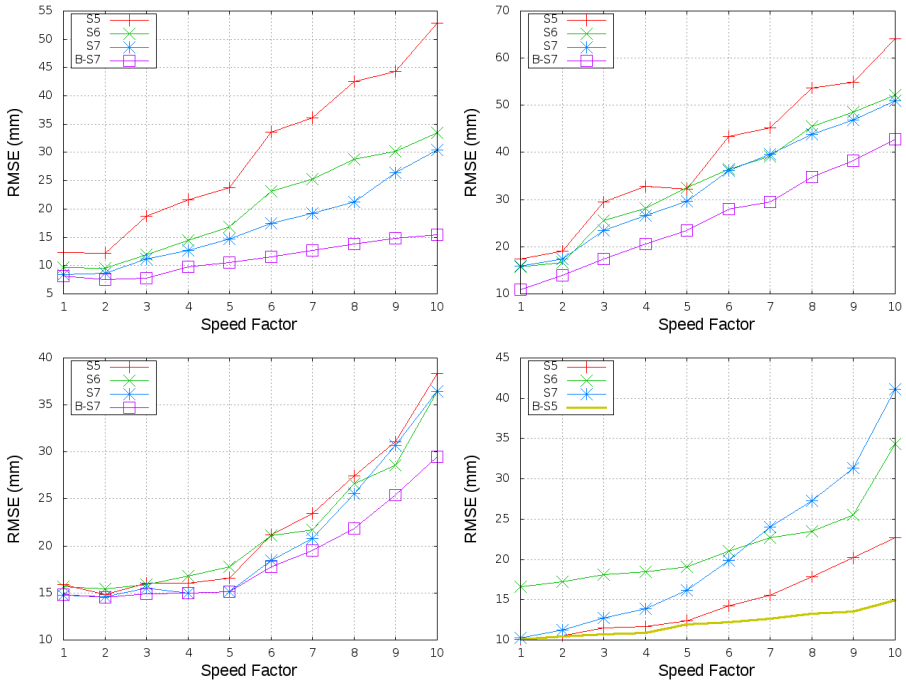

Figure 3-7: RMSE in function of the speed with respect to $P_{ref1_i}(t)$ for all mobile nodes: (a) right wrist - N_5 (b) left wrist - N_6 (c) right ankle - N_7 (d) head - N_8

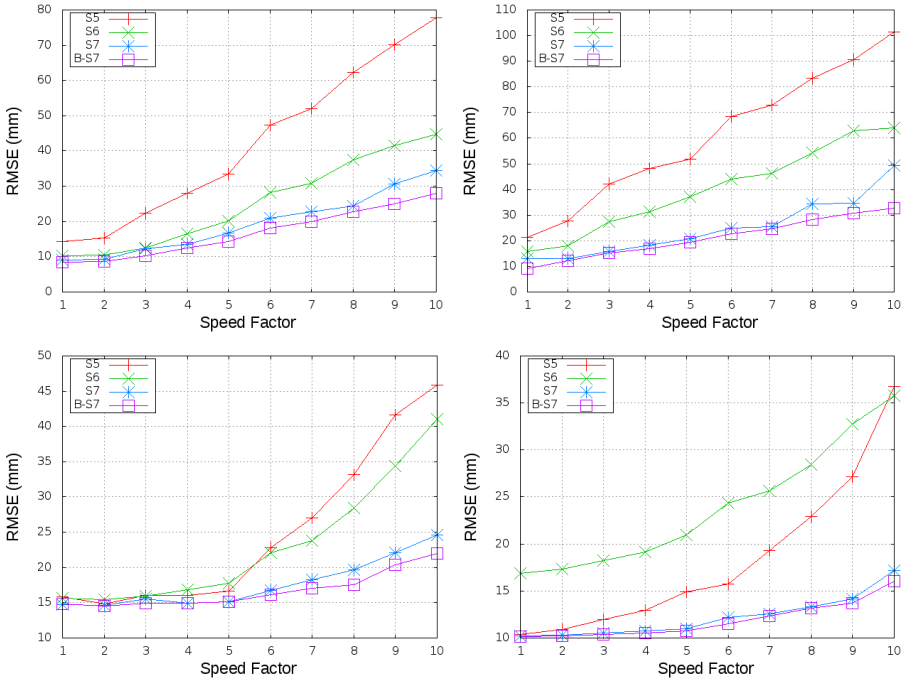

Figure 3-8: RMSE in function of the speed with respect to $P_{ref2_i}(t)$ for all mobile nodes: (a) right wrist - N_5 (b) left wrist - N_6 (c) right ankle - N_7 (d) head - N_8

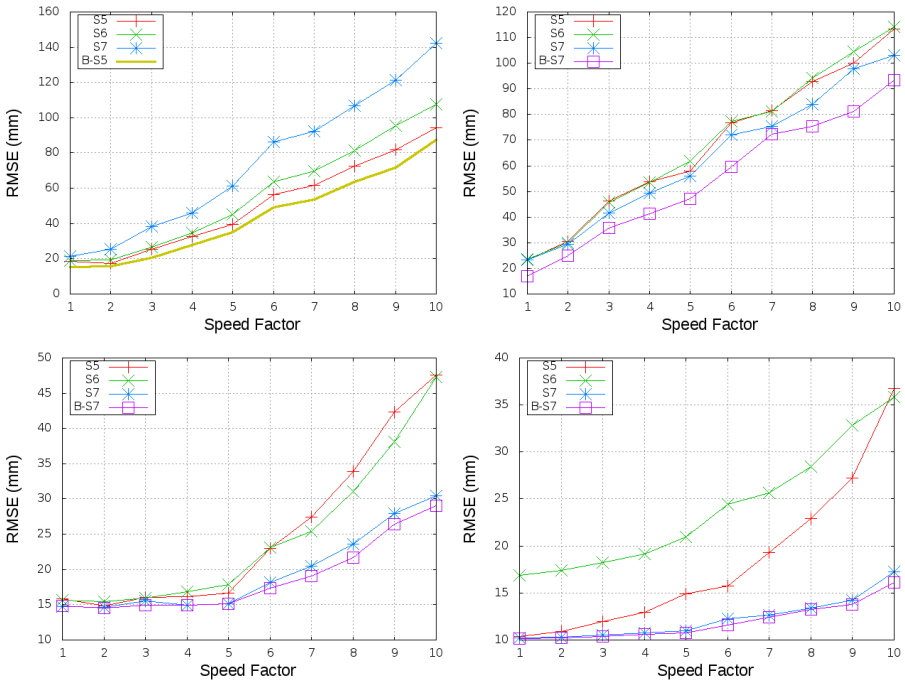

Figure 3-9: RMSE in function of the speed with respect to $P_{final_i}(t)$ for all mobile nodes: (a) right wrist - N_5 (b) left wrist - N_6 (c) right ankle - N_7 (d) head - N_8

3.2.5 CONCLUSION

In this section, the problem of scheduling strategies at MAC layer is addressed to enable an Individual Motion Capture application with IR-UWB systems. For this, we considered our previous results in Section 2.2 and 2.3 presenting the impact of mobility in distance estimation due to the ranging packets delay and speed of nodes. As detailed, the node is always moving and the position of the node may not be the same during the 3-WR transactions, leading to different errors on the localization. To provide increased accuracy, the positioning error can be reduced by proposing the most appropriate scheduling scheme at the MAC layer. For this purpose, we defined different scheduling strategies to minimize the ranging and positioning error. It turns out from simulation studies that an effective scheduling scheme leads to estimate the nodes position one by one rather than doing all nodes at once with the reduction of P2P latency. For the following we would like to extend the study by considering the impact of channel noise under realistic short-term and long-term pedestrian mobility models.

3.3. STUDY OF SLOT RESOURCE ALLOCATION FOR RANGE ESTIMATION

In Section 3.2, we address the scheduling issue to improve the positioning of WBAN nodes under mobility. This is a specific requirement to design appropriate cross-layer protocols to increase both ranging precision and network capacity. Another aspect that can improve the localization accuracy is the slot allocation management-policy. In WBAN context, recent works on slot allocation focus mainly in four strategies: the energy efficiency [61], quality of service (QoS) [62] [63], fairness [64] and reliability [65]. In [61], authors proposed a slot allocation mechanism for medical applications with a WBAN composed by heterogeneous devices. Each sensor has different information to send, sampling rate and power requirements. For this reason, they proposed a TDMA based scheme to allocate a number of resources in function of the energy consumption and the minimum data needed to maintain the medical service (QoS) with short delays. In [64], authors proposed a different approach slot allocation for medical emergency situations depending on the urgency and criticality of information (QoS) to be send. In this mechanism, the coordinator nodes are connected to the devices located on the body. The transmission is based in a non-cooperative evolutionary game algorithm (hawk-dove game) where the coordinators choose how many slots will be allocated to their nodes depending on a fairness transmission factor, the emergency information to be send as well as the energy consumption. However, these last mechanisms were not tested in real or simulated scenarios considering all the WBAN constraints (e.g. channel variations). [62] aims to improve the QoS while deals with channel loss through contention periods for retransmission. But because of the contention period, the channel utilization and energy efficiency decrease. Another slot allocation policy depending on long or short term link quality estimation is proposed in [65], where a coordinator assign the slots in function of its reliability with the devices, i.e. at the beginning the most achievable nodes and at the end the ones with the worst channel. A mixed solution based on TDMA is proposed in [63] to improve the energy efficiency while assigning the slots in function of the QoS and the most recent channel history in a star topology through beacon packets. The packet loss is then improved by assigning a specific number of slots (below to a calculated threshold) to the nodes depending on their channel reliability with the coordinator.

However, in our radio-location context with WBAN, none of these slot allocation solutions fits with our requirements, i.e. the nodes are homogeneous and the main requirements are latency and accuracy to enable localization. Eventually, the short-long term based strategy could be interesting to deal with the WBAN channel under a flexible threshold for reliability, this issue is investigated on Chapter 4. Moreover, the mobility of nodes needs to be considered from the protocol perspective, because it may impact the accuracy of ranging estimation (Chapter 2). In this section, we evaluate the impact of mobility on positioning accuracy with different slot allocation schemes based on the speed of nodes under realistic scenarios [66]. Then, we compare the positioning performance of these slot allocation schemes with different MAC-level scheduling strategies based on TDMA for the transmission of 3-WR packets.

3.3.1 SYSTEM CONFIGURATION

We consider a single full-mesh WBAN in an indoor environment with two categories of nodes: the on-body anchors nodes, which are placed at the most static positions on the body (e.g. on the chest or on the back) composing a Local Coordinate System (LCS) with knowledge of their positions; and the on-body mobile nodes, whose positions are unknown. These nodes communicate through an IR-UWB system to estimate the ToF of pulses accurately (Section 1.2.1). The distances between nodes and anchors are calculated with the transmission of 3-WR packets. Thus, the localization is achieved in a distributed scheme where mobile nodes starts the 3-WR mechanism with the anchors. Then, the position of nodes is calculated through TDOA. Note that the LCS is mobile and generally misaligned relatively to any Global Coordinate System (GCS).

3.3.2 MOBILITY MODELS

We consider two the realistic scenarios of 100 seconds obtained by measurement as presented in Section 2.3.3. The mobile nodes are located on the right wrist (N_5), the left wrist (N_6), the right ankle (N_7) and the head (N_8). Besides, the anchors are on the right chest (A_1), the left chest (A_2), the left hip (A_3) and the back (A_4) as shown in **Figure 3-10**. In the first scenario, called Yoga activity, the subject realizes a series of static positions in the same place, mimicking Yoga postures (as shown in Section2.3.3). The second mobility model consists in a pedestrian walking scenario where the subject starts moving from the middle of the scene. Then, he walks at moderate speed along a rectangular trajectory centered on the starting point. More details on this last scenario can be found in the deliverable D4.1.

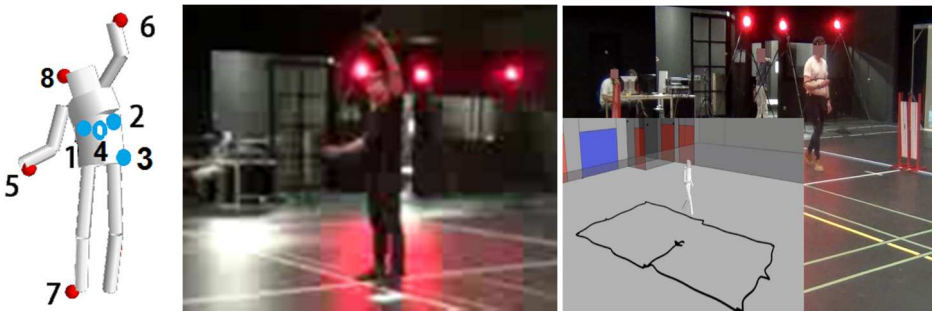

Figure 3-10: Mobility Models for the study. (a) Nodes positions located on a human body (b) Yoga activity scenario (c) Pedestrian Walking scenario

3.3.3 LOCALIZATION-ORIENTED MAC PROTOCOLS AND SLOT ALLOCATION

This work addresses the node speed issue on ranging estimation by analyzing a mobility-level TDMA based slot allocation along with two different scheduling schemes to increase the localization accuracy with 3-WR. For sake of our study, we assume that the channel is perfect and we ignore the effect of body shadowing; therefore, our system detects de first path of pulses. Moreover, the MAC frame is beacon enabled and synchronized.

A. Scheduling strategies for 3-WR packets

First, we propose to compare different MAC scheduling strategies (as proposed in Section 2.3.2) based on our results in Section 3.2 with different properties to improve both latency and positioning accuracy considering the mobility of nodes. For this purpose, we analyze two strategies (**Figure 3-11**):

- **Single nodes localization in Broadcast (P2P-B):** a node *i* broadcasts the request packet Q_i to all anchors. Then, each anchor sends both responses $R1_{ji}$and $R2_{ji}$consecutively, one anchor at a time. Note that broadcasting the requests has the effect to increase the delay $\Delta t1$ for some anchors. Besides, this delay is not uniform across the anchors.
- **Aggregated and Broadcast (A&B):** in a first phase, all requests packets Q_i are transmitted in broadcast. Then, each anchor *j* sends an aggregated response ($R1_j$) to all nodes, followed by the second response ($R2_j$). A&B allows reducing the volume of traffic and hence the size of the TDMA frame, but also results in an increase of the $\Delta t1$ delay for nodes.

Note that A&B and P2P-B can reduce the overall positioning time and save bandwidth, but delay the reception of the first responses. In Section 2.3.2, we show that the nodes speed has an impact on the ranging estimation using 3-WR depending on the MAC strategy to reduce delays, but without focusing to quantify the impact on positioning. In Section 3.2, we show

that the P2P localization, completing the 3-WR ranging estimation for each node, can improve the positioning accuracy compared to other strategies schemes. However, the frame duration of this strategy increases in function of the number of nodes in the network. For this reason, A&B was proposed to limit the packet traffic through broadcast transmission and data aggregation. But, this strategy may lead to higher packet loss in presence of body shadowing. Thus, P2P-B constitutes a compromise between P2P and A&B. This difference is explained in **Figure 3-12** by the number of packets sent by each protocol between m anchors and n mobile nodes. In A&B (resp. P2P-B), the nodes send n Request packets in Broadcast to the anchors. Then, the anchor nodes answer with m (resp. $n * m$) Response 1 packets and m (resp. $n * m$) Response 2 packets. Thus, we have $\prod_{A\&B} = n + 2\,m$ and $\prod_{P2P-B} = n + (2\,m + 1)$ packets for A&B and P2P-B, respectively. In our scenario of 4 anchors and 4 mobile nodes, P2P-B presents a TDMA frame length of $\approx 54\,ms$ against $\approx 18\,ms$ for A&B. This means that for the duration of one P2P-B movement acquisition round, A&B can perform three times more the motion capture, and hence should reduce the impact of nodes mobility.

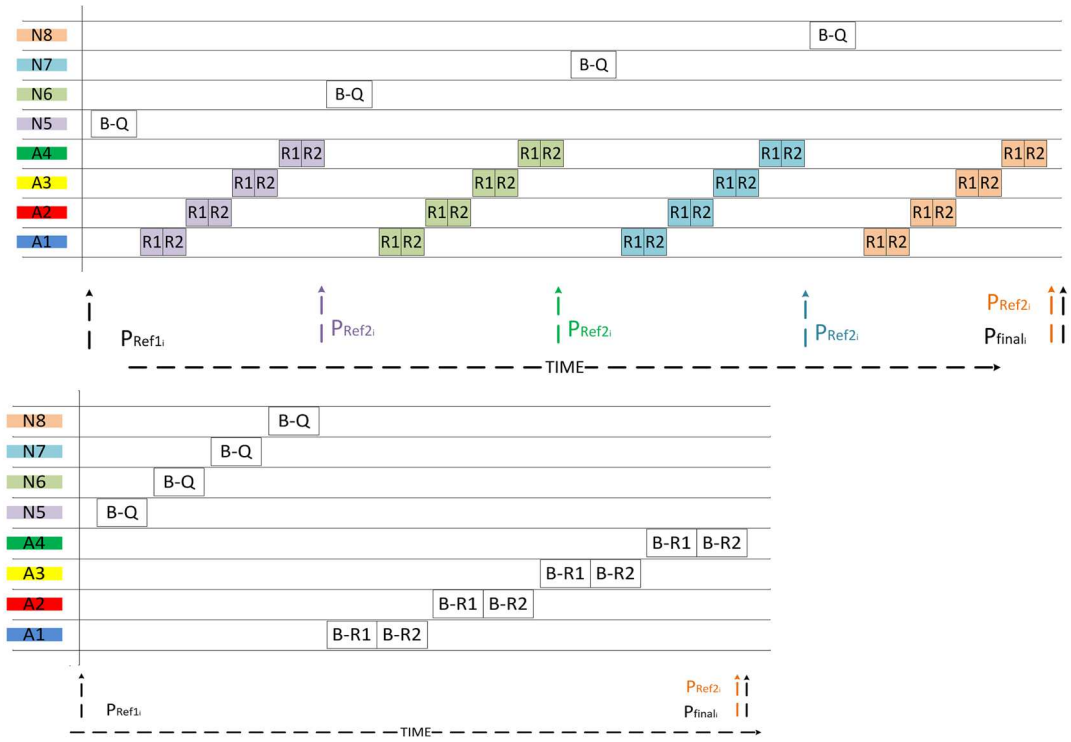

Figure 3-11: MAC scheduling strategies for 3-WR packet transmission (a) P2P-B (b) A&B

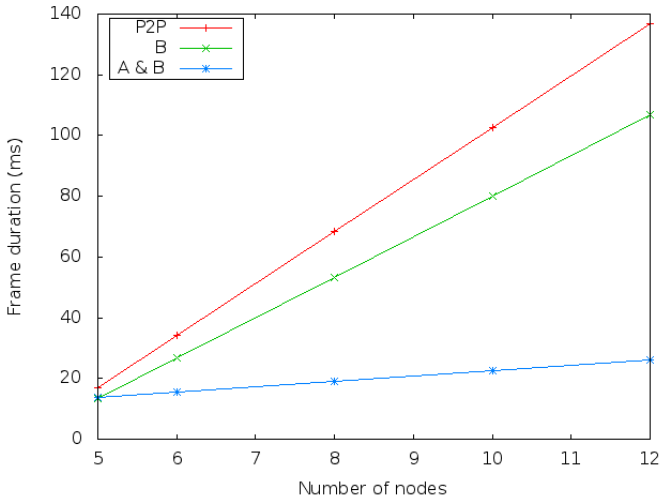

Figure 3-12: Comparison of the MAC frame duration in function of the number of nodes between P2P (red), P2P-B (green) and A&B (blue)

B. Mobility-level slots allocation

Besides the scheduling strategies to reduce the delays for 3-WR transactions, it is possible to play with the MAC allocation of slots to reduce the positioning error of nodes depending on their mobility level. To this aim, we define three levels of mobility depending on the speed of nodes: high, medium and low. Accordingly, we analyze four different permutations of the slot allocated to each node in function of its mobility level, as shown in **Figure 3-13**:

- NS1 where nodes with highest (resp. lowest) mobility are positioned at the beginning (resp. end) of the TDMA frame.
- NS2 where nodes with highest mobility are positioned in the middle of the TDMA frame
- NS3 where nodes with highest (resp. lowest) mobility are at the end (resp. beginning) of the TDMA frame and
- NS4 where nodes with lowest mobility are positioned in the middle of the TDMA frame.

For the present scenario, involving 4 anchor nodes (A_1 to A_4) and 4 mobile nodes (N_5 to N_8), N_5 and N_6 (nodes on the wrists) are considered with high mobility level for both scenarios (walking and yoga), N_7 (node on the ankle) with medium (resp. high) mobility level for the yoga (resp. walking) scenario and N_8 (node on the head) with low level for both scenarios.

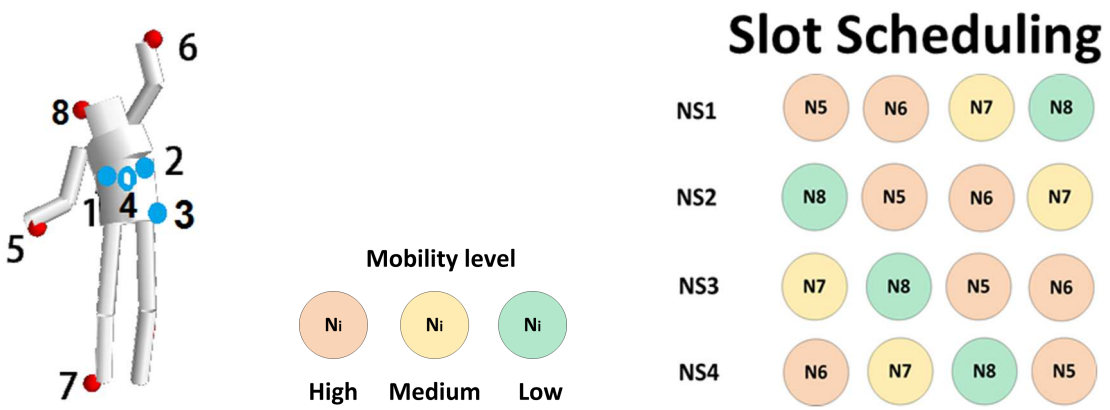

Figure 3-13: Mobility-level slot allocation of nodes with 4 mobile nodes

3.3.4 SIMULATION AND PERFORMANCE EVALUATION

We perform an event-discrete based simulation with WSNet to evaluate the positioning accuracy in function of our mobility-level slots allocation and scheduling strategy. We implemented a physical layer based on IEEE802.15.6 on UWB in default mode (OOK modulation and 0.4875 Mb/s). At the MAC, layer we implemented a TDMA-based medium access protocol, as well as the different algorithms and scheduling approaches, detailed in Section 3.3.3. Finally, we implemented a mobility model that let us exploit the traces for our two scenarios, as explained in Section 3.3.2. We quantify the localization accuracy between a given reference position ($P_{ref_{r,i}}$) and its estimate ($\widehat{P}_i$) with the root mean squared error (RMSE) over N_f as follows:

$$RMSE(i, ref_r) = \sqrt{\frac{\sum_1^{N_f} \left| P_{ref_{r,i}}(t) - \widehat{P}_i(t) \right|^2}{N_f}} \qquad \textbf{(3-2)}$$

Within this framework, each node *i* performs a distributed localization by completing the 3-WR transaction throughout the simulation. At every frame, *i* estimates its position that can be compared with a reference position. which can be the position occupied by the node at the beginning of the MAC frame $P_{ref1_i}(t)$, at the end of the 3-WR with the last anchor $P_{ref2_i}(t)$ or at the end of the TDMA frame $P_{final_i}(t)$, as illustrated on **Figure 3-11.**

A. Impact of MAC scheduling on P2P-B accuracy with the Yoga scenario

First, we evaluate the performance of the different Mobility-level slot allocation schemes using P2P-B under the Yoga scenario. For this, we define a factor from 1 to 10 in order to accelerate the speed of nodes in our scenario (1 correspond to the real scenario). **Figure 3-14** shows the variation of RMSE of the positions estimation (P_{ref1_i}, P_{ref2_i} and P_{final_i}) with each slot allocation

scheme. We observe that the RMSE increases quasi-linearly with the speed factor. The distance covered during 3-WR transaction increases with the node mobility, inducing more errors in the distance estimation and hence in the localization accuracy. **Figure 3-14** (a) shows that NS1 is the best strategy to estimate P_{ref1_i}. This is because the nodes with higher mobility level are located at the beginning of the frame, and its position estimation is closer to the initial reference position. Besides, static nodes positioned later move less, which mechanically leads to a better RMSE. Similarly NS3, in which high mobile nodes are scheduled at the end of the frame, is the best to estimate P_{final_i}, as shown in **Figure 3-14** (c). Finally, **Figure 3-14** (c) shows that there is no gap between the different NS_i strategies when estimating its position (P_{ref2_i}) at the end of the 3-WR exchange. P_{ref2_i} estimation is therefore less sensitive to the mobility-level slot allocation and should be a good candidate when no information on the individual nodes mobility is assumed.

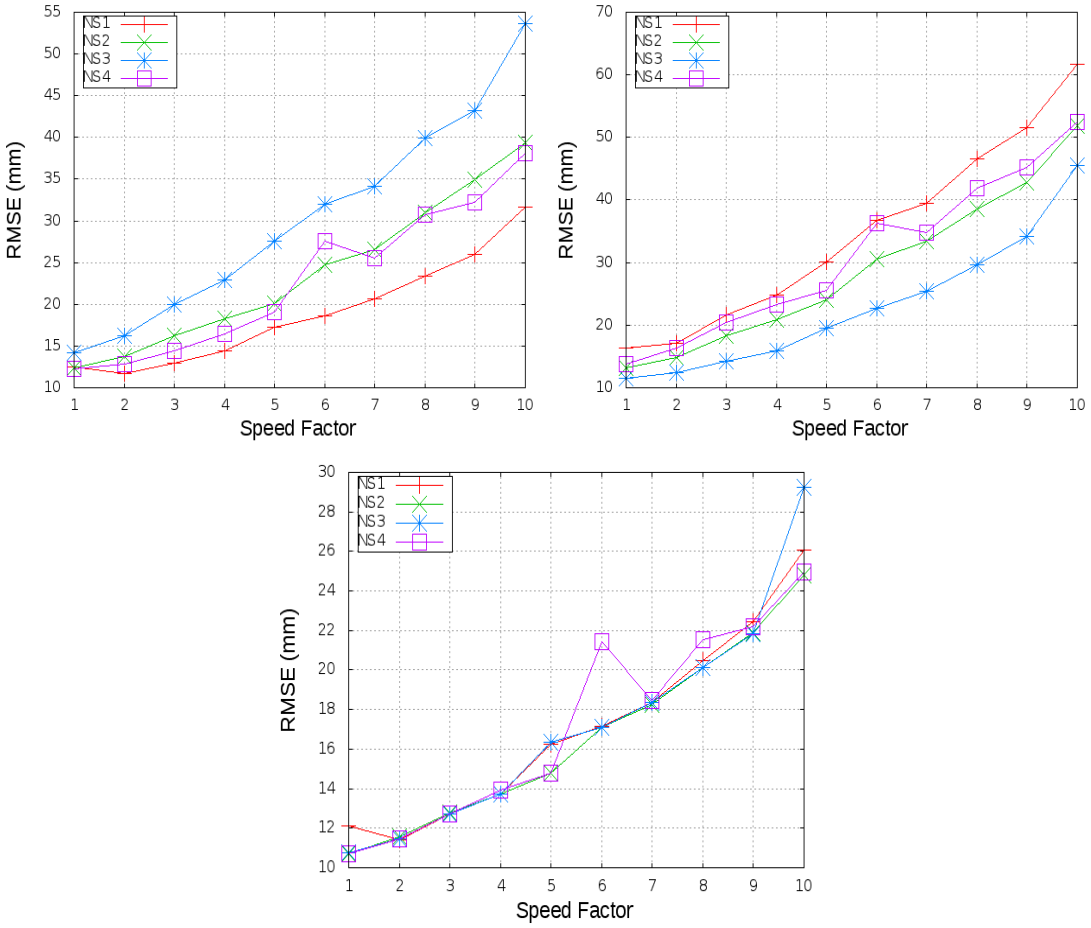

Figure 3-14: Impact of mobility-level slot allocation on positioning accuracy with P2P-B under Yoga activity (a) RMSE w.r.t. P_{ref1_i} (b) RMSE w.r.t. P_{final_i} (c) RMSE w.r.t. P_{ref2_i}

B. Comparison of the MAC scheduling impact between P2P-B and A&B

In this second study, we compare the performance of P2P-B and A&B to estimate the three reference positions with the different mobility-level slot allocation schemes. This analysis relies on the same Yoga scenario as before. **Figure 3-15** compares the distribution of RMSE for all the allocation strategies with P2P-B and A&B. In the case of P2P-B (**Figure 3-15** (a)), we observe a significant gap between the different slot scheduling schemes when estimating P_{ref1_i} and P_{final_i}. Besides, P_{ref2_i} remains the best estimated position with P2P-B and all the slot allocation schemes. On the other hand (**Figure 3-15** (b)), A&B is not affected by the slot scheduling NS_i. Moreover, we note that P_{ref1_i} is the best estimated with A&B, because $\Delta t1$ is considerably reduced and the distances estimated are closer to the initial position. Therefore, A&B permits more freedom with any slot allocation. Compared to P2P-B, A&B reduces the average error by a factor 2 for the estimation of P_{ref1_i} and P_{final_i}. Thus, the consistency in the 4 used distances (A&B), i.e. low ranging dispersion w.r.t any position, is more important than the accuracy of each individual distances (P2P-B).

On the basis of these results we identify the two extreme scenarios concerning the combination of the selection of the reference position and of the MAC scheduling strategy: a *Worst Case (WC)* and a *Best Case (BC)*. The best case, where A&B (resp. P2P-B) performs the localization estimation according to P_{ref1_i} (resp. P_{ref2_i}) independently on the node slot strategy and the worst case, where A&B and P2P-B perform the localization estimation with respect to P_{final_i} with the slot allocation NS1 (high mobile nodes scheduled at the very beginning of the TDMA frame.

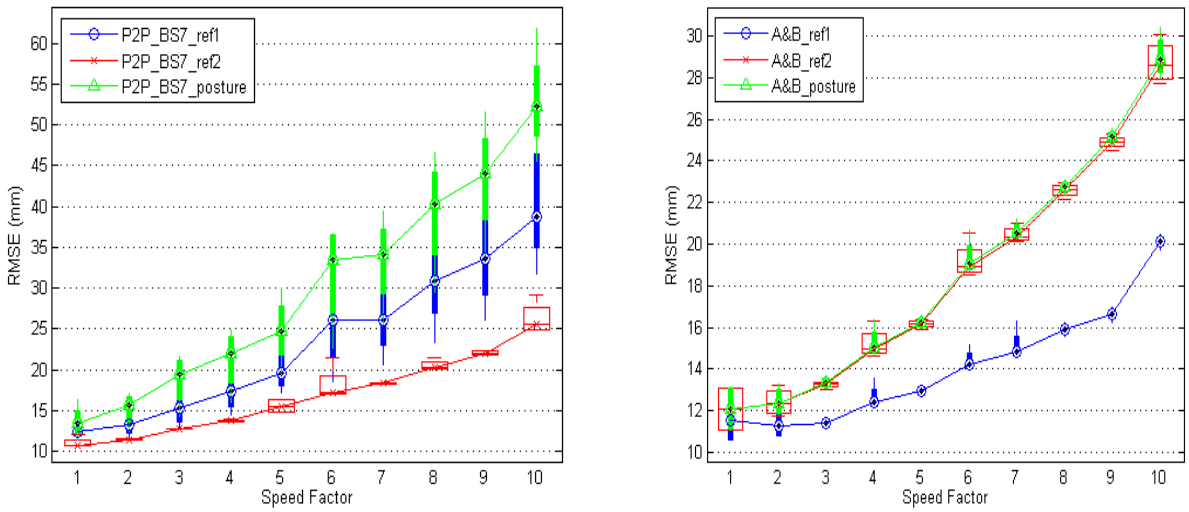

Figure 3-15: RMSE distribution of all NS_i with (a) P2P-B and (b) A&B under Yoga activity

C. Evaluation of position-related errors using P2P-B and A&B under the Yoga and Walking scenarios

In our two last studies, we analyzed the performance of the different Mobility-level slot allocation schemes and 3-WR scheduling strategies to estimate the positions of nodes under a controlled scenario, e.g. Yoga activity. From these studies, we found two scenarios opposed showing the best case and worst case for positioning. In this last study, we extend the evaluation by looking the distribution of the WC and BC positioning error under two different scenarios, Yoga and Walking, as detailed in Section 3.3.2. **Figure 3-16** and **Figure 3-17** presents the cumulative distribution function (CDF) of the RMSE under both mobility scenarios. As expected, the positioning error distribution is dependent on the mobility scenario and on the handshake transaction protocol. If we compare the mobility scenarios, the Yoga scenario, characterized by a low mobility) naturally presents a lower positioning error than the pedestrian walk scenario (characterized with a higher mobility).

Table 3-1 summarizes the average positioning error for all situations. We note that the level of improvement obtained by using the A&B protocol in place of the P2P-B protocol depends on the considered mobility scenarios. In the case of the **Yoga Activity,** the gain of A&B is small for the BC (10%) and more important for the WC (50%). On the other case, the **Walking scenario** shows a gain of 50% with A&B for both WC and BC. To complete this study, we can compare this results with the performance of the ``raw'' P2P algorithm (Section 3.3.3), which does not aggregate requests in a single broadcasted packet. We note that P2P is very close to the performance of P2P-B, which shows that a higher gain results from grouping answers (A&B) rather than requests (P2P-B).

Mean Error (mm)		Yoga	Walk
Worst Case	P2P-B	6.6	10.2
	A&B	3.4	4.8
Best Case	P2P-B	2.8	4.1
	A&B	2.5	2.6

Table 3-1 : Average position estimation error in the WC and BC

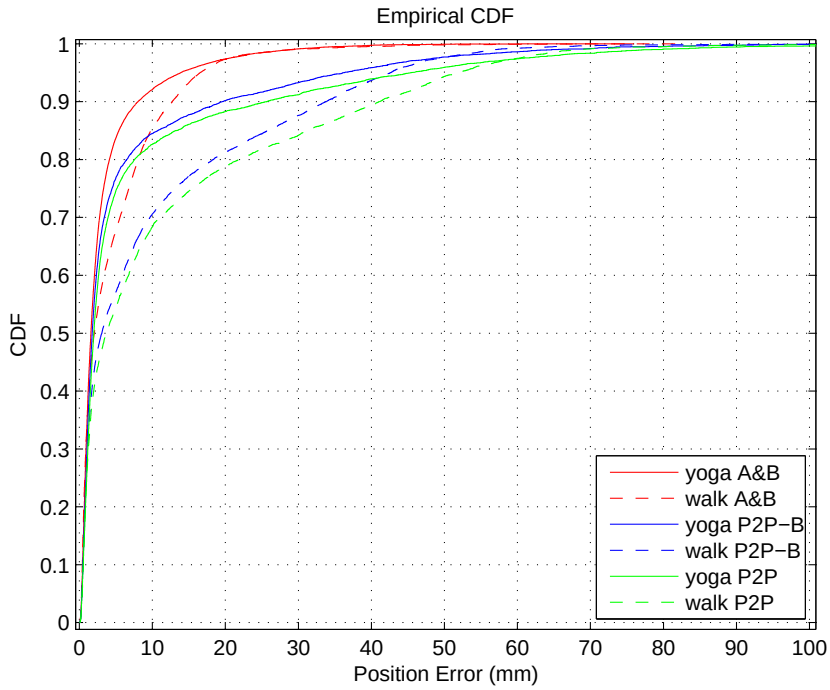

Figure 3-16: CDF of RMSE for the Worst Case: A&B and P2P-B w.r.t $P_{\mathbf{final}_i}$ using NS1

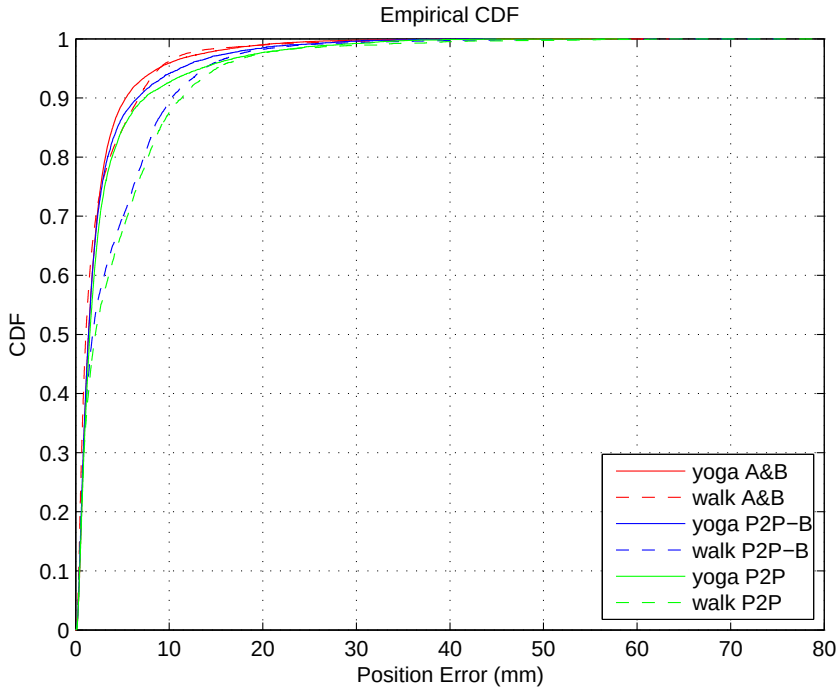

Figure 3-17: CDF of RMSE for the Best Case: A&B (resp. P2P-B) w.r.t . P_{ref1_i} (resp. P_{ref2_i}) independently on the NSi

3.3.5 CONCLUSION

In this second study, we quantified the impact of mobility on the positioning estimation with different MAC schemes on the slot allocation based on real mobility traces. For this, we implemented a full stack cross-layer protocol in an event-based simulator (WSNet) and we compared A&B and P2P-B strategies with different slot allocation policy depending on the nodes mobility level. As the position of nodes change several times during a frame duration, we focused on the estimation of positions at the beginning (resp. end) of the frame and the instantaneous positions. Our preliminary results with P2P-B show that a slot allocation at the beginning (resp. end) of the frame for nodes with high mobility produces a more accurate estimation of P_{ref1_i} (resp. P_{final_i}). Moreover, the mobility level policy has no impact when estimating the instantaneous position P_{ref2_i} with P2P-B. When considering A&B, P_{ref1_i} becomes the best estimated position because of a reduced $\Delta t1$. Besides, A&B allows a greater flexibility with any NS_i. On the basis of this results, A&B yields to a better performance than P2P-B in terms of latency and accuracy for all the scenarios.

3.4. DISCUSSION AND PERSPECTIVES

As explained on the first Chapters, localization with IR-UWB BAN has several constraints in terms of reliability, delay and accuracy. Our previous results highlighted that there is a ranging error due to different ToF of the 3-WR transactions coming from different delays of delivery with nodes under high mobility. Therefore, as the position estimation depends on the distance estimation with different anchors, it is straightforward that on-body nodes will find different positioning errors depending on the scheduling of n-WR packets. Besides, the nodes of a WBAN move with different speed depending on the scenario and their positions on the body and hence, the packets delays have different impact on the positioning. To overcome this, we addressed two main problems of MAC design for localization: scheduling of n-WR packets and slot allocation policy. In Section 3.2, we considered the comparison of different scheduling strategies of 3-WR packets on the position estimation. In our first results to estimate the position of one node, we found a tradeoff between ranging and positioning accuracy, i.e. it is better to choose a strategy that estimates distances closer to the desired position more than the strategies estimating accurate distances. In the case of n nodes, the choice of a scheduling strategy depends on the required application. For instance, in the case of the individual motion capture of nodes (resp. posture recognition), the best scheduling scheme consists on the estimation of nodes position one by one (BS7) with the anchors (resp. estimation of nodes position at once by sending all request first and then each anchor respond one by one (BS5)). In Section 3.3, we compared different slot allocations schemes depending on the speed of nodes. It turns out from our results that when comparing P2P-B and A&B with different mobility scenarios, we found that in the case of a scenario with low motion (e.g. Yoga) the positioning performance gap is smaller between both strategies. But when considering the case where nodes move faster (e.g. Walking), A&B outperforms P2P-B with a greater flexibility on the slot allocation regardless of different speeds between nodes. However, to develop an adequate and flexible cross layer protocol for localization, a fine knowledge about the WBAN channel is required. For this reason, we enlarge the study in the next chapter by considering

the packet error rate over realistic channel models and realistic mobility scenarios to evaluate the impact of short-term and long-term variations on the positioning success rate.

4. CROSS-LAYER PROTOCOL STRATEGIES FOR ENHANCED COOPERATIVE LOCALIZATION UNDER NON-PERFECT CHANNEL CONDITIONS

4.1. INTRODUCTION

As explained in Chapters 2 and 3, the ultimate distance measurement performance, considering ranging accuracy and time measurement, is derived from signal bandwidth. The ranging estimation based on time-of-flight depends on the precision of time measurements which is a direct function of signal bandwidth. UWB offers a pulse width of nanoseconds and a bandwidth of several hundred megahertz; therefore, it enables ranging and position accuracy on the order of centimeters, necessary for indoor location and short term range applications. In WBAN context, the ranging performance can be degraded due to the high nodes mobility and channel instability [25] (Deliverable D2.3 and D2.4). From one side, the mobility has an impact on the distance accuracy at the protocol level during the transmission of packets (e.g. 3-WR), this can be solved by reducing the delays of response packets with scheduling strategies proposing broadcast transmission and data aggregation. In the other side, the nodes located on the body may move producing variations on the channel and the visibility with the anchors will not be possible all the time due to the body shadowing. Therefore, the IR-UWB BAN system will face two problems, the decrease of ToA estimation accuracy and the increase of packet loss. The detection of pulses can be improved with the receiver system implementation at the PHY Layer, while the packet loss can be mitigated through cross-layer cooperative strategies based on Link Quality Estimators (LQEs).

Link quality estimation is a fundamental technique in wireless communications to overcome the unreliability of links due to the channel loss, and on which most of the protocols are based, such as localization algorithms [52], routing [65] and MAC topology control [67]. In literature [68], we can classify the link quality estimators in two categories: hardware-based estimators and software-based estimators. Hardware-based estimators are related with the PHY layer after the signal processing, e.g. Link Quality Indicator (LQI), Received Signal Strength Indicator (RSSI) and Signal to Noise Ratio (SNR). These techniques are easy of implementation and do not need additional computation. However, these metrics are only evaluated for successfully received packets. Therefore, they may overestimate the transmission performance for links under high packet loss. On the other hand, Software-based estimators evaluate the link quality by measuring the successful packet reception or the average number of packet transmissions required for a successful reception, e.g. the Packet Reception Ratio (PRR), the Required Number of Packet Transmissions (RNP), the Expected Transmission Count (ETX) and the Window Mean with Exponentially Weighted Moving Average (WMEWMA). The main advantage of these mechanisms is the increase of accuracy of link quality estimation and reliability. However, most of these LQEs were designed for WSN to detect the presence of links which are reliable on the long-term, and are thus not adapted to the specific context of

highly dynamic WBSNs, as shown in our previous works [67]. In Deliverable D2.3 and D2.4, we showed that on-body links present several channel fluctuations having an impact on stability at short-term. For instance, routing and topology control protocols based on long term estimation might ignore some transient link quality fluctuation, i.e. they do not re-compute information at each time the channel suffers variations to reduce overhead, complexity and energy cost. Therefore, the detection of reliable short-term links is a key requirement along with flexible long-term evaluation.

In our localization context, the long-term LQE can help to evaluate the positioning success rate to identify the anchor nodes having bad channel conditions with the mobile nodes. While the short-term LQE may detect the contact and inter-contact duration [69] between the nodes and thus predict the periodicity and duration of reliable links. Thus, if we take advantage of both LQE, we can detect mobile nodes with better channel conditions to be assigned as dedicated anchors to other mobile nodes once they have estimated their own positions. In [70], the authors proposed a probabilistic routing protocol exploiting short-term and long-term at the multi-hop selection process to route inertial information of body movements. The obtained experimental results show that the proposed routing schema outperforms existing approaches in terms of packet delivery ratio and delay performance. However, this is not suited in our scenario since they exploit inertial data, such as speed and acceleration estimation for the long-term prediction of reliable nodes. In [52], authors compared the performances of non-cooperative and cooperative localization with simultaneous mobile-to-anchor and mobile-to-mobile ranging estimation (i.e. virtual anchor nodes). Obtained simulation results show that thanks to the spatial diversity and the measurement redundancy, cooperative localization approaches are more robust to packet loss and provide a better positioning success rate at the cost, however, of slightly increased positioning error, higher latency and energy consumption. However, they did not consider an efficient choice of virtual anchor nodes with a non-realistic mobility model. In our last results in [71], we confirm with a realistic scenario (mobility and channel models) that the cooperative localization precision and the obtained frame duration at big network size, could be highly compatible with the coarse motion capture applications (as detailed in Deliverable D3.5 and D3.6). In this Chapter, we propose a distributed-cooperative algorithm to increase the localization performance of WBAN nodes. For this, we quantify the positioning success rate defined as a long-term LQE measuring the probability to complete the ranging estimation with the minimum anchors needed for a three dimensional positioning. Then, we analyze the (short-term) channel variations of different WBAN mobile nodes under realistic scenarios in order to find the best mobile nodes to become cooperative virtual anchors.

4.2. LINK BETWEEN RANGING PACKET LOSS AND POSITIONING

In our previous work, we considered a perfect channel in order to quantify only the impact of mobility. However, mobility is not the only issue for WBAN positioning, the channel variations can produce high packets loss. In fact, each node needs to perform the ranging estimation with several anchors depending on the geometrical localization suited, e.g. one node needs to estimate its distance with at least 3 anchors (resp. 4) for a 2-dimensional positioning (resp. 3-D). If one of these transactions is affected by the channel, it might lead into

a packet loss and therefore positioning errors. In this Section, we evaluate the positioning success rate of nodes placed on the body using a PHY layer based on IR-UWB with two different channels [72]: (a) a theoretical channel model based on the on-body CM3 channel (Anechoic chamber) and (b) a simulated channel calculated with the PyLayers ray-tracing simulator. For this purpose, each node calculates its relative position with the estimation of its distances with the on-body anchors. Accordingly, the distance between two nodes can be estimated with the transmission of three packets, as defined by the 3-WR. Moreover, we analyze the positioning success rate with three scheduling strategies (Single node localization (P2P), Broadcast Single node localization (P2P-B) and Aggregated & Broadcast (A&B)) with a MAC layer based on time division multiple access (TDMA) and under a realistic pedestrian walking scenario.

4.2.1 NETWORK TOPOLOGY AND MOBILITY SCENARIO

We consider a WBAN in full-mesh connectivity where all nodes can communicate pair-to-pair. We define two types of sensors: the on-body anchor nodes *j* with perfect knowledge of their relative and absolute positions at any time and the on-body mobile nodes *i* who want to estimate their relative positions. These sensors communicate with a physical layer based on IR-UWB pulses to estimates their distances ($\hat{d}_{ij}(t)$) through 3-WR. Then, each mobile node estimates its position ($\hat{P}_i(t)$) with all the distances estimated.

In this study, we evaluate the performance of an IR-UWB based WBAN system in a daily context, such as the walking scenario. The mobility model was obtained during the measurement campaign related to the CORMORAN project at the M2S laboratory, ENS Cachan, France in June 2014, as detailed in Section 2.3.3. We deployed 16 cameras Vicon based on infrared technology at a rate of 100 Hz. Thus, the motion capture was performed in a confined space of 10x6 m². Accordingly, we consider a pedestrian walking scenario of 100s. The person starts in the middle of the scene performing a 360° rotation with pause of 5 seconds every 90°, then he starts moving at moderate speed along a rectangular trajectory centered on the starting point. The WBAN is composed by 4 anchors and 6 mobile nodes, as shown in **Figure 4-1**. The on-body anchors are positioned on: the right chest (A_1), the left chest (A_2), the left hip (A_3) and the back (A_4). The mobile nodes are located on the right wrist (N_5), left wrist (N_6), right ankle (N_7), right head (N_8), left ankle (N_9) and left knee (N_{10}).

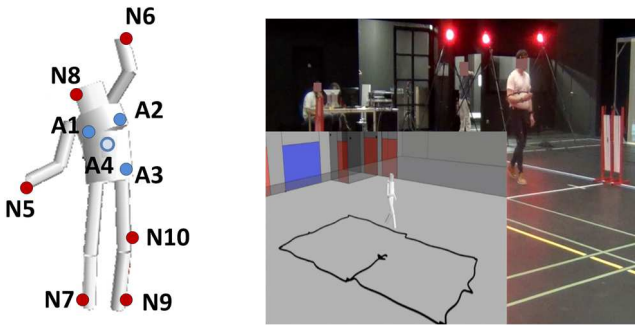

Figure 4-1: Mobility Model (a) Network topology with 4 on-body anchors (blue) and 6 mobile nodes (red) (b) Pedestrian Walking scenario

4.2.2 CONSIDERED MAC SCHEDULING PROTOCOLS

We consider that a positioning is achieved if a node *i* is able to complete the 3-WR transactions (r) with the M anchors on the network. Accordingly, the 3-WR packets are delivered with all the anchors using a MAC frame composed by enough slots. Then, we evaluate the positioning success rate with 3 different MAC strategies (**Figure 4-2**) based on TDMA (beacon-enabled and synchronized), as proposed in Section 2.3.2:

- **Single node localization (P2P)** where each node *i* send the request packets Q_{ij} to the anchors in order. Then, each anchor answers with $R1_{ji}$and $R2_{ji}$ successively in single-links to the nodes.
- **Broadcasted single node localization (P2P-B)** where each node *i* intend to send the requests Q_i to the anchors in broadcast. Thereafter, each anchor answers with $R1_{ji}$and $R2_{ji}$ successively in single-links.
- **Aggregated and Broadcast (A&B)** where nodes send the requests Q_i in broadcast. Then, each anchor *j* gathers the ToA of each request and sends a response ($R1_j$) with all the aggregated timers, followed by the response ($R2_j$).

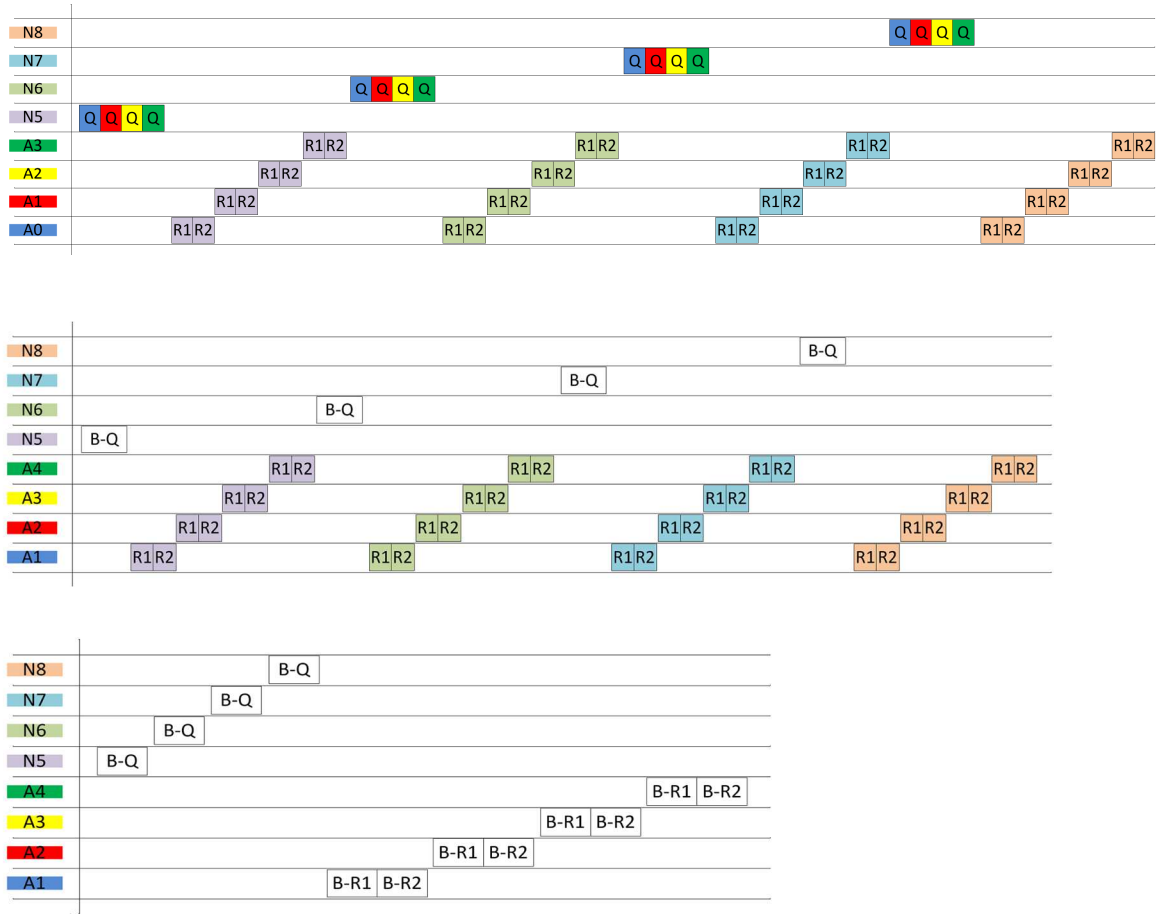

Figure 4-2: MAC scheduling for 3-WR packet transmission (a) P2P (b) P2P-B (c) A&B

4.2.3 PACKET LOSS RELATED TO THE WBAN CHANNEL

In this work, we evaluate the positioning success with three different channel models under the same realistic mobility scenario. We mimic the motion capture process where mobile try to find their positions in the LCS with the anchors nodes embedded on the body. For all the channel models, we define the Packet Error Rate (PER_r) as the probability to lose a 3-WR packet r when it is received with a Rx power P_{Rx} lower than a certain Rx threshold (ρ):

$$PER_r = \mathbb{P}(P_{Rx}(d_{ij}) \leq \rho) \quad \textbf{(4-1)}$$

Empirical channel model. First, we consider an empirical theoretical model for the on-body links. For that, we implement the path loss model CM3 for the 3.1-10.6 GHz band frequency as described in [22]:

$$PL_{on-Body}(d)[dB] = a * log_{10}(d) + b + N \quad \textbf{(4-2)}$$

where a and b are linear fitting parameters of the model, N is a normal distributed variable with zero mean and standard deviation σ_N, and d is the distance (in mm) between the on-body nodes. In our study we use the parameters defined for the Anechoic Chamber which fits with our mobility scenario: a = 34.1, b = -31.4 and σ_N = 4.85. The power of the received packet is calculated as a function of the transmission power (P_{Tx}) and the gains of the transceiver (G_{Tx}) and receiver (G_{Rx}) as follows $P_{Rx} = P_{Tx} + G_{Tx} + G_{Rx} - PL(d)$. The transmitter power is fixed to P_{Tx} = -10dBm and the antenna gain to $G_{Tx} = G_{Rx}$ = 0dB according to the IEEE802.15.6 standard regulation for IR-UWB (-41dBm/MHz) [44].

Simulated channel model. In this model, we use a full ray tracing simulation of the large band radio links calculated by PyLayers. We consider an antenna model [73] mounted within the mobility model to consider the position and orientation of the simulated devices. Note that this channel presents a shadowing of the body affecting the nodes on the extremities and a selective fading with a delay spread higher than 64 ns, but we reduce the inter-symbol interference with a symbol period higher than the delay spread. The details of PyLayers workflow can be found on Deliverable D2.5 and D4.1.

4.2.4 POSITIONING SUCCESS RATE RELATED TO THE SENSITIVITY THRESHOLD

We use the discrete-event simulator WSNet to implement the different channel models. We implemented a MAC a protocol based on TDMA with the strategies P2P, P2P-B and A&B, as detailed in Section 4.2.2. The duration of the MAC frame is designed according to the standard IEEE802.15.6 UWB PHY layer on default mode (OOK modulation and 0.4875 Mb/s). Finally, we exploit the traces of the walking scenario acquired during the CORMORAN project, as described in Section 4.2.1. For all the channel, we fix the sensitivity threshold to ρ = -91 dBm (w.r.t the standard default mode).

Figure 4-3 and **Figure 4-5** (resp. **Figure 4-4** and **Figure 4-6**) represent the positioning success rate when distances are estimated with 2-WR (resp. 3-WR) with the different channel models. We observe that 2-WR compensates the 3-WR loss and increases the positioning success rate,

especially with the simulated channel. However, this cannot be a final conclusion because it is necessary to evaluate the ranging error (clock drift) with 2-WR. Moreover, the results show that nodes located on the ankles (N_7 and N_9) have the lower positioning success rate with all the channels and MAC strategies. This is due to the higher mobility of these nodes compared to the nodes placed on the head or wrists and hence the shadowing and multipath affects more these nodes. When comparing our results from empirical model, they seem to be similar but they are not the same, this is because of the sensitivity threshold. If we analyze the evolution of links Rx power (not presented here), we observe that almost all the decays (e.g. the path loss from the empirical model) are over the Rx threshold; therefore, there is low packet loss. On the contrary, the simulated channel is affected by strong slow/fast fading below the sensitivity threshold. Finally, it is important to note that the different MAC strategies have similar positioning success rate, but when we compare the number of positions estimated with each scheme (**Figure 4-4 (b)** and **Figure 4-6 (b)**), we observe that A&B is the best choice because it let us estimate more positions.

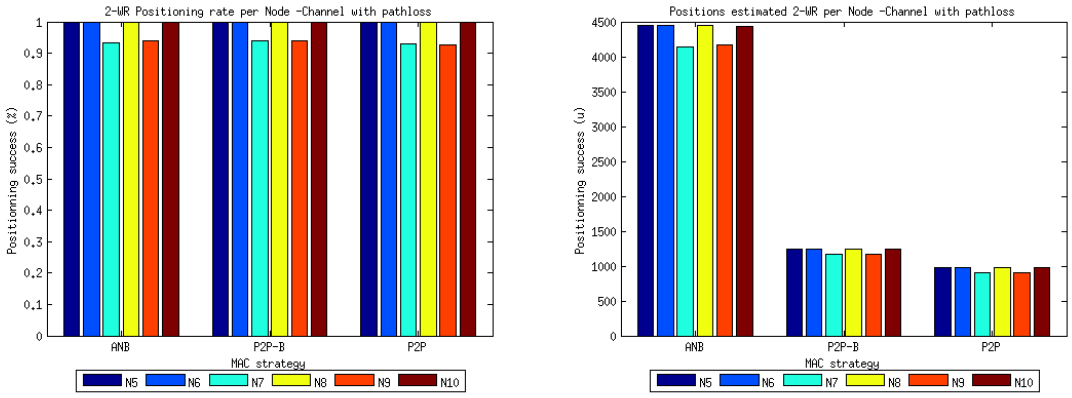

Figure 4-3: Evaluating (a) Positioning success rate and (b) Positions estimated for all mobile nodes using 2-WR and different MAC strategies (A&B, P2P-B and P2P) with the empirical channel model (CM3)

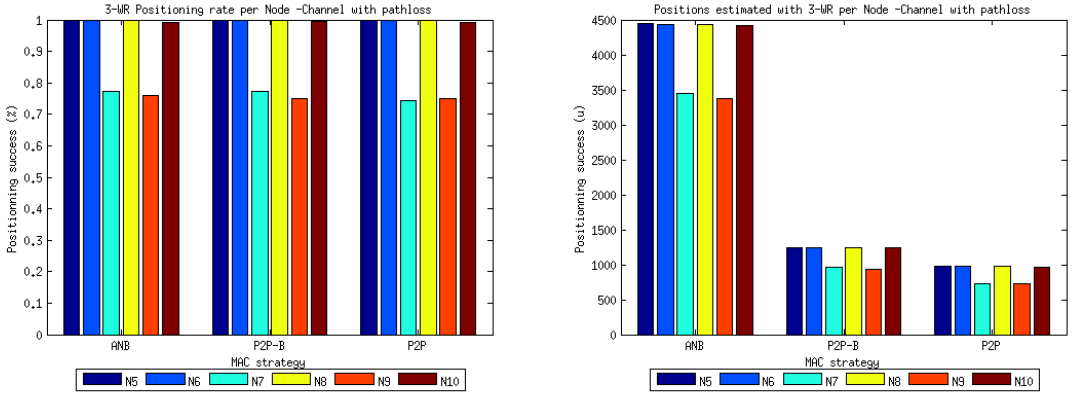

Figure 4-4: Evaluating (a) Positioning success rate and (b) Positions estimated for all mobile nodes using 3-WR and different MAC strategies (A&B, P2P-B and P2P) with the empirical channel model (CM3)

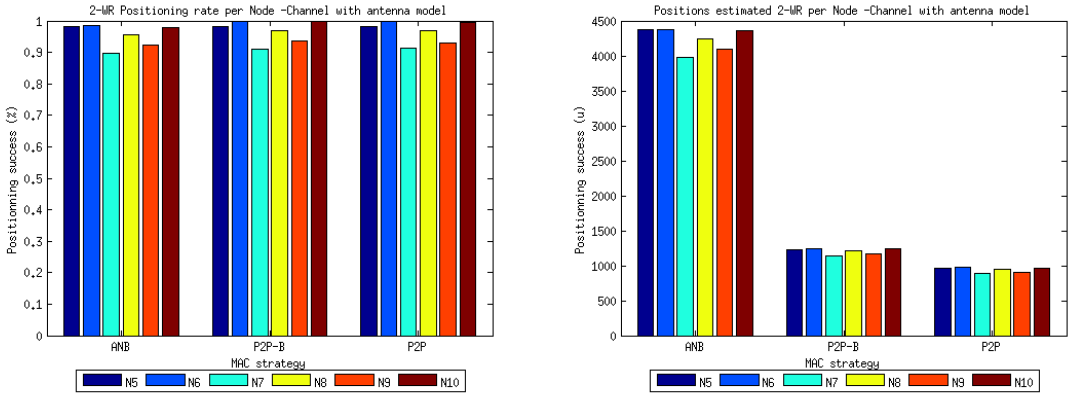

Figure 4-5: Evaluating (a) Positioning success rate and (b) Positions estimated for all mobile nodes using 2-WR and different MAC strategies (A&B, P2P-B and P2P) with the simulated channel model (PyLayers)

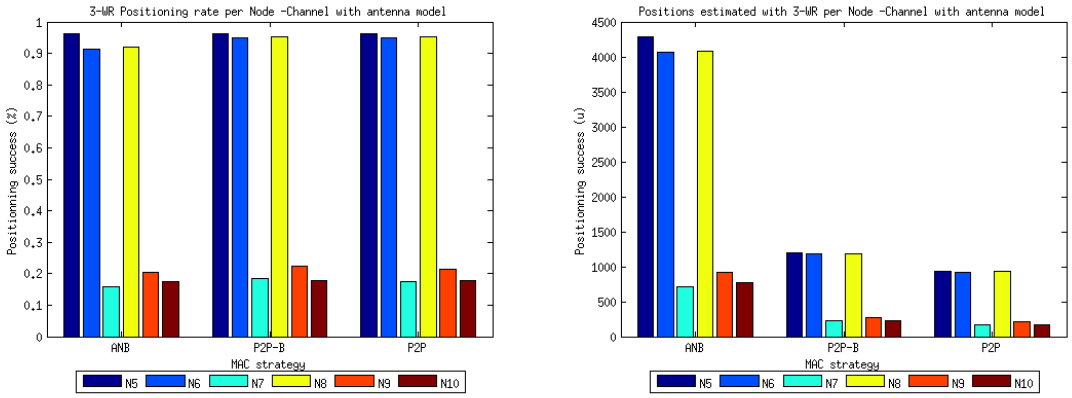

Figure 4-6: Evaluating (a) Positioning success rate and (b) Positions estimated for all mobile nodes using 3-WR and different MAC strategies (A&B, P2P-B and P2P) with the simulated channel model (PyLayers)

4.2.5 CONCLUSION

This first analysis shows the impact of channel variations on the positioning success rate. We observe that the positioning success rate is affected by all the implemented channel models with a fixed sensitivity threshold at the receiver (ρ = -91 dBm). The main finding is that A&B is the best choice because it let us estimate more positions even through channels with slow and fast fading. As explained in Section 3.3.3, A&B has a smaller frame duration than P2P and P2P-B. This means that under this sensitivity condition at the receiver A&B performs more ranging transactions, and even with higher packet loss than P2P or P2P-B, the number of estimated positions is higher and this compensates the positioning success rate. However, it is necessary to quantify the positioning success rate with different sensitivity threshold to validate these results.

4.3. EVALUATION OF THE POSITIONING SUCCESS RATE

As discussed earlier, we aim to design a cross-layer algorithm to improve the localization protocol with IR-UWB WBAN. In our last results, we observed that the channel variations lead to the packet loss of 3-WR transactions and hence the decrease of positioning success. By this time, we fix the same sensitivity threshold for the reception of packets for all the nodes. In practice, the sensors may have different sensitivity at the reception of signals and the packet error rate might be different between them. For this reason, we quantify the upper and lower bounds of the positioning success in function of the sensitivity threshold at the receiver. We consider that a positioning is achieve if a mobile node i is able to complete the 3-WR transactions with the N_A anchors on the network. Accordingly, we evaluate the positioning success rate (P_{Succ}) for all the mobile nodes N_M with a MAC frame composed by enough slots to deliver the 3-WR packets with different scheduling strategies (e.g. P2P, P2P-B and A&B), as described in Section 4.2.2.

4.3.1 PROBLEM FORMULATION

Throughout the rest of the study, we will use the following notation: $\{P_i^M(t)\}_{i=1\dots N_M}$ and $\{P_i^A(t)\}_{i=1\dots N_A}$ denotes the unknown (resp. known) positions of the N_M on-body mobile nodes (resp. N_A on-body anchor nodes). Each node calculates its position $\hat{P}_i(t)$ after estimating their distance $\hat{d}_{ij}(t)$ with the anchors. The distance is evaluated with the ToF of the 3-WR packets ($r = \{Q_{ij}, R1_{ji}, R2_{ji}\}$). Let us note $\hat{d}(t) = [\hat{d}_{11}(t), \hat{d}_{12}(t), \dots, \hat{d}_{1\,N_A}(t),\ \hat{d}_{21}(t), \dots, \hat{d}_{N_M\,N_A}(t)]$ the matrix of distances estimated of all nodes during a MAC frame duration. Thus, the position estimation can be seen as a function of the estimated distances and the anchors positions collected with 3-WR at each frame. The function differs depending on the position algorithm, e.g. conventional algorithms (Linear Least Square Error (LLSE), Time Difference of Arrival (TDOA) [24]) and cooperative techniques (Maximum Likelihood (ML), Cooperative Constrained (CDWMDS) [27]). Therefore, in this work we focus on the collect of enough distances through cooperative MAC scheduling to increase the positioning success of nodes.

In this context, we analyze the channel effects (path loss, shadowing and fast fading) during each transaction on the 3-WR packets success, especially when taking into account the temporal correlation in the channel state due to the body movements. We define $l_{ij}(t)$ as the perceived link quality of packets. Accordingly, we denote the vector of links quality as $l(t) = [l_{11}(t), l_{12}(t), \dots, l_{1\,N_A}(t),\ l_{21}(t), \dots, l_{N_M\,N_A}(t)]$. It is important to note that during a frame duration, the links are not symmetrical [67], therefore, $l_{ij}(t) \neq l_{ji}(t)$ and $\hat{d}_{ij}(t) \neq \hat{d}_{ji}(t), \forall\, i \neq j$. Moreover, during the MAC frame each node can listen to all the on-body nodes transmission in order to collect all the links quality at its range.

In this study, we evaluate the received power (P_{Rx}) when considering three different channel models for the on-body links under the same realistic mobility scenario (as detailed in Section 4.2.3). We consider that a packet is loss when it is received with a reception power P_{Rx} lower than a the Rx threshold (ρ), as described in Equation 4-1. Thus, we measure the P_{Succ} in function of the 3-WR packet loss (PER_r).

4.3.2 SIMULATION AND PERFORMANCE EVALUATION

We consider the same scenario as that described in Section 4.2, i.e. a WBAN in full-mesh connectivity where all nodes can communicates in pairs. The WBAN is composed by 4 anchor nodes and 6 mobile nodes embedded on the body to evaluate their positioning success rate (P_{Succ}). We use the discrete-event simulator WSNet to implement the different channel models (Section 4.2.3). This simulator has implemented a MAC protocol based on TDMA with the P2P, P2P-B and A&B algorithms, as detailed in Section 4.2.2. The duration of the MAC frame is designed according to the standard IEEE802.15.6 UWB PHY layer on default mode (OOK modulation and 0.4875 Mb/s). Finally, we exploit the traces of the walking scenario acquired during 100s of measurement, as described in Section 4.2.1. Within this framework, we evaluate the impact of the channel effect on the P_{Succ} of each mobile node. The on-body anchors are positioned on: the right chest (A_1), the left chest (A_2), the left hip (A_3) and the back (A_4). The mobile nodes are located on the right wrist (N_5), left wrist (N_6), right ankle (N_7), right head (N_8), left ankle (N_9) and left knee (N_{10}).

Figure 4-7, Figure 4-8 and **Figure 4-9** show the P_{Succ} as a function of the Rx threshold ρ for each MAC strategy (P2P, P2P-B and A&B respectively) with all channel models. As expected, the P_{Succ} decays when the threshold increases for all the nodes in all the scenarios. This is because the 3-WR packet error rate increased as well and hence the mobile nodes do not achieve the estimation of the minimum required distances for the positioning.

Observation 1 (body shadowing has an important impact on positioning). If we compare the P_{Succ} between the different channels, we observe that the shadowing due to the body obstruction (included in the simulated model) has higher effect on the P_{Succ} than the free space path loss of the empirical model. For instance, the P_{Succ} in the empirical case (**Figure 4-7 (a)**, **FIGURE 4-8 (a)** and **FIGURE 4-9 (a)**) decays for all the nodes and the difference is due to the distances between the nodes and anchors, e.g. the nodes in the ankles (N_7 and N_9) show the worst P_{Succ}. In the simulated channel case (**Figure 4-7 (b)**, **FIGURE 4-8 (b)** and **FIGURE 4-9 (b)**), the nodes placed on the legs (N_7, N_9 and N_{10}) have a lower P_{Succ} due to the higher shadowing of the body compared to N_5, N_6 and N_8.

Observation 2 (scheduling robustness – the packet loss is more critical in A&B). We can also note that there is different P_{Succ} between the MAC strategies (**Figure 4-7, FIGURE 4-8** and **FIGURE 4-9**), specially with A&B. In the case of P2P and P2P-B, there is a similar performance on positioning. This is because the short-term channel condition does not change fast enough during the 3-WR transactions of one node to create a different packet loss on the Request packets between P2P and P2P-B. In other words, sending one broadcasted request packet instead of 4 pair-to-pair request packets does not improve the reliability against packet loss. On the other hand, if we compare P2P or P2P-B with A&B, we observe that A&B show a smaller P_{Succ}. This is more visible with the simulated model. In fact, in Section 4.2.4 we showed that broadcasting 3-WR packets with a sensitivity threshold of -91dBm reduces the latency of positioning and the number of positions estimated is higher. However, when the receiver is

less sensitive to loss, the criticality of broadcasted packets loss is higher and the P_{Succ} might decrease considerably.

From this study, we conclude that from a certain sensitivity threshold, P2P and P2P-B have better positioning success rate than A&B. This result is important to consider depending on the regulations of each country and the radio capabilities of the sensor. Thus, P2P-B may be better to consider for localization purposes when the channel is expected to be high time-varying (e.g. running case). For the remaining of our study, we will compare only the positioning performance between P2P-B and A&B.

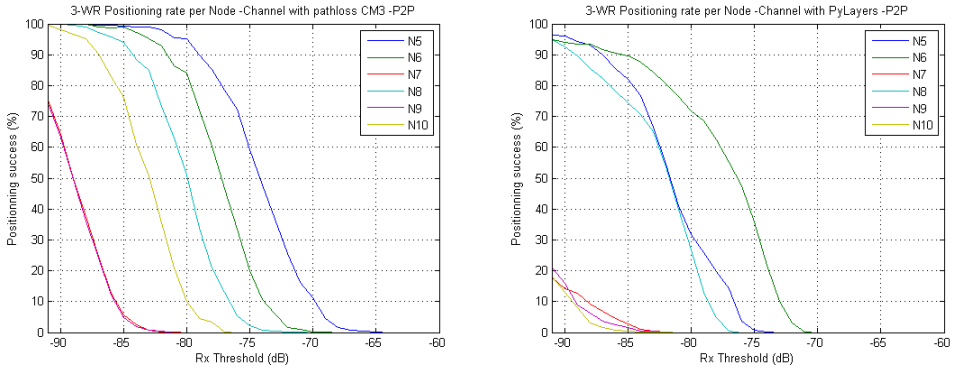

Figure 4-7: Comparison of P_{Succ} using P2P with different channel models: (a) empirical model – CM3 (b) simulated model – PyLayers

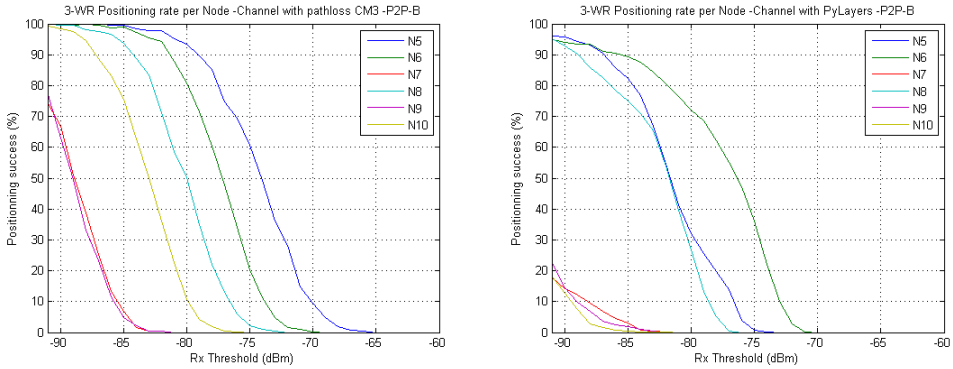

Figure 4-8: Comparison of P_{Succ} using P2P-B with different channel models: (a) empirical model – CM3 (b) simulated model – PyLayers

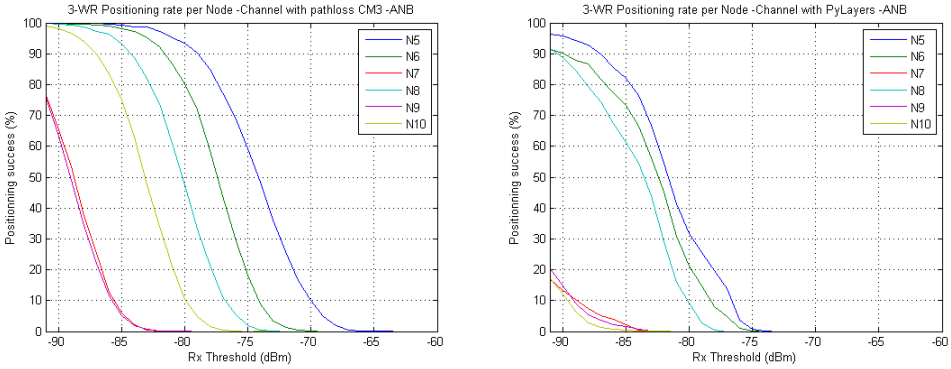

Figure 4-9: Comparison of P_{Succ} using A&B with different channel models: (a) empirical model – CM3 (b) simulated model – PyLayers

4.3.3 CONCLUSION

As explained in Section 4.1, cooperative localization between mobile nodes can improve the P_{Succ}. Authors in [52] show that using virtual anchors for positioning mitigates the packet loss. However, their results are not optimal since they do not consider realistic scenarios and they assume that the localization can be done with any node that had already estimated its position. In practice, depending on the nodes positions and mobility, the communication between the nodes is not always possible. Therefore, not all the mobile nodes can become virtual anchors, it is necessary to choice them with long-term and short-term to avoid the waste of resources without improving the localization performance.

To illustrate this, let us consider the worst positioning case from our results, N_7 and N_9 in A&B using the simulated channel (**Figure 4-8 (b)**). Here we can observe that these nodes located on the legs present less than 30% positioning success rate. This means that their communication with some anchors is obstructed in almost all the simulation and hence the ranging estimation may be compromised. For this reason, we aim to replace the anchors with bad ranging success rate with other on-body nodes with a better link quality.

Figure 4-10 shows the evolution of the average reception power (dBm) of links at each frame for nodes N_7 and N_9. If we observe the evolution of the channels variation of these nodes with the network, we note that the links with anchors A_1 and A_2 are under -91dBm almost all the time. On the other hand, the links with the other on-body nodes seems to be better, especially with the node located on the right wrist (N_5) which has a better P_{Succ}. This is normal because N_5 remained quasi-static during our mobility scenario, i.e. the subject mimic a person looking to his smartphone during the walking. Thus, in this scenario, we can imagine N_5 as a possible virtual anchor for the nodes on the legs. However, this assumption need to be validated with long/short-term LQEs.

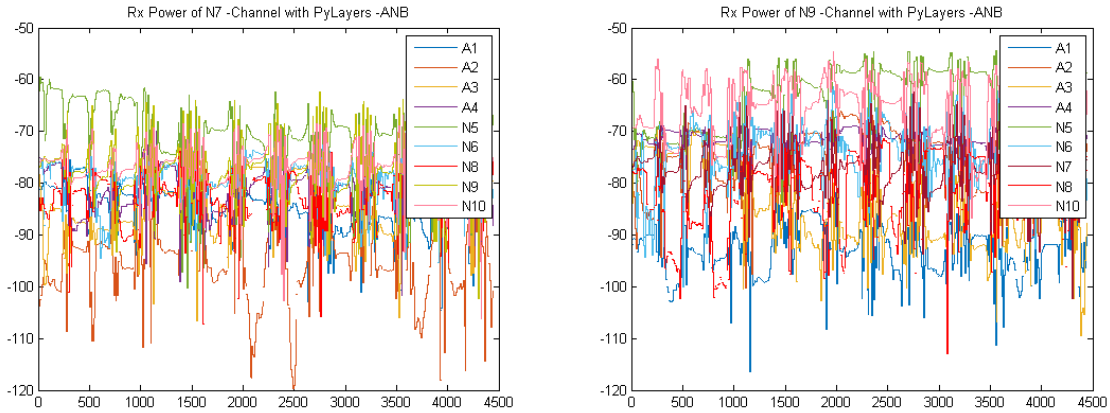

Figure 4-10: Comparison of the reception power of packets between the nodes having the worst P_{Succ} with the simulated channel model a) N_7 b) N_9

4.4. COOPERATIVE SOLUTION FOR INCREASED POSITIONING SUCCESS RATE

4.4.1 PROBLEM FORMULATION

The contribution of this section is two-fold. First, we propose to observe two LQEs based on long-term link reliability: i) the positioning success rate (P_{Succ}) to identify the nodes having the worst positioning performance and ii) the ranging success rate to indicate the anchors that need to be replaced by virtual anchor nodes to increase the P_{Succ}. At this stage, each node analyzes the short-term reliability with the other nodes over a period of time. For this, the nodes exploit the periodic 3-WR packets exchanges to collect instantaneous link quality estimation with all the on-body sensors at its range. During the second phase, each node computes the short-term quality to find the links with higher packet reception rate. Then, they estimate the probability of ranging success to achieve a long-term positioning success rate. The resulting is a time-varying matrix showing which are the best virtual anchors for each mobile node to increase its P_{Succ}. With this matrix we propose a conditional on-body anchor permutation to choose the virtual anchors maximizing the probability of positioning.

4.4.2 METHODOLOGY AND PARAMETERS

For this study we consider the same network topology, walking scenario and simulation parameters presented in Section 4.2.1. However, we will only focus on P2P-B and A&B performances with the three channel models. Moreover, in order to evaluate the behavior of our proposed mechanism, we will fix the sensitivity threshold where some mobile nodes present a poor P_{Succ}. For instance, if we observe our results in **Figure 4-8** and **Figure 4-9,** we note that when the threshold is $\rho = -80\ dBm$, the nodes decrease their P_{Succ} to 50% with both MAC strategies and channels, and they have total loss when $\rho = -70\ dBm$ to $-65\ dBm$. Accordingly, it might be difficult to increase P_{Succ} with total loss because all the links are so affected that the anchors cannot be replaced so easily, especially if there is no nodes able to

estimate its own position. For the following of the study, we will consider the case where the sensitivity threshold is fix on $\rho = -80\ dBm$ for all the nodes.

4.4.3 LONG-TERM POSITIONING ANALYSIS

First, let us analyze **Figure 4-11** which shows the P_{Succ} for 100ms of simulation when $\rho = -80\ dBm$ with all the channels and MAC strategies. In the case of the empirical model (**Figure 4-11 (a)**), N_7 and N_9 present 0% of positioning, while the nodes on the wrist have a good P_{Succ}. In **Figure 4-11 (b)**, we observe that the shadowing from the simulated channel affects more A&B with less than 30% of P_{Succ} for all the nodes. Moreover, N_7, N_9 and N_{10} have 0% of P_{Succ} with all the strategies. For instance, only the nodes on the wrists and the head can help to improve the positioning of nodes. However, as we explained in Section 4.3, the P_{Succ} is not a sufficient long-term metric to evaluate the localization performance because it depends on the ranging success rate (R_{Succ}) with the minimum required anchors for positioning.

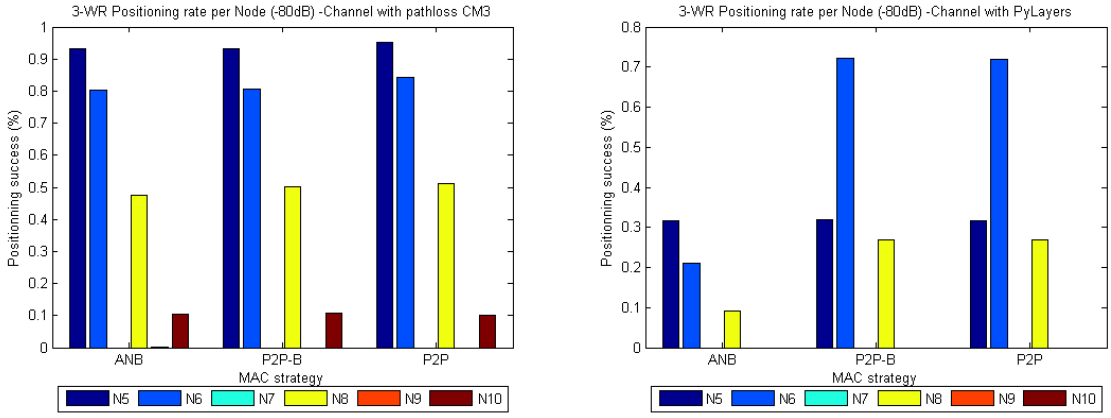

Figure 4-11: Comparison of the positioning success rate for all mobile nodes using different MAC strategies (A&B, P2P-B and P2P) and a sensitivity threshold $\rho = -80\ dBm$ with the channel models (a) empirical channel – CM3 (b) simulated channel – PyLayers

Figure 4-12 and **Figure 4-13** permit to give an insight on the reason of position loss. They show the underlying ranging success rate between the mobile nodes and the on-body anchor with when $\rho = -80\ dBm$. We observe that the ranging statistics is varying depending on the anchor position. For example, in the empirical case (**Figure 4-12**), N_7 and N_9 have a R_{Succ} lower than 30% for all the anchors, especially with A_1, A_2 and A_4 as the worst. Here, it would be necessary to replace these three anchors to increase the P_{Succ}. In the case of the simulated channel (**Figure 4-13**), the nodes N_7, N_9 and N_{10} show at least one anchor with 0% of ranging success. This explains why the positioning rate for these three nodes becomes critical. Therefore, it is only necessary to find one virtual anchor. From these results, we propose to look for other on-body nodes with a better link quality than the anchors having a bad R_{Succ}.

Therefore, these nodes could be seen as possible virtual anchors once they have estimated their own positions.

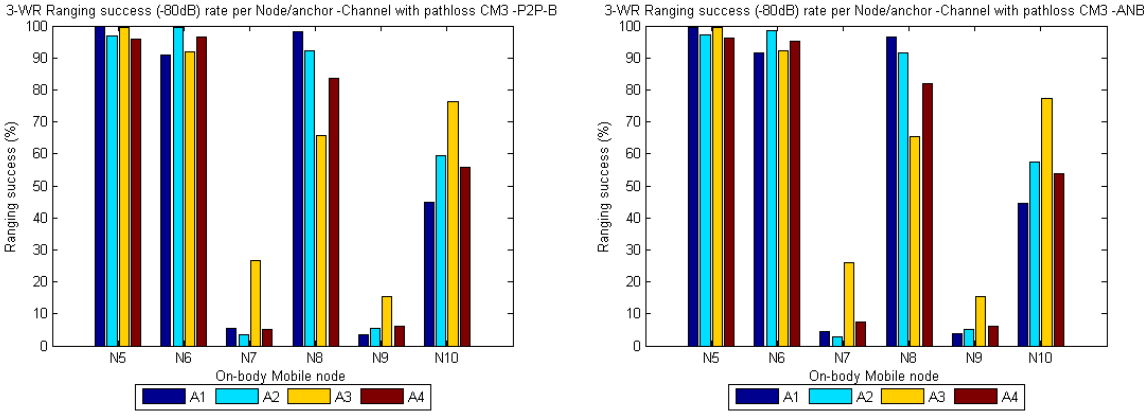

Figure 4-12: Comparison of the ranging success rate between (a) P2P-B and (b) A&B using the empirical channel model CM3 and a sensitivity threshold $\rho = -80\ dBm$

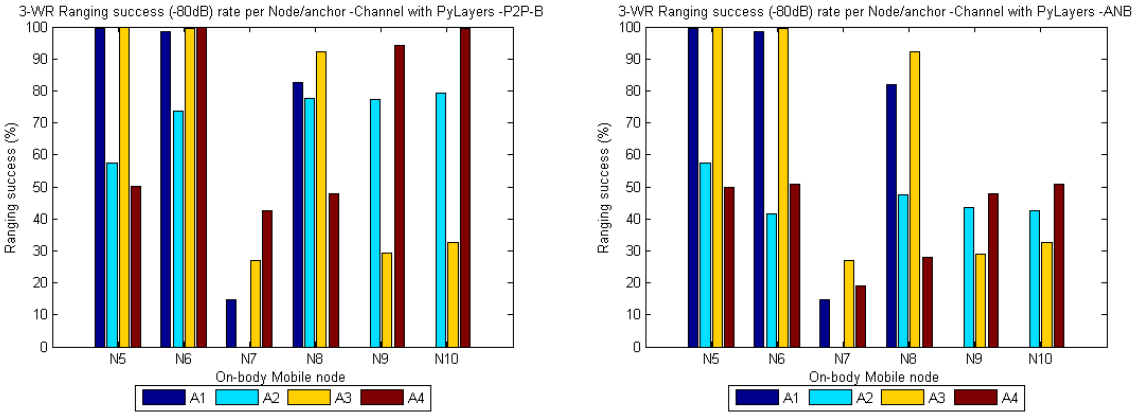

Figure 4-13: Comparison of the ranging success rate between (a) P2P-B and (b) A&B using the simulated channel model with PyLayers and a sensitivity threshold $\rho = -80\ dBm$

4.4.4 SHORT-TERM LINK RELIABILITY FOR COOPERATIVE AND DISTRIBUTED POSITIONING

In this second phase, we suppose that each node estimates its ranging success rate with each anchor and can collect the link quality of the 3-WR transactions. From this information, we propose a Bayesian approach to increase the probability of positioning success $\mathbb{P}(P_{Succ}\,|\theta)$ with the knowledge of two parameters (θ): the link quality distribution and the ranging success rate with the anchors. Let us note $\theta_{ik} = \{L_{ik}, D_{ik}\}$ the vector of parameters containing the distribution of the links quality and the ranging success rate collected during a defined positioning activity period (T_L) higher than the MAC frame period (T_F). As the positioning rate decreases because of a lower ranging success each node looks for the anchors presenting a

lower probability of R_{Succ}. Then, each node will identify the links with a higher probability of packet reception. Accordingly, we define the probability of packet reception (PRR) as follows:

$$\mathbb{P}_x(X \geq \rho) = \begin{cases} \int_{\rho}^{\rho_{max}} L_{ik}^{(r)}(x)dx, & for\ r = Q_{ik} \\ \int_{\rho}^{\rho_{max}} L_{ki}^{(r)}(x)dx, & for\ r = \{R1_{ki}, R3_{ki}\} \end{cases} \quad \textbf{(4-3)}$$

where X represents the random variable of link quality obtained during each T_L. For sake of simplicity, we assume that the channel decoder works correctly under this threshold and the probability of packet loss is bounded by the antenna capacities of reception which means that $\mathbb{P}_x(X \geq \rho)$ converge and it can be calculated in $[\rho, \rho_{max}]$, where ρ_{max} is the maximum power that we can receive. Accordingly, the probability of ranging success between the node i with the on-body anchor k and the probability of positioning success of node i with N_A' anchors are given by:

$$\mathbb{P}(R_{Succ} \mid \theta)_{ik} = \prod_r \mathbb{P}_x^{(r)}(X \geq \rho) \quad \textbf{(4-4)}$$

$$\mathbb{P}(P_{Succ} \mid \theta)_i = \prod_{k=1}^{N_A'} \mathbb{P}(R_{Succ} \mid \theta)_{ik} \quad \textbf{(4-5)}$$

Figure 4-14 and **Figure 4-15** represent the packet reception rate for A&B and P2P-B when the threshold is $\rho = -80\ dBm$. We observe for all the channels and MAC strategies that the on-body nodes, with low packet error success with some anchors (e.g. N_7, N_9 and N_{10}), have a better link quality with other on-body nodes leading to the possibility to select them as new virtual anchors. For instance, in the simulated channel, we observe that N_9 and N_{10} have 0% of PRR with A_1. In this case, we need to replace at least one anchor, **Figure 4-15** show N_5 and N_6 as the best candidates to become anchors. In the empirical case (**Figure 4-12**), N_7 and N_9 have a low R_{Succ} with all the anchors. But when we look at their probability of packet reception (**Figure 4-14**), we identify only two interesting mobile nodes to become virtual anchors, the opposite ankle node and the left knee. From these examples we can conclude that the number of anchors to replace is not a fixed parameter, some nodes will need to replace none or the 4 anchors and depending on their ranging success rate the algorithm for the choice of new virtual anchors is very important. Therefore, the P_{Succ} will be compromised for all the nodes. For this reason, we propose a conditional permutation strategy for the choice of anchors.

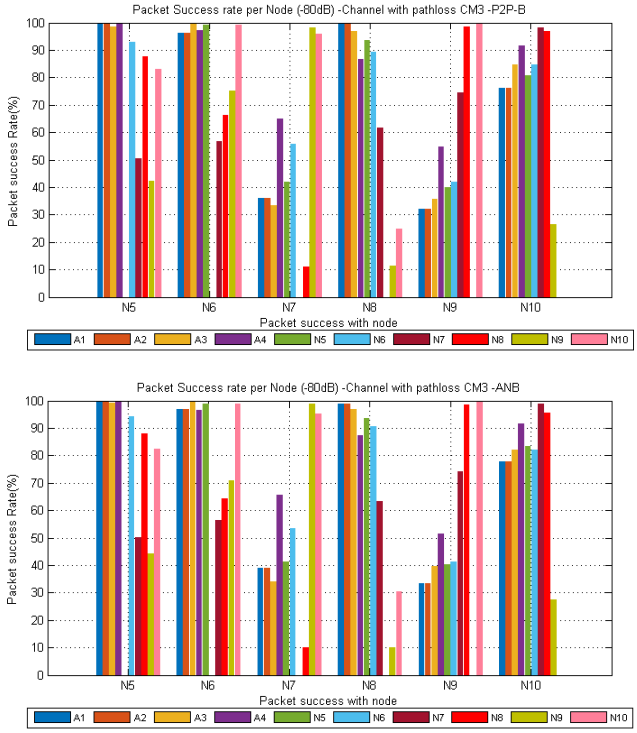

Figure 4-14: Comparison of the packet reception rate between (a) P2P-B and (b) A&B using the empirical channel model CM3 and a sensitivity threshold $\rho = -80\ dBm$

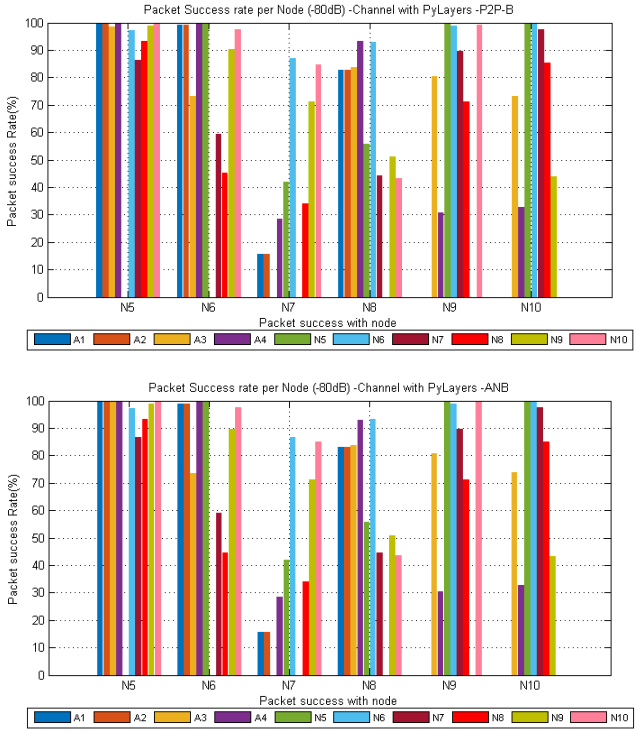

Figure 4-15: Comparison of the packet reception rate between (a) P2P-B and (b) A&B using the simulated channel model and a sensitivity threshold $\rho = -80\ dBm$

4.4.5 CONDITIONAL ON-BODY ANCHOR PERMUTATION

In this last section, we propose a combinatorial permutation mechanism for the choice of on-body virtual anchors to increase $\mathbb{P}(P_{Succ})$ used at the end of each positioning activity period. We note $\{s_i \mid i = 1 \dots N_M\}$ and $\{s_j \mid j = 1 \dots N_A\}$ as the sets of on-body mobile nodes and on-body anchors respectively in a WBAN, where $\{s_{-i}\}$ represents the on-body nodes different than s_i. Each node s_i is attached to a set of N_A' anchors denoted as $A_i = \{a_i^k \mid k = 1 \dots N_A'\}$, where a_i^k can be an anchor node s_j or a mobile node s_{-i} acting as virtual anchor for a given positioning activity period. Accordingly, a *pure strategy* [74] of anchor scheduling for the node s_i is a permutation of a_i^k, given by $\phi_i^w \in \Phi_i$, where w is the index in the set of N_ϕ possible pure strategies Φ_i. Moreover, the utility function of s_i is given by:

$$\mathrm{u}_i(s_i, \phi_i^w) = \mathbb{P}(P_{Succ} \mid \theta)_i^w \qquad \textbf{(4-6)}$$

In this sub-problem, each on-body node search for the pure strategy maximizing its $\mathbb{P}(P_{Succ})$ on Φ_i. Thus, the conditional on-body anchor permutation corresponds to the best strategy maximizing the positioning utility for all the nodes:

$$\theta^+ = \underbrace{argmax}_{w \in 1 \dots N_\phi} \sum_{i=0}^{N_M} \mathrm{u}_i(s_i, \phi_i^w) \qquad \textbf{(4-7)}$$

In practice, it might be difficult to process the utility matrix for the N_ϕ strategies, especially with the sensors of a WBAN. For this reason, we reduce the problem by prioritizing the mobile nodes with the worst P_{Succ}. Moreover, each node compares its P_{Succ} with a defined positioning quality threshold (α). If the current $\{P_{Succ}\}_i$ is under this threshold, then the on-body node triggers the search of new virtual anchors. The goal is to increase its $\{P_{Succ}\}_i$ through our cooperative positioning mechanism with other on-body mobile nodes. In order to avoid the case where two mobile nodes can be their virtual anchors mutually, we start with those with the worst positioning rate. Thus, if a mobile node A finds a mobile node B as its new anchor, then the anchor B cannot choose the node A as an anchor. **Figure 4-16** and**Figure 4-17** show the comparison between the P_{Succ} without the cooperative positioning mechanism (red) and the $\mathbb{P}(P_{Succ} \mid \theta)$ following the conditional permutation strategy (blue) when the threshold is $\rho = -80\ dBm$.

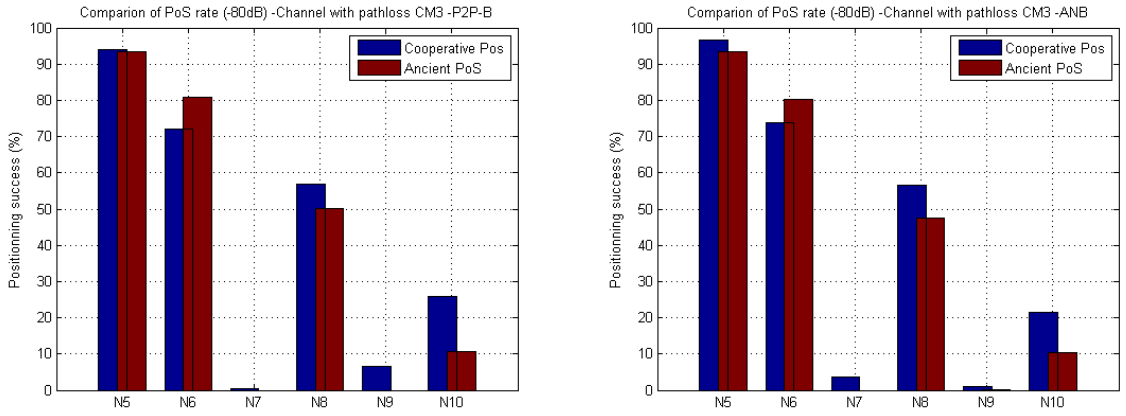

Figure 4-16: Comparison of the P_{Succ} with the conditional anchor permutation between (a) P2P-B and (b) A&B using the empirical channel model CM3 and $\rho = -80\ dBm$

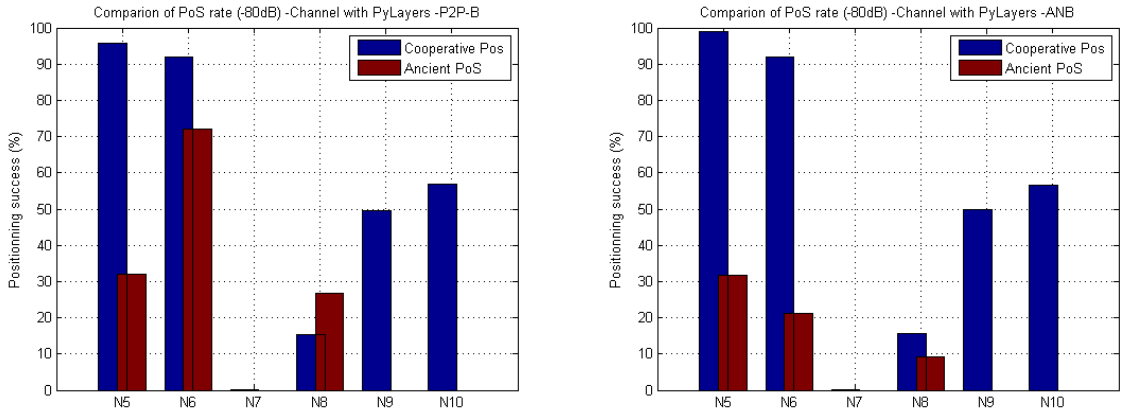

Figure 4-17: Comparison of the P_{Succ} with the conditional anchor permutation between (a) P2P-B and (b) A&B using the simulated channel model and $\rho = -80\ dBm$

As desired, we observe that our anchor choice strategy is favorable for the mobile nodes with low positioning success rate. In the empirical case (**Figure 4-16**), we observe that P_{Succ} increases less than for the other channels. The order of anchor choice for A&B (resp. P2P-B) was $[N_7, N_9, N_{10}, N_8, N_6, N_5]$ (resp. $[N_9, N_7, N_{10}, N_8, N_6, N_5]$). As N_7 (resp. N_9) is served first with A&B (resp. P2P-B), the gain in performance is interchanged between these 2 nodes. However even with our strategy, the P_{Succ} is very low, that's because their packet reception rate with other nodes is not enough even with the other mobile nodes. This means that even if 3 virtual anchors shows a good ranging success rate, if the 4th anchor has low ranging success rate, then the P_{Succ} is conditioned to be low as well. We note that N_6 decreases its $\mathbb{P}(P_{Succ} \mid \theta)$ even when he did not perform permutation, this is due to an statistical error with the real $\mathbb{P}(P_{Succ})$ where the long-term channel effect is considered.

In the case of the simulated channel (**Figure 4-17**), both MAC strategies perform the same anchor permutation $[N_{10}, N_9, N_7, N_8, N_6, N_5]$ and they found the same anchors replacement for

all the nodes. Accordingly, N_{10} and N_9 increases their $\mathbb{P}(P_{Succ})$ first. N_7 could not increase its P_{Succ} because its PRR is low enough to not find 4 good anchors.

Finally, we can conclude that our proposed algorithm leads to an increase of positioning success rate (even when the initial P_{Succ} was null), for whichever tested MAC protocol, and whichever tested channel. We thus believe that the algorithm is generic. This is a real advantage for WBAN where the person corpulence and behavior highly impacts the network topology. Besides, it is necessary to consider the allocation of some slots for the virtual anchors at the end of the existing frame, which can lead to accuracy errors as explained in the precedent chapters.

4.5. DISCUSSION AND PERSPECTIVES

In this Chapter, we analyzed the impact of the channel on the positioning success rate with WBAN using IR-UWB. We considered the scenario where the on-body nodes communicate with on-body anchors to perform motion capture. For this purpose, we used three different channel models: i) the CM3 path loss model as defined by the standard IEEE 802.15.6 and ii) a channel model calculated with the PyLayers ray-tracing simulator. In Sections 4.2 and 4.3, we showed that the channel affects the reception of the 3-WR packets inducing the positioning loss as a function of the sensitivity threshold at the receiver. In particular, the shadowing of the body is the principal cause of low positioning success rate. When comparing the positioning performance with different the scheduling strategies P2P, P2P-B and A&B, it turns out that even if they show a similar level of positioning success rate, A&B performs better in terms of number of positions estimated. However, this is severally decreased with higher packet loss and hence, P2P-B based strategies might be more suited for the case of dynamic scenarios.

From these results, we proposed and tested a cooperative algorithm based on long-term and short-term LQEs to improve the number of estimated positions with a conditional permutation of the on-body anchors. With our algorithm, we showed an improvement of the positioning success rate for the nodes with the worst localization performance for all the scheduling strategies and different channel models.

Future work will consist in testing our cooperative and conditional algorithm in other scenarios with group navigation and several WBANs. Nevertheless, in this study we did not considered the positioning and ranging error with respect to the channel variations. This is because of the complexity to use a suited ranging error model for all the links. In Deliverable D3.5 and D4.1, we will discuss more about this issue by exploring the performance of our different propositions.

5. CONCLUSIONS

Throughout this Deliverable, we explored WBAN cooperative cross-layer functionalities, which were partly presented in Deliverable D3.1. More specifically, the focus is put on the optimization of cooperative communications (mostly at the PHY/MAC layers level) for the sake of improving on-body nodes localization. One final aim is to cope with the initial requirements listed in Deliverable D1.1. Such requirements are recalled in Table 1-1 (Section 1.1.3), primarily for individual motion capture (LSIMC) applications, but also (even though more marginally here) coordinated group navigation (CGN) applications. Besides, the early analysis of a dynamic measurement campaign (Deliverable D4.1) highlighted the needs to define specific models depending on the radio link and human movement, thus motivating the refined simulation-based validation means adopted herein.

In Chapter 1, we briefly presented the different constraints to deal with, while considering WBAN and IR-UWB radio for localization purposes. In particular, we underlined that the required communication protocol has to deal mainly with the nodes synchronization, WBAN channel variations and mobility of the human body. We also explained that most of the works have been focused on the radio issues and localization algorithms performances without rigorous scope on cross-layer cooperative strategies. For this reason, we proposed to study different strategies at PHY/MAC levels to overcome the positioning errors due to the channel variations and mobility of nodes. To this aim, we implemented a complete cross-layer protocol stack in the discrete-event simulator WSNet coupled with PyLayers (Deliverable D2.5) to study our different strategies presented in this document under realistic scenarios (Deliverable D4.1).

In Chapter 2, we investigated and characterized the impact of nodes mobility and the WBAN channel variations on the ranging estimation. For this, we considered both LSIMC and CGN scenarios and we compare the ranging performance between the different on-, off- or inter-body links. When evaluating the impact of the mobility on the ranging accuracy, we found that the error is due to the packets delivery latency and the speed of nodes. From one side, the delays taken by the n-WR packets when nodes are moving yield an erroneous distance estimate because of the different evaluated ToF of different packets. Moreover, this error is increased when nodes moves faster. Thus, we found a tradeoff between the ranging accuracy and the delays of 3-WR packets. Thereafter, if we compare the ranging impact of mobility with different kind of links, we found that the level of error varies considerably depending on the MAC strategy and the mobility for all the links.

On the basis of the previous results, Chapter 3 focused on adapted cooperative cross-layer mechanisms. In this second study, we enlarged the mobility problem on the ranging accuracy to quantify its impact on the positioning estimation with different strategies at the MAC layer. In particular, we considered the study of scheduling of n-WR packets and the slot allocation. To sake of this study, we assumed the case of a perfect channel with the detection of first path of pulses. Accordingly, the system is beacon enabled and synchronized without packet loss.

First, we evaluated different scheduling strategies in pair-to-pair localization (P2P) proposing different features to reduce the packet delay or ranging error. In the case of the relative positioning of one on-body node with on-body anchors (e.g. at least for anchors for 3-D localization), we found a tradeoff between the estimation of precise distances and the positioning accuracy, i.e. it is better to choose a strategy that estimates distances closer to the desired position more than the strategies estimating accurate distances. More generally, when considering several on-body nodes trying to estimate its relative position, the accuracy performance of each scheduling strategy is different depending on the application. In the case of the individual motion capture, we found that the estimation of positions individually and in order with the anchors (BS7) leads to a better accuracy. In the case of posture recognition, it is preferable to consider a strategy that reduces the packets delays to estimate the distances closer to the desired position to estimate (BS5). Finally, the slot allocation study was evaluated with two different scheduling protocols (P2P-B and A&B) and a resource allocation policy depending on the mobility level of nodes. It turns out from our results that when comparing the positioning accuracy using P2P-B and A&B the positioning performance gap is smaller between both strategies in scenarios with low mobility (e.g. Yoga activity). Besides, in more dynamic scenarios with nodes moving faster (e.g. Walking), A&B outperforms P2P-B with a greater flexibility on the slot allocation regardless of different speeds between nodes. It is important to keep in mind that the parameters studied in this Chapter were not evaluated or quantified in literature. This analysis let us quantify the overall error on positioning estimation due to the mobility of nodes when using typical ranging protocols (e.g. n-WR). The latter results are essential to understand the impact of the MAC design to propose enhanced functionalities dedicated to the localization purposes. However, we only considered two basic scenarios with moderate mobility and fixed topology network. For this reason, it could be interesting in future works to enlarge the study with dynamic scenarios (such as running or random movements) and observe the ranging and position accuracy evolution in function of the number of mobile nodes / anchors and the different type of links (on-, inter- and off- body).

Finally, in Chapter 4, we introduced the packet error due to the WBAN channel during the localization scenario. For this study, we considered two different channel models: a) an empirical model from the literature (CM3) and b) a simulated channel model calculated (D2.2, D2.3 and D2.4) with PyLayers (D2.5). Within this models we quantify the impact of the packet loss on the positioning success rate depending on the sensitivity condition at the radio reception and we compare it using P2P, P2P-B and A&B from our previous studies. As expected, we found that the shadowing of the body provokes higher packet loss. Moreover, in the case of moderate channel conditions A&B is able to realize more position estimations than P2P strategies even with a similar packet success rate. However, when the channel conditions decreases, the loss of broadcasted transmissions in A&B becomes a critical problem for the positioning. From these results, we proposed an algorithm to increase the localization success by choosing cooperative virtual anchors for the ranging estimation based on link quality estimation. Our results show an improvement on the positioning success rate of nodes with the worst localization performance. This approach should be developed with a dynamic ranging error model at the PHY layer to compare the impact on the ranging error with an analysis of short-term and long-term variations.

6. REFERENCES

[1] M. A. Hanson, H. C. P. Jr., A. T. Barth, K. Ringgenberg, B. H. Calhoun, J. H. Aylor and J. Lach, “Body Area Sensor networks: Challenges and opportunities”, University of Virginia: 0018-9162/09/ © IEEE Computer Society, January 2009.

[2] R. Cavallari, F. Martelli, R. Rosini, C. Buratti and R. Verdone, "A Survey on Wireless Body Area Networks: Technologies and Design," *IEEE Communications Surveys & Tutorials,* vol. 16, no. 3, pp. 1635-1657, 2014.

[3] S. Ullah, H. Higgins, B. Braem, B. Latre, C. Blondia, I. Moerman, S. Saleem, Z. Rahman and K. S. Kwak, “A Comprehensive Survey of Wireless Body Area Networks: On PHY, MAC, and Network Layers Solutions,” *Springer Science+Business Media, LLC,* 2010.

[4] M.Chen, S.Gonzalez, A. Vasilakos, H. Cao and V. C. M. Leung, "Body Area Networks: a Survey", Springer Science+Business Media, LLC, 18 August 2010, p. 171–193.

[5] U. Sana, H. Henry, B. Bart, L. Benoit, B. Chris, M. Ingrid, S. Shahnaz, R. Ziaur and K. K. Sup, "A Comprehensive Survey of Wireless Body Area Networks: On PHY, MAC, and Network Layers Solutions," *Springer Science+Business Media, LLC,* 2010.

[6] M. Lauzier, P. Ferrand, H. Parvery, A. Fraboulet and J.-M. Gorce, "WBANs for live sport monitoring: An experimental approach," in *EURO-COST*, Bristol, UK, 2012.

[7] P. Ferrand, "Rapport de Thèse - Communications coopératives dans les réseaux autour du corps humain," Ecole Doctorale E.E.A, Lyon, 2013.

[8] J. Dong and D. Smith, "Opportunistic Relaying in Wireless Body Area Networks: Coexistence Performance," in *IEEE ICC 2013 - Wireless Communications Symposium*, 2013.

[9] B. Miscopein, J. Schwoerer and J.-M. Gorce, "Cooperative beacon-free MAC layer for body area networks," in *Personal, Indoor and Mobile Radio Communications, 2009 IEEE 20th International Symposium on , vol., no., pp.2157,2161*, 13-16 Sept. 2009.

[10] M. Dohler and Y. Li, “Cooperative Communication: Hardware, Channel and PHY”, John Wiley & Sons, Ltd, 2010.

[11] A. Nosratinia, T. E. Hunter and A. Hedayat, "Cooperative Communication in Wireless Networks," *IEEE Commun. Mag.,* vol. 42, no. 10, pp. 74-80, Oct 2004.

[12] J. M. Gorce, C. Goursaud, C. Savigny and G. Villemaud, "Cooperation mechanisms in BANs", University of Lyon: COST 2100, TD(09)862, 2009.

[13] G. Kramer, I. Maric and R. D. Yates, "Cooperative Communications. Foundations and Trends in Networking", Hanover, MA: NOW Publishers Inc., vol. 1, no. 3-4, 2006.

[14] K. J. R. Liu, A. K. Sadek, W. Su and A. Kwasinski, “Cooperative Communications and Networking”, Cambridge, MA: Cambridge University Press, 2009.

[15] Y. Chen, J. Teo, J. Lai, E. Gunawan, K. S. Low and C. B. R. P. Soh, “Cooperative Communications in Ultra-Wideband Wireless Body Area Networks: Channel Modeling and System Diversity Analysis,” *IEEE Journal on Selected Areas in Communications,* vol. 27, pp. 5-16, 2009.

[16] "IEEE Standard for Local and metropolitan area networks – Part 15.6: Wireless Body Area Networks," 29 Feb. 2012.

[17] S. Gezici, Z. Tian, G. B. Biannakis, H. Kobayashi, A. F. Molisch, H. Poor and Z. Sahinoglu, "Localization via Ultra-Wideband Radios: a look at positioning aspects for future sensor networks," *IEEE Signal Processing Magazine,* vol. 22, no. 4, pp. 70-84, July 2005.

[18] N. Patwari, A. O. Hero, M. Perkins, N. S. Correal and R. O'Dea, "Relative location estimation in wireless sensor networks," *IEEE Trans. on Signal Processing,* vol. 51, no. 8, pp. 2137-2148, Aug. 2003.

[19] D. Neirynck, K. Philips, H. D. Groot and J. Espina, "Practical comparison of ranging in IEEE 802.15.4 and IEEE 802.15.4a medicalbody sensor networks," *Proc. BodyNets’10,* pp. 16-22, Sept. 2010.

[20] Y. Qi and H. Kobayashi, "On relation among time delay and signal strength based geolocation methods," *Proc. IEEE Global Telecommunications Conf (GLOBECOM’03),* vol. 7, p. 4079–4083., Dec. 2003.

[21] P. Ferrand, M. Maman, C. Goursaud, J.-M. Gorce and L. Ouvry, "Performance evaluation of direct and cooperative transmissions in body area networks," *Annals of telecommunications, "Special issue on Body Area Networks Applications and Technologies",* no. 66, pp. 213-228, 2011.

[22] K. Y. Yazdandoost and K. Sayrafian-Pour, "Channel Model for Body Area Network (BAN)," *IEEE P802.15-08-0780-09-0006,* 2009.

[23] H. Poor, "An Introduction to Signal Detection and Estimation," *2nd ed. New York: Springer-Verlag,* 1994.

[24] Z. Xiao, Y. Hei, Q. Yu and K. Yi, "A survey on impulse-radio UWB localization," in *Sci. China Inf. Sci.,vol. 53, pp. 1322–1335, Jul 2010.*.

[25] J. Hamie, B. Denis, R. DErrico and C. Richard, "On-body toa-based ranging error model for motion capture applications within wearable UWB networks," *Journal of Ambient Intelligence and Humanized Computing,* Dec 2013.

[26] D. Macagnano, G. Destino, F. Esposito and G. Abreu, "MAC performances for localization and tracking in wireless sensor networks," in *4th Workshop on Positioning, Navigation and Communication*, 2007.

[27] J. Hamie, B. Denis and C. Richard, "Decentralized Positioning Algorithm for Relative Nodes Localization in Wireless Body Area Networks," *Mobile Networks and Applications,* vol. 19, no. 6, pp. 698-706, 2014.

[28] H. Soganci, S. Gezici and H. Poor, "Accurate positioning in ultra-wideband systems," *IEEE Wireless Communications,* vol. vol. 18, no. no. 2, p. pp. 19–27, April 2011.

[29] Y. Shimizu and Y. Sanada, "Accuracy of relative distance measurement with ultra wideband system," *in Proc. IEEE Conf. Ultra Wideband Systems and Technologies (UWBST'03),* pp. 374-378, 2003.

[30] Y. Ying, M. Ghogho and A. Swami, "Code-Assisted Synchronization for UWB-IR Systems: Algorithms and Analysis," *IEEE Transactions on Signal Processing,* vol. 56, no. 10, pp. 5169-5180, October 2008.

[31] B. Miscopein and J. Schwoerer, "ow complexity synchronization algorithm for non-coherent UWB-IR receivers," *n Vehicular Technology Conference 2007 VTC2007-Spring IEEE 65th,* pp. 2344-2348, April 2007.

[32] B. Miscopein, "Systèmes UWB impulsionnels non cohérents pour les réseaux capteurs: Coexistence et coopération," *PhD thesis,* 2010.

[33] M.-G. D. Benedetto and G. Giancola, " Understanding Ultra Wide Band," *Prentice Hall PTR, Ed.: Radio Fundamentals,* 2004.

[34] S. Yang and J.-C. Belfiore, "Towards the optimal amplify-and-forward coope-rative diversity scheme," *IEEE Transactions on Information Theory,,* vol. 50, no. 12, pp. 3114-3126, 2007.

[35] B. Talha and M. Patzold, "Channel models for mobile-to-mobile cooperative communication systems : A state of the art review," *IEEE Vehicular Technology Magazine,* vol. 6, no. 2, pp. 33-43, june 2011.

[36] E. Telatar, "Capacity Of Multi-antenna Gaussian Channels," *European Trans. Telecommun,* vol. 10, no. 6, pp. 585-595, 1999.

[37] M. Maman, B. Denis and L. Ouvry, "An intuitive prioritised medium access scheme for tracking applications in UWB ldr-lt networks," in *IEEE 19th International Symposium on Personal, Indoor and Mobile Radio Communications*, 2008.

[38] G. E. Garcia, L. S. Muppirisetty and H. Wymeersch, "On the trade-off between accuracy and delay in UWB navigation," *IEEE Commun. Lett.,* vol. vol. 17, no. no. 1, pp. pp. 39-42.

[39] B. Denis, M. Maman and L. Ouvry, "On the scheduling of ranging and distributed positioning updates in cooperative IR-UWB networks," in *IEEE International Conference on Ultra-Wideband*, 2009.

[40] L. De Nardis and M.-G. D. Benedetto, "Medium Access Control design in UWB networks: review and trends," *Journal of Communication and Networks, Special Issue on Ultra-Wideband Communications,* vol. 5, no. 4, pp. 386-393, December 2003.

[41] M. M. Alam and E. B. Hamida, "Towards Accurate Mobility and Radio Link Modeling for IEEE 802.15.6 Wearable Body Sensor Networks," *in Proceedings of the Seventh IEEE International Workshop on Selected Topics in Wireless and Mobile computing (IEEE STWiMob 2014),* Cyprus, October 8-10th, 2014.

[42] J. Choliz, A. Hernandez and A. Valdovinos, "A framework for UWB-based communication and location tracking systems for wireless sensor networks," in *Sensors, vol. 11, pp. 9045–9068, Sep 2011.*.

[43] A. Guizar, A. Ouni and C. Goursaud, "Impact of Mobility on Ranging Estimation using UltraWideband," in *Proceedings of the Fourth Networking Networking Women Workshop - N2Women {ACM} SIGCOMM*, Chicago, USA, August 2014.

[44] IEEE Std 802.15.4-2006: Wireless Medium Access Control (MAC) and Physical Layer (PHY) Specifications for Low-Rate Wireless Personal Area Networks (WPANs), IEEE Std., September 2006.

[45] A. Guizar, C. Goursaud and J. Gorce, "Modeling the Impact of node speed on the ranging estimation with UWB Body Area Networks," *In 26th IEEE Annual International Symposium on Personal, Indoor and Mobile Radio Communication (PIMRC'26),* Hong Kong, China, Sept, 2015.

[46] M. Maman, B. Denis, M. Pezzin, B. Piaget and L. Ouvry, "Synergetic MAC and Higher Layers Functionalities for UWB LDR-LT Wireless Networks," *In Proceedings of the 2008 IEEE International conference of ULTRA-WIDEBAND (ICUWB2008),* vol. 3, 2008.

[47] B. Denis, N. Amiot, B. Uguen, A. Guizar, C. Goursaud, A. Ouni and C. Chaudet, "Qualitative Analysis of RSSI Behavior in Cooperative Wireless Body Area Networks for Mobility Detection and

Navigation Applications," *In 21st IEEE International Conference on Electronics Circuits and Systems (ICECS'21),* Marseille, France, Dec. 2014.

[48] Vicon, "http://www.vicon.com".

[49] G. Chelius, A. Fraboulet and E. B. Hamida, "http://wsnet.gforce.inria.fr".

[50] A. Ouni, J. Hamie, C. Chadet, A. M. Guizar and C. Goursaud, " From the Characterization of Ranging Error to the Enhancement of Nodes Localization For Group of Wireless Body Area Networks," *In the 7th International Conference on Ad Hoc Networks (AdhocNets'15),* San Remo, Italy, Sept, 2015.

[51] R. Bharadwaj, S. Swaisaenyakorn, C. G. Parini, J. Batchelor and A. Alomainy, "Localization of Wearable Ultrawideband Antennas for Motion Capture Applications," *Antennas and Wireless Propagation Letters, IEEE,* vol. 13, pp. 507-510, 2014.

[52] E. Ben Hamida, M. Maman, B. Denis and L. Ouvry, "Localization performance in Wireless Body Sensor Networks with beacon enabled MAC and space-time dependent channel model," *IEEE 21st International Symposium on Personal, Indoor and Mobile Radio Communications (PIMRC) Workshops,* 2010.

[53] N. Amiot, M. Laaraiedh and B. Uguen, "Pylayers: An open source dynamic simulator for indoor propagation and localization," *in 2013 IEEE International Conference on Communications Workshops(ICC),* pp. 84-88, June 2013.

[54] A. Guizar, A. Ouni, C. Goursaud, N. Amiot and J. Gorce, "Impact of MAC scheduling on positioning accuracy for motion capture with UWB body area networks," *In 9th International Conference on Body Area Networks (BodyNets'9),* London, Great Britain, October, 2014.

[55] A. Bachir, M. Dohler, T. Watteyne and K. Leung, "MAC essentials for wireless sensor networks," *IEEE Communications Surveys & Tutorials,* vol. 12, no. 2, pp. 222-248, 2010.

[56] U. Sana, S. Bin, I. S. Riazul, K. Pervez, S. Shahnaz and K. K. Sup, "A Study of MAC Protocols for WBANs," *Journal of Sensors,* vol. 10, pp. 128-145, April 2010.

[57] H. A. Shaban, M. A. El-Nasr and R. M. Buehrer, "Toward a Highly Accurate Ambulatory System for Clinical Gait Analysis via UWB Radios," *IEEE Transactions on Information Technology in Biomedicine,* vol. 14, no. 2, 2010.

[58] M. Mhedhbi, M. Laaraiedh and B. Uguen, "Constrained LMDS technique for human motion and gesture estimation," *9th Workshop on Positioning Navigation and Communication (WPNC),* 2012.

[59] Z. W. Mekonnen, E. Slottke, H. Luecken, C. Steiner and A. Wittneben, "Constrained maximum likelihood positioning for UWB based human motion tracking," *International Conference on Indoor Positioning and Indoor Navigation (IPIN),* 2010.

[60] J. Hamie, C. Chaudet and B. Denis, "Improved Navigation Capabilities in Groups of Cooperative Wireless Body Area Networks," *9th International Conference on Body Area Networks (BodyNets),* 2014.

[61] R. Kong, C. Chen, W. Yu, B. Yang and X. Guan, "Data priority based slot allocation for Wireless Body Area Networks," *International Conference on Wireless Communications Signal Processing (WCSP),* pp. 1-6, 2013.

[62] B. Liu, Z. Yan and C. W. Chen, "CA-MAC: A hybrid context-aware MAC protocol for wireless body area networks," *in Proc. 13th IEEE International Conference on e-Health Networking Applications and Services (Healthcom),* Columbia, MO, Jun. 2011, pp. 213–216.

[63] Z. Yan, B. Liu and C. W. Chen, "QoS-Driven Scheduling Approach Using Optimal Slot Allocation for Wireless Body Area Networks," *IEEE 14th International Conference on e-Health Networking, Applications and Services (Healthcom),* 2012.

[64] S. Misra and S. Sarkar, "Priority-Based Time-Slot Allocation in Wireless Body Area Networks During Medical Emergency Situations: An Evolutionary Game-Theoretic Perspective," *IEEE Journal of Biomedical and health informatics,* vol. 19, no. 2, 2015.

[65] E. B. Hamida, M. M. Alam, M. Maman and B. Denis, "Short-Term Link Quality Estimation for Opportunistic and Mobility Aware Routing in Wearable Body Sensors Networks," *in Proceedings of the 2014 IEEE 10th International Conference on Wireless and Mobile Computing, Networking and Communications (IEEE WiMob 2014),* Cyprus, October 8-10th, 2014.

[66] A. Guizar, A. Ouni, C. Goursaud, C. Chaudet and J. Gorce, " Quantifying the Impact of Scheduling and Mobility on IR-UWB Localization in Body Area Networks," *In 12th IEEE International Conference on Body Sensor Networks (BSN'12),* MIT, Cambridge, USA, June, 2015.

[67] M. Lauzier, P. Ferrand, A. Fraboulet, H. Parvery and J.-M. Gorce, "Full Mesh Channel Measurements on Body Area Networks under Walking Scenarios," in *7th European Conference on Antennas and Propagation (EuCAP)*, 2013 .

[68] N. Baccour, A. Koubaa, M. B. Jamaa, H. Youssef, M. Zuniga and M. Alves, "A Comparative Simulation Study of Link Quality Estimators in Wireless Sensor Networks," *in 17th IEEE/ACM MASCOTS'09,* Sept. 2009.

[69] E. B. Hamida, R. D'Errico and B. Denis, "Topology Dynamics and Network Architecture Performance in Wireless Body Sensor Networks," *in 4th IFIP NTMS, Paris, France, 2011.*

[70] S. Yang, J.-L. Lu, F. Yang, L. Kong, W. Shu and M.-Y. Wu, "Behavior-Aware Probabilistic Routing For Wireless Body Area Sensor Networks," *IEEE Globecom 2013.*

[71] J. Hamie, A. Ouni and C. Chaudet, "Is Cooperative Localization in Wireless Body Area Networks Accurate Enough for Motion Capture Applications?," *in 12th IEEE International Conference on Sensing, Communication and Networking (SECON), Seattle, USA,* jun 2015. .

[72] A. Guizar, C. Goursaud and B. Uguen, " Impact of On-Body Channel models on positioning success rate with UWB Wirelss Body Area Networks," *In 10th International Conference on Body Area Networks (BodyNets'10),* Sydney, Australia, September, 2015.

[73] M. Mhedhbi, N. Amiot, S. Avrillon and B. Uguen, "Human Body Perturbed Antenna Integration in Indoor Propagation Simulator," *Journées scientifiques 2014 de l'URSI France, Paris, France,* 2014.

[74] L. Wang, C. Goursaud, N. Nikaein, L. Cottatellucci and J. Gorce, "Cooperative Scheduling for Coexisting Body Area Networks," *Wireless Communications, IEEE Transactions on,* vol. vol.12, no. no.1, pp. pp.123,133, January 2013.